A QUANTITATIVE EVALUATION OF CLOSED-CYCLE OCEAN THERMAL ENERGY CONVERSION (OTEC) TECHNOLOGY IN CENTRAL STATION APPLICATIONS

PREPARED FOR THE U.S. DEPARTMENT OF ENERGY

E. C. GRITTON, R. Y. PEI, J. AROESTY, M. M. BALABAN,
C. GAZLEY, R. W. HESS, W. H. KRASE

R-2595-DOE
MAY 1980

Rand
SANTA MONICA, CA. 90406

The work upon which this publication is based was performed pursuant to Contract No. DE-AC01-79-PE70078 with the U.S. Department of Energy.

Library of Congress Cataloging in Publication Data

Main entry under title:

A Quantitative evaluation of closed-cycle ocean thermal energy conversion (OTEC) technology in central station applications.

([Report] - Rand Corporation ; R-2595-DOE)
Bibliography: p.
1. Ocean thermal power plants. I. Gritton, E. C. II. United States. Dept. of Energy. III. Series: Rand Corporation. Rand report ; R-2595-DOE.
AS36.R3 R-2595 [TK1056] 081s [621.31'243] 80-13615
ISBN 0-8330-0222-8

Published by The Rand Corporation

A QUANTITATIVE EVALUATION OF CLOSED-CYCLE OCEAN THERMAL ENERGY CONVERSION (OTEC) TECHNOLOGY IN CENTRAL STATION APPLICATIONS

PREPARED FOR THE U.S. DEPARTMENT OF ENERGY

E. C. GRITTON, R. Y. PEI, J. AROESTY, M. M. BALABAN,
C. GAZLEY, R. W. HESS, W. H. KRASE

R-2595-DOE
MAY 1980

Rand
SANTA MONICA, CA. 90406

PREFACE

The Office of Energy Research (OER) has a department-wide oversight responsibility for the conduct of research and development programs within the U.S. Department of Energy (DOE). These programs not only represent a major commitment of DOE resources but also provide a basis for the eventual full commercialization of advanced energy conversion technologies. Budget cycles and the need to couple proposed experimental programs to the effective definition of future system requirements and to long-term program goals underscore the need for a quantitative evaluation methodology with which OER can discharge its oversight responsibility. More specifically, a methodology is needed which can be readily implemented to study the cost sensitivities and engineering uncertainties of advanced energy conversion systems.

Rand has developed such a methodology for the OER and has successfully applied it to evaluate the Ocean Thermal Energy Conversion (OTEC) technology. The results of this evaluation are reported here. The authors emphasize the total system approach and the identification of information needed to bound the uncertainties.

The approach described in this report should be a useful contribution to the overall effort of reducing uncertainties and achieving a better understanding of the cost/performance interactions of large, complex energy systems under development. Consequently, the information contained here should be of interest to both policy and program offices in the Department of Energy, as well as to those outside the DOE who are concerned with energy system development.

This research has been conducted as part of Rand's program of policy studies for the Department of Energy under contract DE-AC01-79PE 70078.

SUMMARY

This report summarizes the results of an independent quantitative evaluation by Rand of Ocean Thermal Energy Conversion (OTEC) for central station applications. The methodology developed and implemented for the quantitative analysis of cost sensitivities and engineering uncertainties provides the Office of Energy Research (OER) with the capability for evaluating the effects of alternative OTEC R&D strategies. The analysis also provides a general quantitative approach to assess advanced energy technologies.

Ocean Thermal Energy Conversion (OTEC) is a solar technology. Like all solar technologies, it is a renewable energy source. By exploiting the temperature difference between warm surface waters and cold water from the depths to operate a thermodynamic cycle to generate electricity, OTEC is a heat engine that taps the surface waters of tropical and subtropical oceans of the earth as a heat source and the cold water originating in the polar regions as a heat sink. The oceans are massive natural storage basins for solar energy. Subject to seasonal variations, the energy collected is available 24 hours a day, which means that OTEC is usable for base-load power. This characteristic is almost unique to OTEC among renewable power systems.

The available temperature difference of 30° to 45°F results in remarkably large proportions for a thermal power plant. Proposed OTEC designs use standard engine cycles that are typical of those used in conventional steam power plants, where the temperature difference is on the order of hundreds to thousands of degrees. The lower temperature difference available to OTEC leads to smaller Carnot cycle net efficiencies, larger heat exchanger areas, and larger flows of warm and cold water. Major objectives of OTEC R&D are to demonstrate that a system can be built at a projected life cycle cost that is competitive and to reduce the uncertainties in estimates of engineering performance and cost.

This study focuses on closed-cycle OTEC for delivery of electric power to the United States. Performance and costs of complete

commercial OTEC systems are analyzed at the system level using inputs from component analyses and thermal-resource data for sites in the Gulf of Mexico. Such sites could feed the Gulf Coast from the west coast of Florida to the New Orleans areas.

In this evaluation, the energy conversion analysis, i.e., the study of the power system, is based on a thermodynamic analysis of the complete system, which includes allowances for losses in all circuits. A cost-minimization scheme is used to ensure that the cycle component choices are near optimal. To make these cost-minimization calculations, cost algorithms are developed for the principal components.

Off-design operations are of great importance in the Gulf of Mexico because of significant seasonal surface temperature variations and the quite large resulting variations of output power. These effects are accounted for in this study by calculating the off-design performance of the power systems and by selecting the cycle that maximizes the average power over the year. The value of the generated electricity was assumed constant throughout the year.

Capital cost estimates are made for the complete system. Costs for commercial-size plants for delivery of electricity to shore, including the power system, platform, cold- and warm-water systems, mooring, and transmission of electricity to shore are estimated based on both contractors' estimates and independent analyses. These estimates include major variations in concept. All costs are computed in 1978 dollars. The total system cost is then minimized using the nonlinear Sequential Unconstrained Minimization Technique (SUMT). The optimization is carried out with respect to the engineering design variables entering into the system performance calculations. Cost sensitivity is then analyzed for several areas of engineering and cost uncertainty to identify factors having potentially significant impact on total system cost.

The results of our engineering analysis indicate that the power system and platform appear to be within the state of the art. Biofouling, the fouling of the system components by aquatic microorganisms, remains a major concern in OTEC. The principal countermeasures are chlorination (or other chemical treatment) and mechanical cleaning.

The long-term environmental acceptability of chlorination in pristine oceans is still in question. Mechanical cleaning introduces additional technical and cost uncertainties. Long-term realistic demonstrations of potential cleaning systems have been initiated and require further support. Some novel heat exchanger configurations have been proposed that promise significant performance advantages, but they need commercial-scale verification. Mooring and station-keeping technologies require further development and adaptation for commercial-size platforms. Tests to be conducted in the first systematic at-sea experimental program, designated OTEC-1, are expected to yield useful information about heat exchanger performance and biofouling countermeasures. Follow-on scaled-up and pilot plant test programs currently being planned will further contribute to a much needed data base for the development and commercialization of OTEC technology.

The submarine cable system and cold-water pipe (CWP) present major technical risks. The cable design parameters remain uncertain. The optimal configuration for the riser cable needs to be established and validated. A major development program including large-scale tests may be necessary to validate CWP designs. Materials such as fiberglass-reinforced plastic (FRP) appear promising, but a more extensive data base than is currently available for FRP needs to be developed, particularly for fatigue properties. Both the CWP and the riser cable are amenable to numerical analysis. The amount of engineering information that can be generated with appropriate computer modeling could be extremely useful and cost effective in complementing the necessary experimental work. A systematic effort in this direction is required.

Estimates of the total system cost are highly sensitive to costing methodologies, financing schemes, and incentives. In this study, a reference design was selected to provide a basis for comparison with a number of variations in design concepts and for the sensitivity analysis of cost estimates. This reference design consists of a 400 MWe plant located approximately 150 n mi west of Tampa, Florida. The power system is based on a tube-and-shell heat exchanger using titanium for tube material. The construction period was taken to be 5 years, with an annual rate of inflation and cost of capital assumed to be 6 percent

and 10 percent, respectively. The total system capital cost was estimated to be $3400/kWe for this reference design at start of operation. The estimate does not reflect any tax preference and/or financing incentives. Consequently, comparison with other energy conversion technologies that are subsidized or expected to benefit from favorable financing schemes or tax provisions will not be meaningful unless appropriate adjustments are made.

No single component dominates or drives the cost of the system. The largest contributor to the capital cost is the heat exchanger, which is 25 percent of the total. The research and development of advanced heat exchangers constitute a large portion of DOE's current OTEC program. An advanced flat plate designed by Alfa-Laval Thermal, Inc., is under investigation. Evaluation of preliminary performance data in our systems model shows that successful development of this heat exchanger will reduce the overall capital cost of OTEC by 15 percent.

Current DOE OTEC research programs on heat exchanger enhancement are concentrated on the ammonia vapor side of the tube-and-shell heat exchanger. Enhancement on the water side is a technical opportunity that has not been investigated to any great extent. Our preliminary analysis shows that the effect can be quite large, leading to a possible reduction of capital cost by 8 to 15 percent depending on the cost of incorporating the required tube roughness. Of the potential technical improvements we have examined, water-side enhancement is one of the most promising, although it may entail complex cleaning requirements. Heat transfer performance, cleanability, and manufacture should be verified.

Only a small fraction of past OTEC program R&D funding has been aimed at the engineering design and development of prototype CWP and cable designs. Therefore, our cost estimates for these components are much more uncertain than those for the power system. Our sensitivity studies show that substantial cost variations in these components will not change the overall system cost drastically. The sucessful development of a cold-water pipe and cable is critical to the feasibility of a commercial OTEC system. An accelerated progam in these two areas to

show feasibility and develop confidence in future cost estimates and engineering performance is desirable.

Lower cost estimates for OTEC can be achieved by using projected low-cost components such as plate type heat exchangers and an FRP cold-water pipe, eliminating most technical and design uncertainty (contingency) and accelerating the construction period by one year. For this case, the capital cost of our OTEC reference design is reduced to $2500/kWe. However, this lower capital cost estimate is contingent on the realization of a number of favorable assumptions.

Estimates of OTEC cost of electricity are highly uncertain. Using the Electric Power Research Institute methodology and assuming a fixed charge rate of 18 percent and a maintenance availability factor of 90 percent, we estimate the cost of electricity (COE) for the reference OTEC plant to be 96 mills/kWh. Decreasing the fixed charge rate to 15 percent (effectively assuming a tax preference of 3 percent) and using the favorable assumptions described above reduces the COE to 60 mills/kWh. This clearly indicates the sensitivity of COE estimates to costing methodologies and incentives. Thus, it is important to use the same cost methodology and financing assumptions when comparing COE estimates for alternative energy systems.

The economic viability of the OTEC system is a very sensitive function of the plant's availability. High availability may be aided by modularity and on-line cleaning, although conditions peculiar to ocean operation will introduce uncertainties. However, it is the capacity factor, the product of availability and a second factor related to the seasonal variation of the surface-to-bottom temperature difference (10 percent reduction in this quantity leads to about a 30 percent loss in output), that determines power cost. For the Gulf region, a range of capacity factors from 60 to 80 percent has been considered.

The OTEC plant is a complex system with many components. Because no single component dominates the cost of the total system, perturbations of any single engineering or cost variable will not cause dramatic changes in the total system cost. We found that a one percent variation in any of the important engineering and cost variables resulted in less than one-fourth of one percent variation of the system cost. Therefore,

we cannot expect a dramatic reduction in overall system cost to occur even with a large cost reduction or engineering performance improvement in only a single OTEC component. Cost and performance improvements will only occur with improvements in the system as a whole. This characteristic leads to the conclusion that the successful development of an OTEC commercial plant will require a total systems approach by DOE in establishing an appropriate OTEC R&D program.

ACKNOWLEDGMENTS

We acknowledge the support of the Office of Energy Research, Department of Energy, and the cooperation of the Ocean Systems Branch. With the latter's approval, the three principal contractors to the Department's OTEC program--TRW, Lockheed, and Westinghouse--have made available to us information and staff expertise, without which this study could not have been completed. Our thanks also to the experts from the Applied Physics Laboratory and the MITRE Corporation who have met with us on many occasions to share their insights.

Carolyn Huber provided all the programming support for the project. Thomas F. Kirkwood and David J. Dreyfus reviewed the report and provided many helpful suggestions. Robert Douglas (TRW), Murray Leitner (LMSC), and William Richards (DOE) also read the draft and offered valuable comments.

CONTENTS

I. INTRODUCTION

Ocean Thermal Energy Conversion (OTEC) is a solar technology. Like all solar technologies, it is based on a renewable energy source. First enunciated by d'Arsonval (known for his work on the galvanometer) in 1881, the OTEC concept uses the temperature difference between warm surface waters and cold water from the depths to operate a thermodynamic cycle and generate electricity. Thus the idea has the makings of a heat engine that taps the tropical and subtropical oceans of the earth as a heat source and uses the polar regions as its heat sink.

The oceans are massive natural storage basins for solar energy. The energy collected is available 24 hours a day. The natural collection and storage capacity of the oceans eliminate problems associated with the sporadic availability of energy that marks most other systems for direct use of solar energy. This round-the-clock availability makes the energy usable for base-load power. The sun and tropical currents continue to warm the surface ocean water while polar currents and other factors continue to chill the deep waters. Thus, there is a natural dependable fuel supply. These characteristics, coupled with the expectation that use of the stored solar energy will be nonpolluting, make ocean thermal energy conversion attractive.

There have been a number of pioneering efforts by French scientists and engineers in this century. The most famous, G. Claude's attempt in 1930 in Cuba to generate power at a shore-based site, generated 22 kWe with a temperature difference of only 13°C (24°F) (Claude, 1930). In the forties and fifties, French utilities planned several OTEC plants for sites off the coast of West Africa and in the Caribbean. Construction was cancelled, however, because of technological and economic uncertainties (Massart, 1974).

In Claude's scheme, cold water was drawn in through a 1-1/2 mile pipe. Warm surface water was pumped through a much shorter pipe. The warm water (81°F) was flash-evaporated in a partial vacuum and the resulting steam rotated a turbine coupled to a generator to produce electricity. The steam was then cooled in a condenser by the cold water.

This concept using seawater as the working fluid is called the open-cycle concept and is shown schematically in Fig. 1.

The closed-cycle concept shown in Fig. 2 uses ammonia or a similar liquid as the working fluid. Because ammonia boils at a lower temperature than water, it is not necessary to use a partial vacuum. Instead, heat from the warm ocean water is transferred to liquid ammonia in a heat exchanger known as an evaporator. The ammonia vaporizes and passes through a turbine, turning a generator and producing electricity. Then it is cooled and condensed by the cold ocean water in another heat exchanger known as a condenser. The ammonia is then reused and the cycle is thus closed.

A number of factors limit the means of extracting useful ocean thermal energy. Practical OTEC systems need to be located at favorable sites offering (1) high thermal differences between the warm surface and the cold deep water, (2) low velocity currents, (3) low frequency and severity of storms, and (4) nearness to the market for the OTEC products.

The temperature difference between the surface water and deep water has the most bearing on extraction of ocean energy. As the temperature difference decreases, the energy output will decrease drastically and the effective cost of each unit of energy will increase. Current concepts for extracting ocean energy require a temperature difference of 33° to 40°F. With a temperature difference of 30°F, a plant would produce approximately 51 percent less output than with a temperature difference of 40°F. With a temperature difference of less than 30°F, there is a marked loss of output. For that reason, 30°F can be considered a minimum usable temperature difference to generate net power from a turbine.

Even a temperature difference of 40°F presents technical problems. For example, the technology proposed for OTEC designs uses standard engine cycles that are typical of those used in power plants where the heat from burning fuel is converted into electrical power. In conventional power plants, the temperature difference is on the order of hundreds to thousands of degrees. An OTEC design will attempt to create useful power from a temperature difference that is usually discarded as

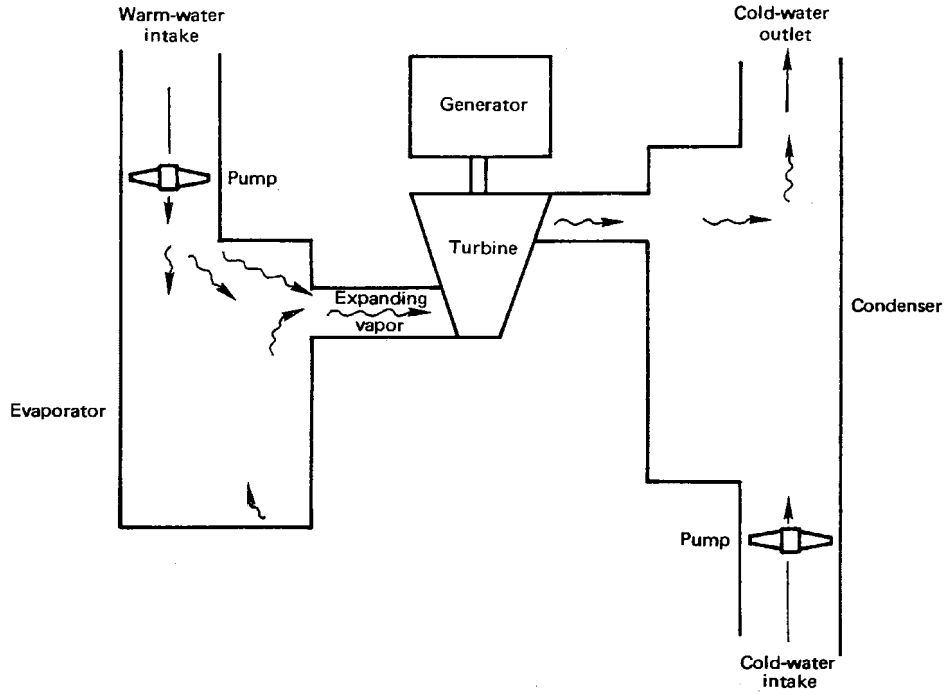

Fig. 1 — Open-cycle OTEC

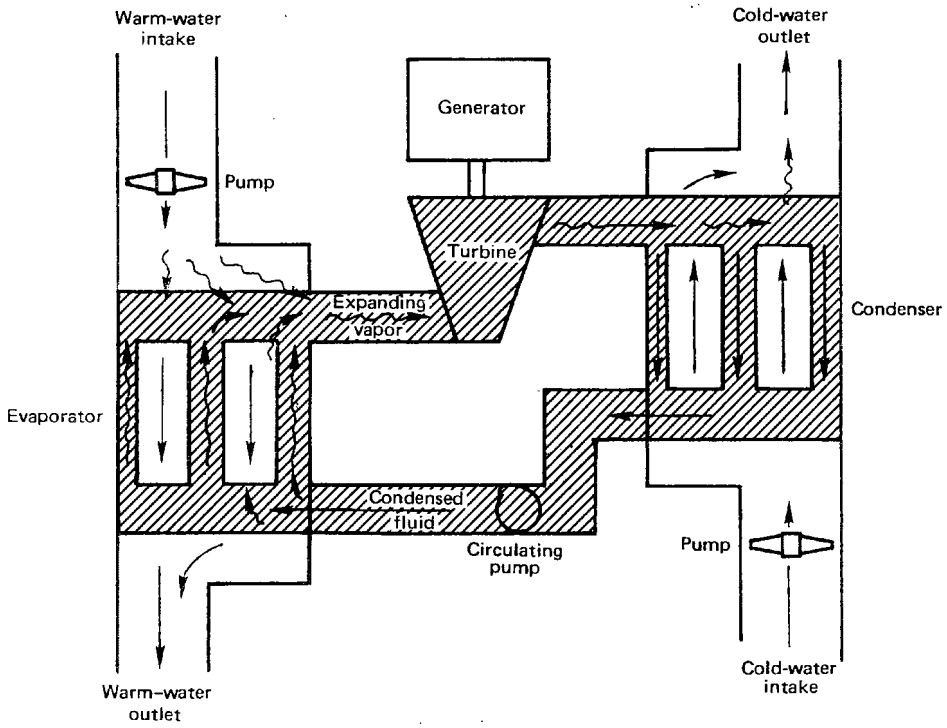

Fig. 2 — Closed-cycle OTEC

infeasible in conventional power plants. This lower temperature difference leads to a lower Carnot net efficiency. Useful amounts of net power output will require large volumes of flow of both the warm water (heat source) and cold water (heat sink) with correspondingly large heat exchanger surface areas for energy transfer to and from the working fluid. A major objective of OTEC R&D, then, is to achieve an acceptable system performance at a reasonable cost.

Only two regions of the continental United States appear to be promising sites--the Florida stream and the Gulf of Mexico. Other areas of interest to the United States exist off Hawaii, Puerto Rico, the Virgin Islands, Guam, Micronesia, and international waters. A detailed assessment of the oceans' thermal resources and their relationship to the amount and kind of energy needed in specific places has not been made.

The near-term (through 1985) objective of DOE's OTEC program is to develop a technology for demonstrating the technical and economic feasibility of commercial offshore OTEC power plants capable of economically converting ocean thermal energy into substantial quantities of base-load electrical energy. To assess OTEC performance, a 1 MWe closed-cycle component platform (OTEC-1) is planned for ocean tests starting in 1980. Major system procurement began in FY 1977. Work has also begun on engineering test facilities. It has been suggested that seawater systems and ocean platforms sizes of 10 to 40 MWe are necessary to verify OTEC feasibility. Design of closed-cycle 10 MWe power modules has been completed and subsequent procurements of scaled units are in negotiation. This could lead to a major commitment of DOE resources and have ramifications for the eventual full commercialization of OTEC systems.

Three industrial contractor teams are developing candidate designs for commercial-size OTEC power systems, using state-of-the-art heat exchangers as well as more advanced configurations. The prime power system contractors are Lockheed Missiles and Space Company, Inc., Sunnyvale, California, teamed with Alfa-Laval, Thermal, Inc.; TRW, Inc., Redondo Beach, California; and Westinghouse Electric Corporation Power Systems Company, Philadelphia, Pennsylvania. Other industrial contractors are

developing candidate concepts for OTEC platforms, cold-water intake pipes, and submarine cables. On the whole, however, the power system is in a much more advanced state of development than the other major components.

The OTEC program has been qualitatively assessed on a number of occasions (U.S. Congress, 1978; National Academy of Sciences, 1977). These assessments have delineated a number of problem areas over a wide range of proposed OTEC applications. However, these assessments should be complemented with a systematic effort in quantitative evaluation, especially for the case of base-load power generation. More specifically, there is need for a methodology that can be readily implemented to study the cost sensitivities and engineering uncertainties of OTEC systems. This report presents such a methodology and the results. Emphasis has been placed on the full exploitation of the existing data base and on the identification of information needed to bound the uncertainties. The study also addresses the potential impact of larger scale experimental programs on the narrowing of such uncertainties, as well as new technologies that might be expected to resolve some of the questions. Supporting studies include component-level analyses of performance and cost, identification and analysis of critical areas of uncertainties, review and assessment of existing estimates of resources magnitude, and a review of potentially critical material and possible production shortages. The results should contribute to the overall effort to reduce uncertainties and better understand the interaction between cost and system performance.

The U.S. OTEC program has emphazed the closed-cycle configuration because the technology required for its implementation is more advanced at this time compared with the open-cycle. Accordingly, this study focuses on closed-cycle OTEC for cable delivery of electric power to the continental United States. System-level analyses of performance and cost of complete commercial OTEC systems are made from inputs from components analyses and thermal resource data for given sites. Sites considered for full-scale commercialization are in the Gulf of Mexico, feeding the west coast of Florida and New Orleans areas.

The study consists of three interconnected areas of investigation:

- o Applied Sciences
  - Resource analysis
  - Heat transfer
  - Biofouling and corrosion
- o Engineering
  - Energy conversion
  - Ocean engineering
  - Power transmission
- o Systems
  - Off-design performance
  - Cost estimating relations
  - Modeling and optimization
  - Sensitivity analysis

The study of the energy conversion power system is based on a thermodynamic analysis of the complete system, which includes allowances for losses in all circuits. An appropriate cost-minimization scheme ensures that the cycle choices are near optimal. To make these cost-minimization calculations, cost algorithms are developed for the principal components.

Off-design operations are of great importance in the Gulf of Mexico because of significant seasonal surface temperature variations and the quite large resulting variations of output power. These effects call for optimization of the cycle based on annual variations and for a definition of the power plant rating on that basis.

Capital cost estimates are made for the complete system. Costs for commercial-size plants for delivery of electricity to shore, including the power system, platform, cold- and warm-water systems, mooring, and transmission of electricity to shore are estimated based on both contractors' estimates and independent analyses. These estimates include major variations in concept.

The cost model consists of a set of estimating relationships keyed to a cost breakdown structure. These cost estimating relationships are

driven by three types of inputs: results of the thermodynamic analysis and system design parameters, default factors, and model options. The model options are required to identify the more important cost and design considerations, such as platform capacity, overload capacity, site, type of platform, etc. All costs are computed in 1978 dollars. The total system cost is then minimized using the nonlinear Sequential Unconstrained Minimization Technique. The optimization is carried out with respect to the engineering design variables entering into the system performance calculations. Cost sensitivity is then analyzed for several areas of engineering and cost uncertainty to identify factors having potentially significant impact on total system cost.

Figure 3 illustrates the relation of the major tasks in our total system analysis. More detailed descriptions of the methodologies for the engineering, systems, and cost analyses, as well as the modeling and optimization techniques, are given in the following sections.

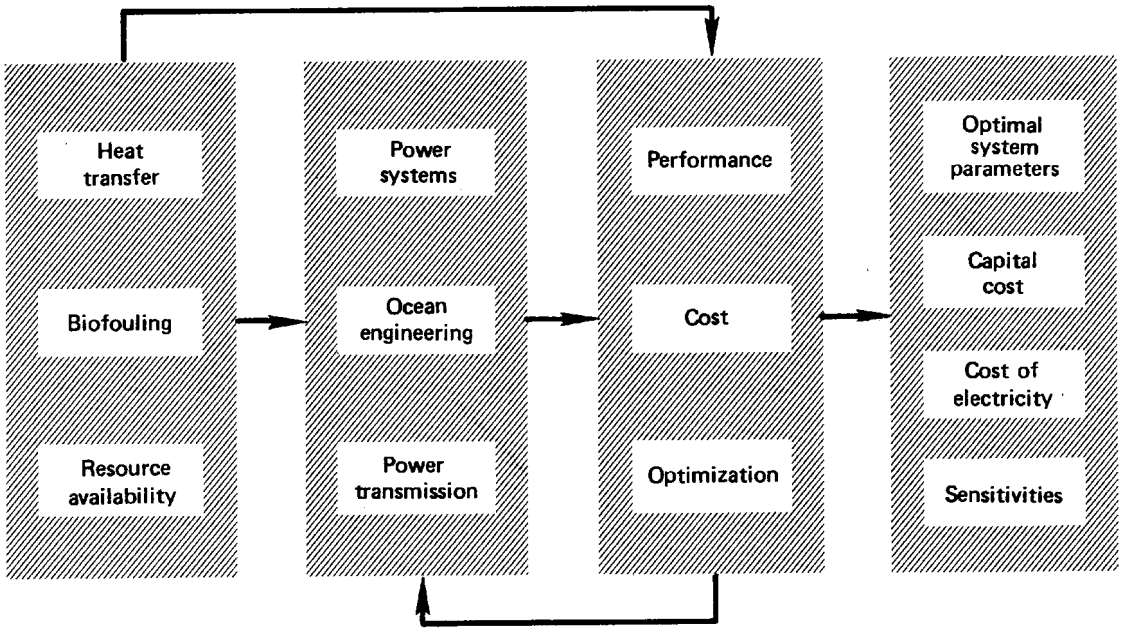

Fig. 3—OTEC engineering performance and cost model

II. ENGINEERING ANALYSES

A closed-cycle OTEC system for the generation of electric power, to be delivered ashore by submarine cable, consists of three major components: the power system, the ocean system, and the transmission system. These are illustrated schematically in Fig. 4.

The power system includes all the modules housed on the platform responsible for the conversion of the thermal energy to electricity ready for transmission. The heart of the power system is the heat exchanger where energy from the warm surface water is transferred to the working fluid--the evaporator--and where after expanding and performing work through the vapor turbine, the same working fluid rejects its unusable sensible heat to the cold bottom water--the condenser. The heat exchanger (evaporators and condensers) provides the interface between the two media: seawater and the working fluid, e.g., ammonia. Other major components in the power system may be conveniently grouped

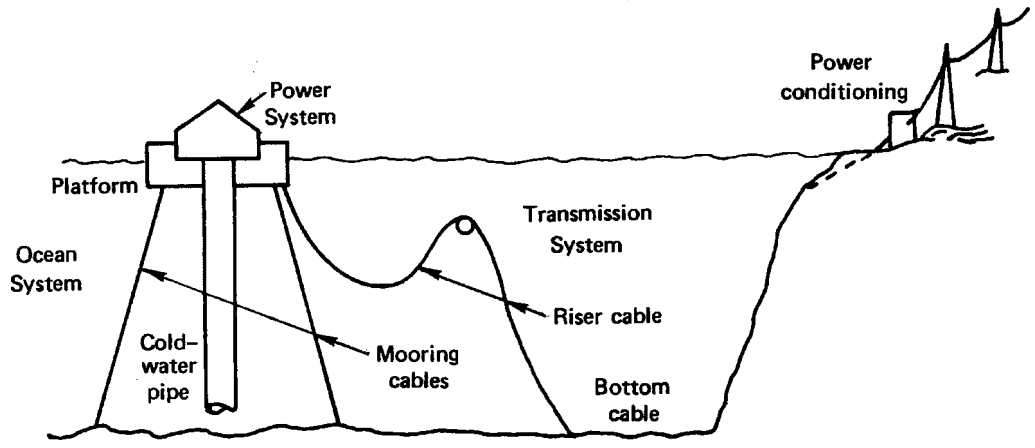

Fig. 4—OTEC system

according to the associated medium. For example, in the seawater circuit, there are pumps to circulate the warm water taken from the ocean surface and the cold water drawn up from the ocean bottom. The need to control biofouling to maintain an acceptable level of thermal resistance to heat transfer calls for chemical (e.g., chlorination) and/or mechanical cleaning installations. In the ammonia loop, there are the turbines and the feed and recirculating pumps. The electrical circuit consists of the generators, motors to drive the pumps and other electrical auxiliaries, instrumentation and control, and start-up/stand-by power source.

The ocean system provides for the seaworthy operation of the power system and access to the cold water. It consists of the platform, the cold-water pipe, the mooring system, and possibly some form of active station-keeping capability. The platform is the structure housing OTEC equipment in the open ocean. To date, five configurations have been suggested: a ship, a submarine, a vertical column (stabilized and semi-submersible), a disk, and an axisymmetric spar.

The purpose of the cold-water pipe is to bring cold water from the deep ocean to provide cooling water for the condensers. The cold-water pipe is one of the largest engineering challenges in OTEC design. Several types and materials have been considered to date, including structures of steel, aluminum, reinforced concrete, fiber-reinforced plastic, and rubberized materials. All these materials raise questions about the size of the structures that can be built and deployed at the depth required. The cold-water pipe problem is best described in terms of its requirement for conveying water from a depth of about 3000 feet to the platform and, secondly, its projected (equivalent) diameter of 60 to well over 100 feet* for plants in the 250 to 400 MW range. The positioning system should be designed to hold the platform in place with a given surface current and winds on the surface at some prescribed sea state and wave heights.

The transmission system includes the riser cable, the bottom cable, and the power conditioning equipment aboard and ashore.

---

*It is conceivable that clusters of pipes of smaller diameters could be used to yield equivalent cross-sectional areas.

The engineering analyses focus on the system parameters, off-design performance, and the engineering uncertainties and technological risks of the total OTEC system. In the following subsections, these issues will be addressed for heat transfer, biofouling, materials and corrosion, thermodynamics, site-specific seasonal variations in available thermal gradient, naval architecture, and submarine cable technologies.

HEAT TRANSFER

The heat exchangers in the currently contemplated closed-cycle OTEC systems represent an important component of the system cost. Each of the OTEC heat exchangers (evaporator and condenser) must transfer about 40 MWt for each MWe generated by the plant. Because of this large factor and because of the relatively low temperature differences (typically less than 10°F), the heat transfer area requirements are very large--on the order of an acre per MWe.

Different designs have been proposed for the OTEC heat exchangers. Some are of the shell-and-tube type with the warm or cold seawater inside the tubes and the evaporating or condensing ammonia on the shell side. In some cases, the tubes are oriented horizontally, and in others, vertically. Plate-type exchangers are also being considered. Although our discussion is devoted primarily to the shell-and-tube types of evaporator and condenser, many of the general observations on the heat transfer and pressure drop problems apply to both types of heat exchangers and their differences will be discussed.

Because of the large size and cost of the OTEC shell-and-tube heat exchangers, considerable program effort has been devoted to heat transfer enhancement--particularly on the ammonia side of the exchangers. By the use of porous surfaces and fluted tubes, the evaporation and condensation heat transfer coefficients can be increased by factors on the order of three to five. The ammonia-side coefficients are then large enough so that the water side is controlling. The advisability of water-side enhancement depends on the relative increases of heat transfer and pressure drop, the additional cost of the enhanced surface, and the effect of biofouling on the enhanced surface.

The effects of various parameters on the heat exchanger performance may be judged graphically by the method developed in Appendix A. For example, biofouling on the water side will reduce the overall heat transfer coefficient, U, with a resulting decrease in heat transferred unless the water flow rate is increased. The amount of this increase depends on the value of the parameter $UA/\dot{m}c_p$ for the original design point, where A is the heat transfer area, $\dot{m}$ is the mass flow rate of water, and c_p is the specific heat. This is illustrated in Fig. 5, which shows the design line for a given heat quantity per unit temperature difference ($q/\Delta T$) and two possible design points. A change in U due to biofouling will require different amounts of increase in water flow rate for the two cases. To maintain the desired quantity of heat transferred, the larger design value of $UA/\dot{m}c_p$ is preferable because biofouling can be countered with a smaller increase in water flow rate.

The same type of diagram may be used to visualize the effects of change in the available temperature difference due to, say, seasonal

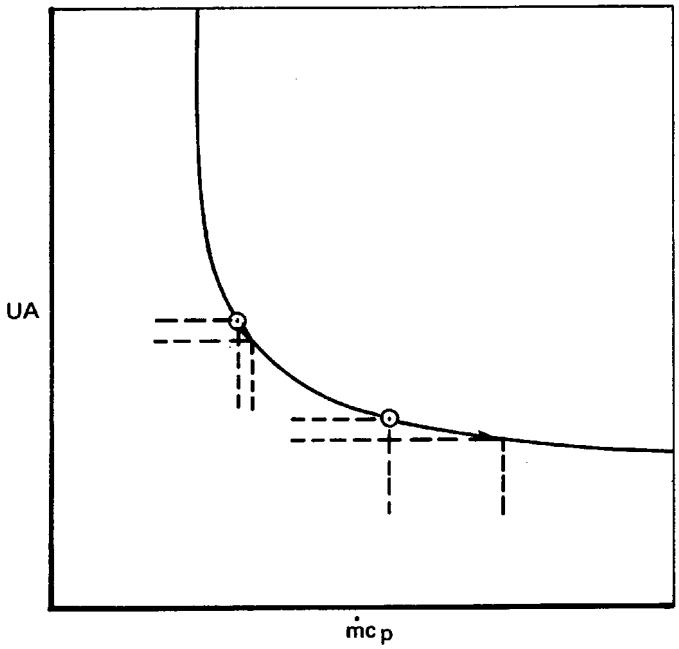

Fig. 5—Effect of fouling of heat transfer surface. U decreases and $\dot{m}$ must increase if the specified heat quantity is to be maintained

variations. In Fig. 6 are shown two points on Line I; Line II is a new design line corresponding to the maintenance of the heat quantity with a decreased temperature difference. Here again, the original design point with a large value of $UA/\dot{m}c_p$ is advantageous because a smaller increase in water flow rate is required to counter the effect of the decreased temperature difference.

The same type of diagram can be used to evaluate the effects of heat transfer enhancement and the resulting design changes that are possible. Figure 7 illustrates some examples of the trade-offs between heat transfer area and water flow rate with enhancement. Two unenhanced design points are shown on the design line for a specified $q/\Delta T$. With enhanced heat transfer, the overall heat transfer coefficient will increase and several possible design options are available. The heat transfer area can be correspondingly decreased and the design point will remain fixed with an unchanged water flow rate. Or, a lesser decrease in area can be accompanied by an increased flow rate, thus sliding the design point downward on the design line. Ultimately, such design choices must depend on the relative costs of heat transfer area, pumping power, and biofouling problems. Also, the details of the heat exchanger geometry must be accounted for. These interactions are developed in more detail in Appendix B.

WATER-SIDE ENHANCEMENT POSSIBILITIES

The size, cost, and complexity of the OTEC heat exchangers require that any mechanism that increases the heat transfer "efficiency" (e.g., special surfaces or geometry) be explored. Although there has been considerable effort devoted to enhancement of the ammonia-side condensation and evaporation, little attention has been given to enhancement of the water-side heat transfer. Some designs (e.g., the TRW/Carnegie-Mellon fluted tube and the Lockheed/Alfa-Laval corrugated plate) provide an area increase with perhaps some increased heat transfer resulting from attendant turbulence. Various types of surface roughness have not been explored extensively--apparently for two reasons: (1) concern that such a surface would complicate biofouling control and make cleaning difficult and (2) belief that the pressure drop would be increased more than the heat transfer.

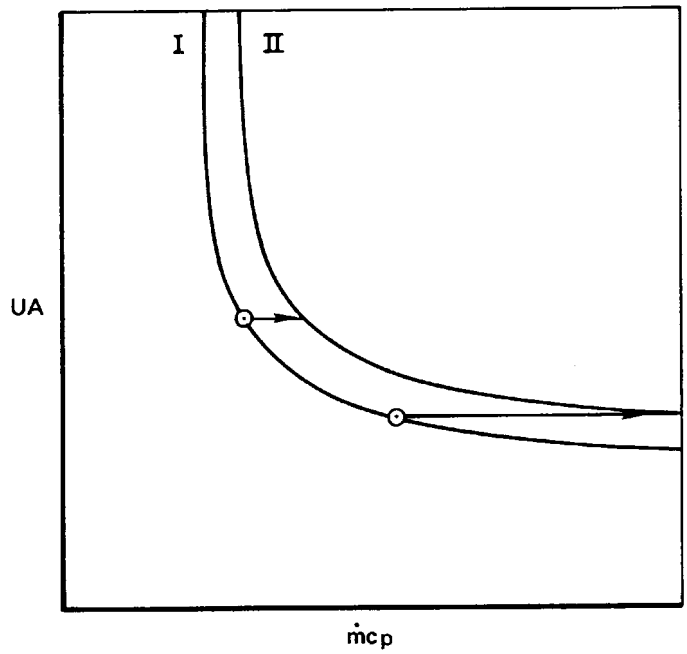

Fig. 6—Effect of a decrease in the available ΔT. ΔT_{in} decreases and $q/\Delta T_{in}$ must be increased by an increase in $\dot{m}$ if the specified heat quantity is to be maintained

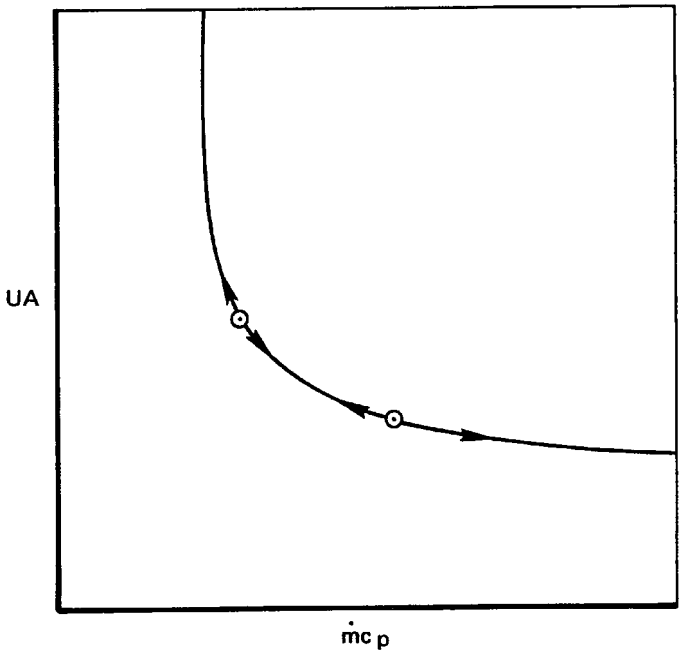

Fig. 7—Effect of heat transfer enhancement. U increases, allowing a corresponding decrease in A, or a lesser decrease in A combined with a decrease in $\dot{m}$, or a greater decrease in A combined with an increase in $\dot{m}$

As will be shown below, the optimum size of roughness elements appears to be large compared with the microfouling film of concern to OTEC and yet small enough so as not to interfere with cleaning. The belief that such surfaces would increase the pressure drop more than the heat transfer apparently was based on experimental studies using air (see, e.g., Bergles and Jensen, 1977); as will be described below, the higher Prandtl number of water allows the heat transfer to be increased just as much as (and perhaps more than) the pressure drop.

Smooth-Surface Convective Heat Transfer

The transfer of heat at a smooth surface in turbulent flow can be related to the fluid properties and to the momentum transfer. This and similar relations (Schlichting, 1968) are the result of analytical and numerical studies which rely on empirical information. The temperature distributions in the viscous sublayer and in the turbulent outer flow are related to the velocity distribution and consequently to the skin friction. The Prandtl number of the fluid determines the relationship between the temperature and velocity distributions and consequently the relative resistances to heat transfer of the viscous sublayer and the turbulent outer flow. As the Prandtl number increases, the resistance of the viscous sublayer increases and begins to dominate. The flow structure and the distributions of velocity and temperature are illustrated schematically in Fig. 8. Note the effect of the Prandtl number on the temperature distribution. It is important in understanding the effects of surface roughness on the heat transfer process.

Rough-Surface Effects

The effects of surface roughness on turbulent velocity friction were established by the classic works of Nikuradse (1932), who used various sizes of sand-grain roughness on a tube wall. Similar classic work for the effects of a sand-grain roughness on heat transfer was done by Dipprey and Sabersky (1963); their work began to establish the effects of Prandtl number for rib-type roughness. Qualitative representation of the results of these works for the skin friction coefficient, C_F, and the heat transfer coefficient, C_H, is shown in

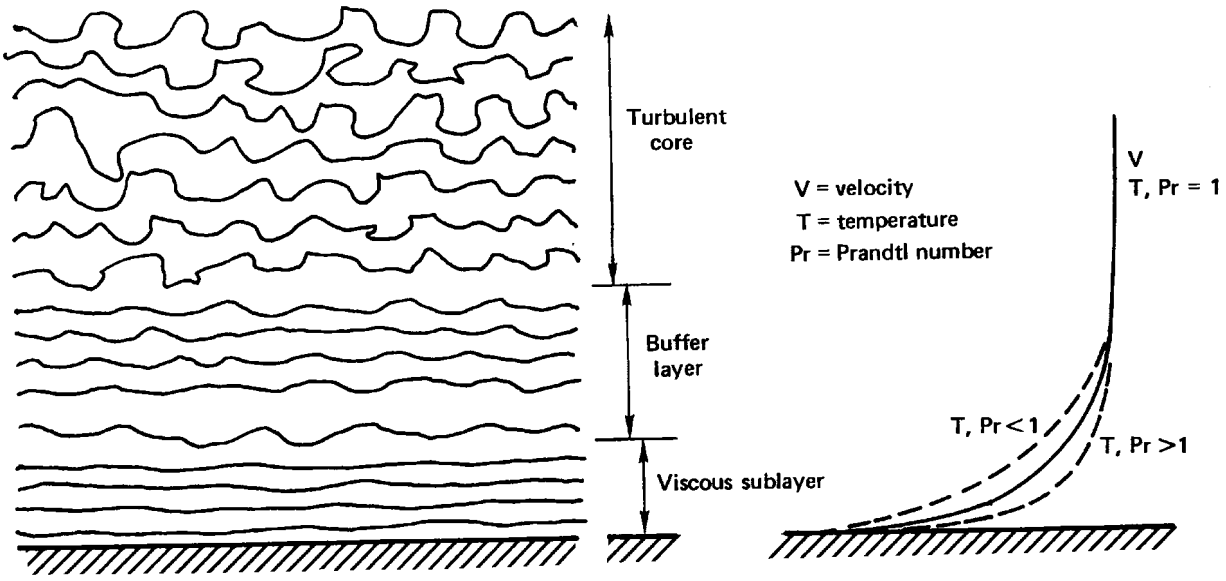

Fig. 8—Schematic representation of turbulent flow structure, velocity, distribution, and the effects of Prandtl number on temperature distribution

Fig. 9 for fluid with a Prandtl number of five--comparable to that of water at about 80°F. The lower dashed lines in this figure are the smooth-surface values, and the solid lines illustrate the increases due to surface roughness. At low Reynolds numbers, the roughness has no effect on the skin friction; in this region, the roughness elements are still buried in the viscous sublayer. As the Reynolds number increases, the viscous sublayer becomes thinner; when the tops of the roughness elements begin to emerge from this layer, the skin friction begins to increase. As this layer continues to thin with increasing Reynolds number, the skin friction continues to increase through this transition region as the roughness element emerges from the viscous sublayer. At high Reynolds numbers, when the roughness is primarily in the turbulent region (and the concept of a viscous sublayer is really no longer valid), the skin friction maintains a constant value whose level is dependent only on the ratio of roughness height to passage diameter.

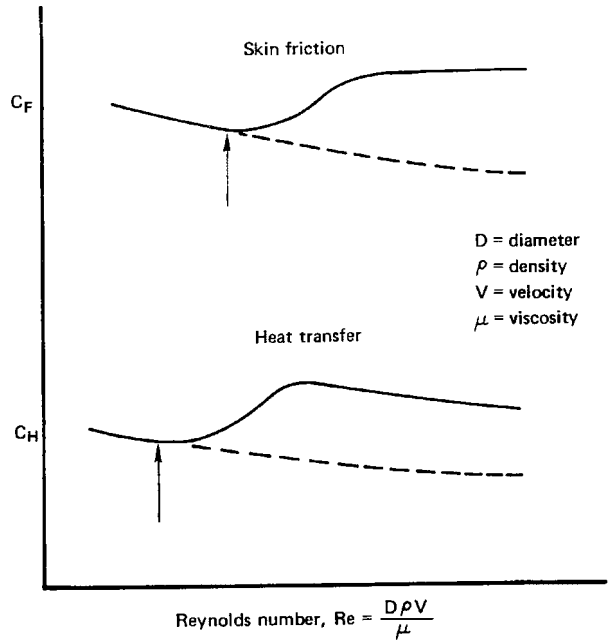

Fig. 9—Schematic representation of the effects of a sand-grain type of roughness on skin friction and heat transfer for a fluid with a Prandtl number of five

In the case of fluids with a Prandtl number greater than unity, the dimensionless heat transfer coefficient begins to rise at a Reynolds number somewhat below that where the skin friction begins to increase (because, for Prandtl numbers greater than unity, disturbances in the viscous sublayer affect the temperature distribution without any appreciable effect on the skin friction). Further increases in Reynolds number through the "transition" region cause the heat transfer coefficient to increase. At higher Reynolds numbers, the heat transfer coefficient decreases slowly with increasing Reynolds number and appears to be independent of roughness height.

For Prandtl numbers somewhat greater than unity (e.g., values of 5 to 12--comparable to the range for water in the OTEC heat exchangers), it is possible in this "transition" range to effect an increase in heat transfer greater than the increase in skin friction.

Optimum Heat Transfer Enhancement

Based on presently available analytical and experimental studies of roughness effects, it is possible only to specify approximately the type and size of elements that would provide optimum enhancement for the OTEC condenser and evaporator. The work of Dipprey and Sabersky (1963) and of Webb et al. (1971, 1972, 1978) suggests that a dimensionless number* in the range of 10 to 30 provides the greatest increase in heat transfer for a given increase in skin friction. For the transverse ribs studied by Webb et al., the heat transfer increase can exceed the skin friction increase for Prandtl numbers above 10. Ribs spaced about 10 rib heights apart appeared to be optimum. Han et al. (1978) recently found that ribs oriented at an angle of about 45 deg to the flow direction are somewhat more effective than transverse ribs. The sand-grain type of roughness used by Dipprey and Sabersky appeared to be more effective than the ribs and produce a heat transfer increase exceeding the skin friction increase for Prandtl numbers above about three. The data and analyses of these investigators as well as the studies of Owen and Thomson (1963), Pilipenko (1977), Dawson and Trass (1972), and Slianciauskas and Drizius (1977) allow an approximate evaluation of the relative effects of rib and sand-grain roughness on the increase in heat transfer compared with the increase in skin friction. Figure 10 illustrates such an approximate variation and it is apparent that, for Prandtl numbers in the range of interest, the heat transfer can be increased more than the skin friction. Note that C_{H_s} and C_{F_s} are smooth-wall reference values.

Although the ratio C_H/C_F, as plotted in Fig. 10, is frequently used as an "efficiency" or figure of merit for heat transfer enhancement, approximate analyses of heat exchanger performance (Webb and Eckert, 1972), of gas-cooled nuclear reactor heat transfer (Melese-d'Hospital, 1973; Gazley et al., 1977), and of OTEC heat transfer (Zener, 1973) indicate that a more appropriate performance

*This is defined as $(eRe\sqrt{C_F/2})/D$, where e is the roughness height, Re is the Reynolds number, C_F is the skin friction coefficient, and D is the tube diameter.

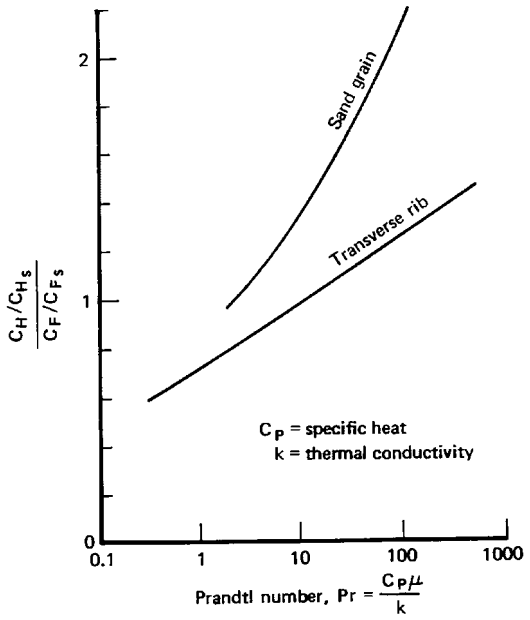

Fig. 10—Approximate variation of heat transfer increase in ratio to skin-friction increase for rib and sand-grain roughness

index is $C_H^{3/2}(C_F)^{-1/2}$. This parameter puts much greater emphasis on the increase of heat transfer than on the increase of skin friction. These approximate analyses indicate that for a given quantity of heat transferred, the required area is inversely proportional to this performance index. As Fig. 10 shows, the heat transfer increase can be greater than the skin friction increase and thus a reduced area would be possible. Preliminary analysis indicated a positive contribution to system performance.

The following tentative remarks on optimizing water-side enhancement in the OTEC heat exchangers are based on the above discussion: (1) three-dimensional roughness appears to be more effective than two-dimensional; (2) sand-grain roughness may be too closely packed and a more widely spaced three-dimensional roughness would be preferable, and (3) a desirable roughness height appears to be on the order of about 0.005 in. Applying the most effective spacing deduced by Webb et al. (1971) for the transverse ribs to a three-dimensional element,

a spacing of about 0.5 in. is obtained. For the plate heat exchangers, the figures are comparable.

Both analytical and experimental work is needed to evaluate more quantitatively the benefits of rough-surface enhancement of heat transfer for a closed-cycle OTEC system and to choose the size and type of roughness for optimum performance. The available theoretical and experimental studies of roughness effects need to be analyzed with particular emphasis on the effects of three dimensionality and of Prandtl number. Although it is now clear that more basic experimental work is needed to delineate these effects, such analytic studies should permit the design of specific experiments to provide the necessary information for OTEC application. At the same time, systems studies of the OTEC power system should be made to determine the range of optimum enhancement. These analytic and systems studies should reveal the experimental parameters to be investigated. The experiments should be designed with three objectives:

1. To determine the heat transfer and skin friction increases of various sizes and shapes of three-dimensional roughness elements over the range of Reynolds numbers of interest for OTEC heat exchangers.
2. To determine the effects of Prandtl number on the heat transfer characteristics of these roughness elements.
3. To determine the susceptibility of these roughness elements to biofouling and the applicability of various cleaning methods.

Preliminary research should also begin on manufacturing techniques and costs of this type of enhanced surface and on concomitant requirements for biofouling countermeasures.

BIOFOULING

Since the inception of the OTEC program, the importance of biofouling, corrosion, and materials in establishing the feasibility, costs, and performance of the OTEC system has been recognized. At

this stage in the program, it appears that satisfactory materials options are available which involve minimal technological risk (Kinelski, 1979a, b). The biofouling question is less clear. It does not seem that biofouling will render the OTEC program infeasible. Rather, it appears that not enough is known about biofouling rates, prevention, and countermeasures in the OTEC environment to design and cost an optimal power system with a thirty-year performance life. A prudent present course is to assume that continuous water treatment, using chlorination or its equivalent, for both evaporator and condenser systems will be required, and that an intermittent mechanical or chemical system will also be necessary to clean the heat exchangers. The completion and use of the OTEC Seacoast Test Facility at Keahole Point in the Hawaiian Islands; early results from OTEC 1 on the effectiveness of the Amertap Ball System and chlorination; continued longer term microfouling experiments; cold seawater quality and fouling data from OTEC 1, mini-OTEC, Keahole Point, and the Gulf of Mexico; and early field data on the Alfa-Laval plate heat exchangers used in mini-OTEC should shortly provide valuable field data for a more refined design analysis.

Our approach to assess the effects of biofouling is to review the highlights of that which is known, and to raise questions about that which is not. Unless there are major advances in biochemistry and microbiology, we can expect no biological "fix" or coating that will prevent or combat fouling, require little maintenance, and have negligible adverse effects on performance or the environment. Rather, we expect that the ultimate OTEC biofouling system will be a specifically engineered amalgram of methods that are currently available--biocides, brushes, rubber balls, strainers, screens, acoustics, ultraviolet light, etc.

Biofouling is ubiquitous in marine and aquatic environments. However, the familiar types of macrofouling--visible organisms and deposits such as algae, mussels, barnacles, shellfish, and seaweed--are less important than microfouling from the viewpoint of OTEC performance. This is because microfouling films are measured in micra and constitute an early stage in the development of macrofouling; the OTEC heat exchangers would operate at considerably reduced levels

even prior to the accumulation of visible macrofouling layers. Thus microfouling is of considerable importance for OTEC power systems. Macrofouling of the more conventional type would be important in the design and performance of screens, pumps, hull, cold-water pipe, warm-water pipe, etc. However, the impact on heat exchanger performance is the central biofouling problem for OTEC systems.

Only preliminary data are now available for engineers to design heat transfer surfaces which will remain suitably clean over long periods of time in seawater, and to evaluate the effectiveness of potential methods for fouling prevention and removal. Customary marine and coastal heat exchanger practice accepts fouling factors considerably greater than those appropriate to OTEC.

The many years of field experience in biofouling control for coastal power plants is not directly applicable to OTEC because of its more stringent requirements. Coastal and estuarine waters, however, are generally richer in both nutrients and organisms than expected OTEC sites. Thus the rate of fouling formation would be less for OTEC than for traditional coastal power plants. Another factor, discussed below, is the greater effect of fouling on high performance heat exchangers than on less efficient designs.

The Seacoast Test Facility for fouling studies should expedite the development of fouling countermeasures and cleaning techniques.

The Qualitative Biology Of Biofilm Development

Marine biologists have described several stages in the development of fouling layers on smooth, noncorroding surfaces. The situation becomes considerably more complex, and less well described, when fouling layers and surface corrosion layers interact, as in the case of aluminum. The stages of fouling film development are (Mitchell, 1977; Corpe, 1977).

1. *Conditioning.* When a clean surface is placed in the sea, a polymeric conditioning film is quickly formed via chemical absorption. The reactions are fast, and depend on local environmental factors. The measurements of DePalma et al. (1979) infer that a glyco-protein layer forms within hours. Naturally occurring macromolecules are

absorbed and denatured, the extent depending on the surface chemistry of the substrate. These surface-attached macromolecules provide nutrients for pioneer bacteria. DePalma's preliminary work suggests that the surface energies of test materials change substantially within 24 hours of exposure to flowing warm seawater, and only slightly thereafter. Attempts to modify the electro-negativity and wettability of surfaces to prevent the formation of this fouling film are not yet sufficiently promising for OTEC use.

2. *Colonization by pioneer bacteria.* Fast growing bacterial species are attracted or otherwise attached to conditioned surfaces. Chemotaxis of motile bacteria as well as random collisions may play a role in this process. Some chemicals have been shown to impede slime formation by repelling motile bacteria. Chet et al. (1976) have shown that tannic acid, benzoic acid, and acrylamide have powerful repellent effects on bacteria. However, paints or other coatings on surfaces must be renewed, and may retard heat transfer. Thus, this approach to biofilm prevention is not promising for OTEC. Pioneer bacteria are first loosely sorbed to a surface, but after a short time (see Fig. 11), macromolecular fibrils that provide a permanent bond are extended. The bacterial glycocalyx (Costerton et al., 1978) provides the strong bond between cell and surface. Within hours, these pioneer rod-shaped bacteria (pseudomonas, flavobacteria, and others) are well established and may produce extracellular polymeric slime. This mixture of exudative polysaccharides and bacteria (see Fig. 12) forms the primary biofilm covering the surface, and is probably responsible for the initial insulating properties of the film.

3. *Secondary colonization.* Once the primary biofilm is established, other bacteria, microalgae, diatoms, and protozoa may develop extensively. The primary film facilitates adhesion of the secondary bacteria. The resulting mixture of trapped detritus, polymers, and organic matter also provides nutrients for attached bacteria.

4. *Accumulative equilibrium.* As the film becomes thicker, an equilibrium develops among growth, entrainments, and sloughing by surface fluid shear forces. Portions of the thickened film may peel away. Sloughing is due to both steady reentrainment of the film by

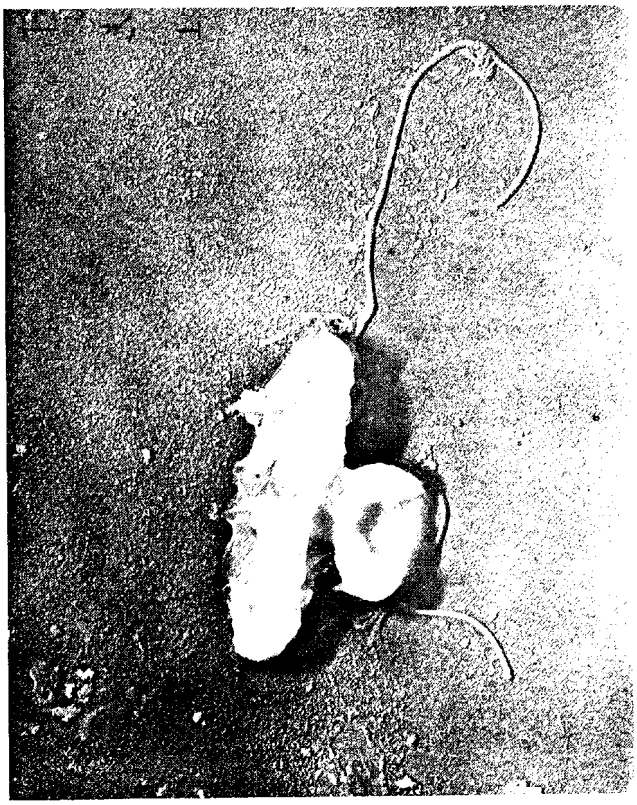

Fig. 11 — A bacterium extruding macromolecular fibrils as it attaches permanently to a marine surface (Mitchell, 1977)

the flowing seawater and a random massive removal of biofilm that is perhaps associated with oxygen and nutrient depletion deep within the film.

Hydraulic and heat transfer considerations suggest that thin biofilms, with irregularities that protrude through the viscous sublayer, are equivalent to surface roughness and waviness in their effect on friction and heat transfer. However, the net impact on heat transfer is largely due to the insulating properties of the polymeric layer, since the thermal conductivity of the biofilm is close to that of water. There is general agreement that biofilm layers after the early stages are dominated by the polymeric exudate released by bacteria. It appears (from early field data) that total organic carbon correlates

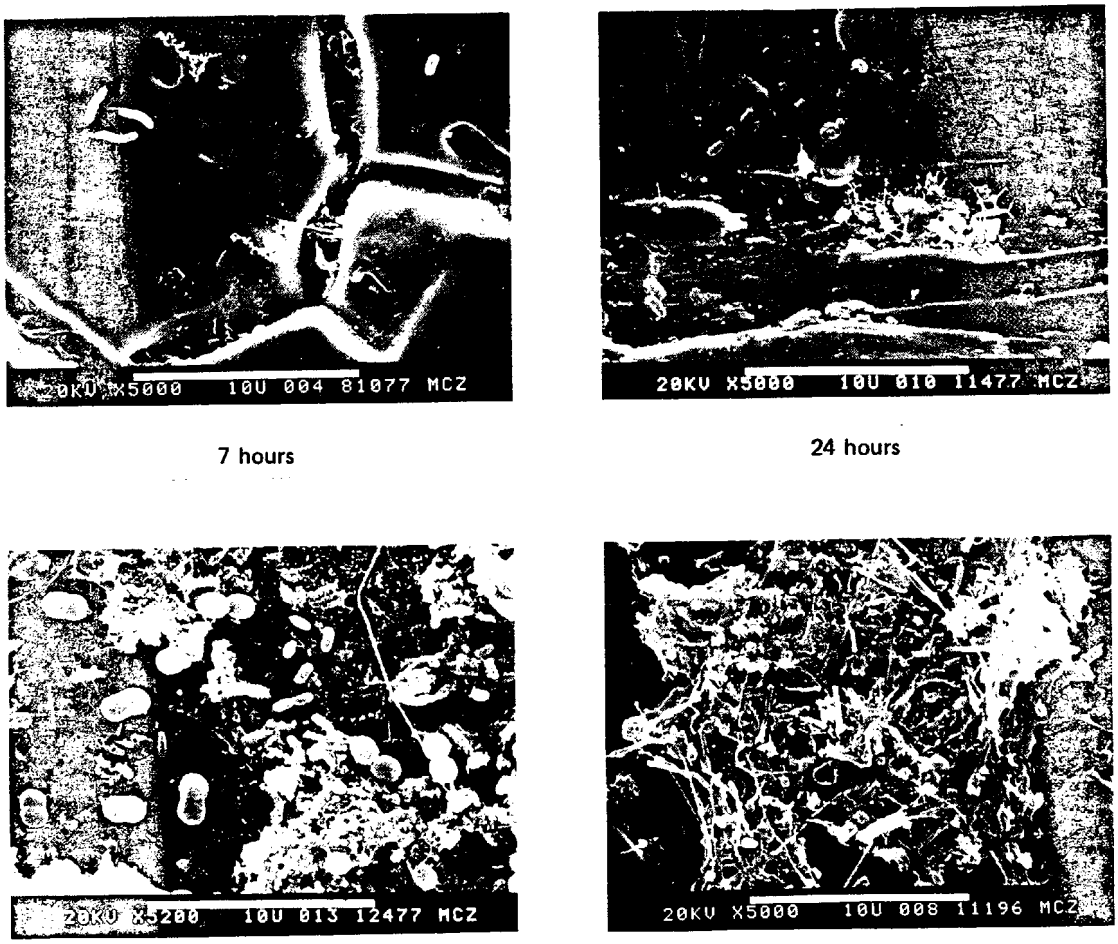

Fig. 12 — Scanning electron micrographs showing development of marine biofilms (Mitchell, 1977)

well with measured film thickness, whereas adenosine triphosphate (ATP) shows poorer correlation. Since ATP is associated with cellular metabolism, this supports the notion that bacterial debris and exudated polysaccharides rather than dividing bacteria are largely responsible for the insulating properties of the biofilm.

As part of the OTEC program, a comprehensive biological study of the properties of warm-water fouling films in the Gulf of Mexico and Hawaii have been undertaken (Berger, 1979).

ATP, organic carbon and iron, protein, inorganic iron and other elements, bacterial biomass, and surface polymers have been assayed. Physical examination of the surface by optical and scanning electron microscopy and x-ray fluorescence has also been performed for a number of engineering materials.

Biological measurements have not yielded data (except perhaps for total organic carbon) that are easily related to parameters of engineering interest. However, the data are preliminary and further biochemical assaying is required to establish the relative importance of micro-organisims and polymer in determining fouling resistence.

Biofouling Effects on Heat Transfer and Hydrodynamics

Although marine biologists can describe the qualitative structure of fouling films and the importance of the conditioning film, it is the engineering aspects that are most germane to OTEC systems design. Only one non-OTEC research study on the interaction between pipe flow hydrodynamics and heat transfer and biofilms has been found. Professor W. Characklis and his students at Rice University (Characklis, 1973; Bryers, 1979) have been studying the fouling of power plant condensers, using a small laboratory tube reactor and water artifically enriched with nutrients, glucose, and synthetic growth media. They found that δ, the biofilm thickness, can be described by a logistic equation:

$$\frac{d\delta}{dt} = k\delta \left[1 - \frac{\delta}{\delta_{MAX}}\right]$$

where k is the rate of fouling film development and δ_{MAX} is the asymptotic or equilibrium film thickness.

Both δ_{MAX} and k decrease with increasing flow velocity and increase with increasing nutrient levels. Measurements of primary biofilm formation also indicate that the rate of initial biofilm development increases with increasing velocity, organism growth rate, and dispersed biomass concentration. Since some measurements were performed with extremely rich biomass concentrations, biofilm thickness sometimes reached 500 μ and pressure drops increased three-fold

after only 80 hours of operation in these experiments. The experiments also confirmed that biofilm peaks must penetrate through the viscous sublayer for the friction factor to increase substantially over the smooth wall value, and that an equivalent sand-roughness could be defined for each biofilm thickness. Because of water-like insulating properties of the biofilm, the increase in friction factor was accompanied by an increase in heat transfer resistance, after a brief initial period during which the increase in mixing and convective heat transfer dominated the increase in film conductive resistance. Chlorination experiments were also performed in Characklis' laboratory, but the data were not yet precise enough to estimate biofilm destruction rates. However, the extracellular polymeric matrix appeared to have been sufficiently weakened by chlorination to permit later removal by fluid shear. Ominously, a residual deposit of microbial cells and associated organic material which was associated with highly filamentous biofilms remained, even after extremely severe chemical treatment. This deposit apparently enhances later regrowth of the biofilm.

Fouling Resistance

The conventional parameter for quantifying biofouling effects on heat exchanger performance is through r_F, the fouling resistance, defined as the additional thermal resistance due to the presence of a fouling film. For both tube-and-shell and plate-and-shell heat exchangers, total heat transfer is $Q = UA\Delta T_{LM}$, where A is the heat transfer area, U is the overall heat transfer coefficient, and ΔT_{LM} is the log mean temperature difference. It can be shown* that the heat exchanger is more sensitive to r_F at large values of U_o, and enhanced OTEC heat exchangers may suffer greater reductions than do conventional unenhanced systems. This is illustrated in Fig. 13 where two different, but representative, heat exchangers are considered. In this illustration, the percentage of performance is defined as Q/Q_o. The case $U_o \sim 650$ BTU/hr-ft^2-°F is representative of values that are predicted for tube-and-shell exchangers with ammonia-side

*See Appendix D.

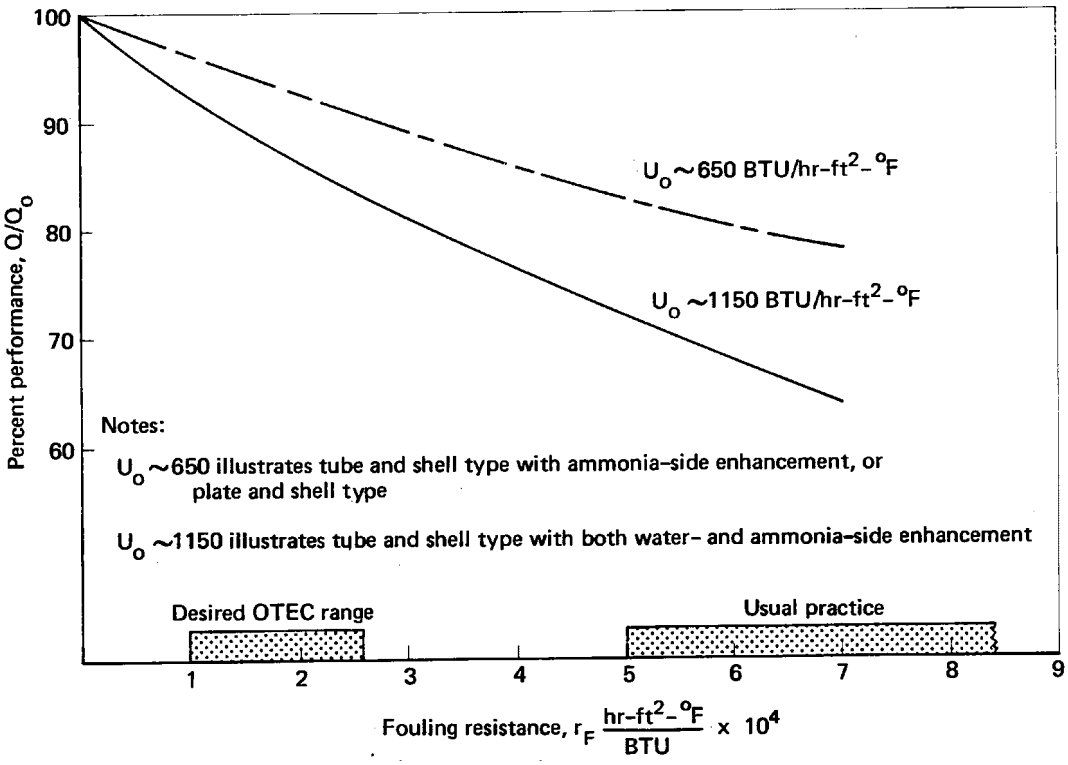

Fig. 13 — Heat exchanger performance vs fouling resistance

enhancement and also for plate heat exchangers of the Lockheed/Alfa-Laval type. The case $U_o \sim 1150$ corresponds to heat exchangers where both ammonia- and water-side enhancement is employed. Note that an r_F of 2×10^{-4} hr-ft^2-°F/BTU degrades performance by 7 percent when $U_o \sim 650$, and 13 percent when $U_o \sim 1150$. The usual practice in marine and coastal power plant heat exchangers is to maintain r_F in the range $0.0005 \sim 0.001$. The desired range for OTEC performance is in the low range $r_F \sim 0.0001$ to 0.0005, with a mean of 0.00025. Figure 13 also illustrates, in a qualitative way, the impact on heat exchanger performance when cleaning and biofouling countermeasures are unable to maintain target r_F values.

Field Measurements of r_F

Laboratory measurements are useful for understanding the mechanisms of biofilm growth, hydrodynamic effects, and heat transfer phenomena, but field measurements of fouling resistance, r_F, are clearly required for quantitative design estimates. Fortunately, the original National Science Foundation OTEC project supported the development of a precise heat transfer instrument for measurement of r_F in a pipe flow. This instrument, developed by F. G. Fetkovich (1978, 1979) of Carnegie Mellon University and modified by Argonne Laboratory for field use, has become an integral part of the OTEC biofouling program. It measures the heat transfer film coefficient between flowing seawater and tube surface with sufficient accuracy to permit accurate serial estimation of fouling resistance. Preliminary field data have been obtained under a number of different conditions and encourage speculation that a carefully instrumented and monitored test program at the Keahole Point Seacoast Test Facility will minimize the need for extensive and difficult field measurements in the open ocean. The accuracy of the instrument, in experienced hands and in benign environments, is limited by the accuracy of flow velocity measurement. (Some of the early data were obtained under adverse conditions, both from the viewpoint of poorly trained operating personnel and unstable environmental conditions.)

The work of Fetkovich has, however, been exemplary. Figure 14, taken from his early work, shows the time course of r_F, measured on a barge off the Virgin Islands. Notice that r_F appears to increase faster at low velocities. Figure 15 is a collection of r_F data taken off the Kona Coast. There appears to be little dependence here on pipe material or flow rate. Figure 16 is a schematic of the "good" data. Above a certain value of r_F (corresponding to $\sim$ 20 μ), there is a linear growth of r_F with time. The initiation period and characteristics may vary with location, tube material, water quality, season, etc., but once the linear behavior is observed, the slope dr_F/dt appears to be invariant, with a value equivalent to an increase of 0.0001 every ten days. Fetkovich has proposed a model of this process, and fits the data with the relation $\delta_{FILM} \sim 20\mu(1 + t/T_2)$,

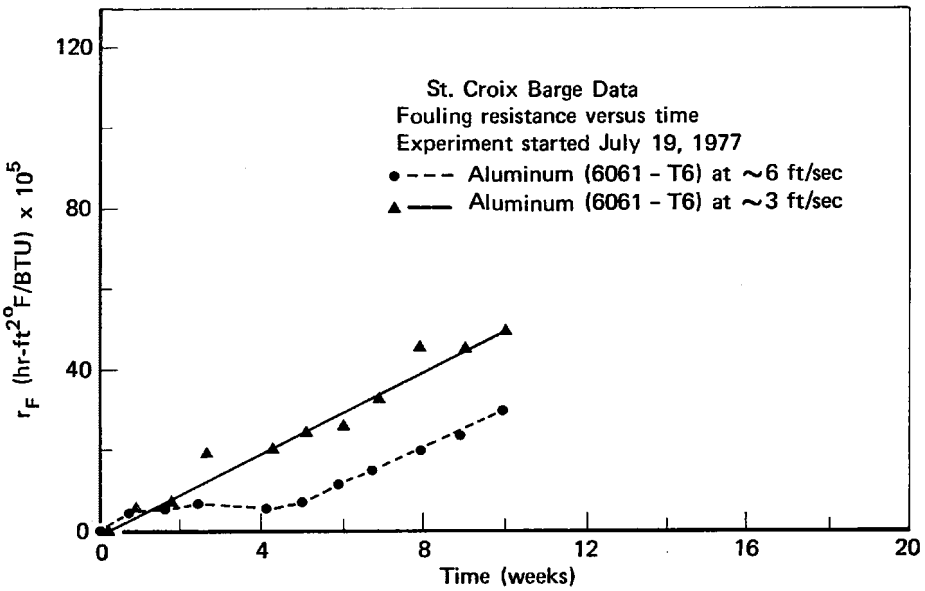

Fig. 14 — Fouling resistance (r_F) vs. time for St. Croix experiments (From Fetkovich, 1978)

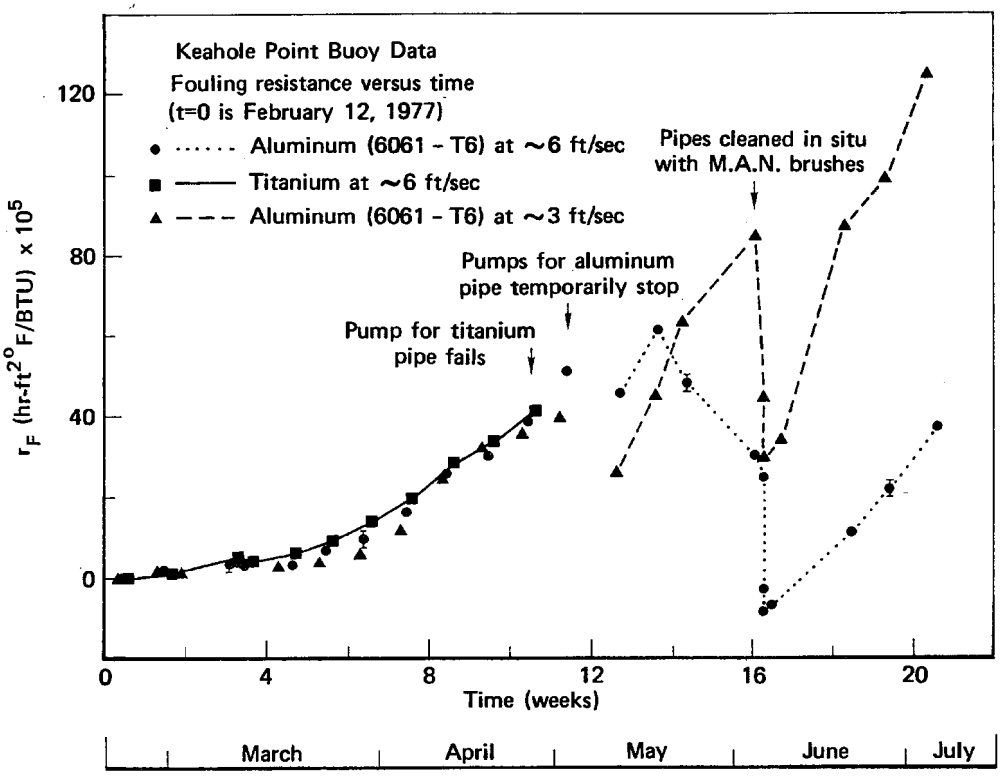

Fig. 15 — Fouling resistance (r_F) vs. time for Buoy Series I experiments at Keahole Point (From Fetkovich, 1978)

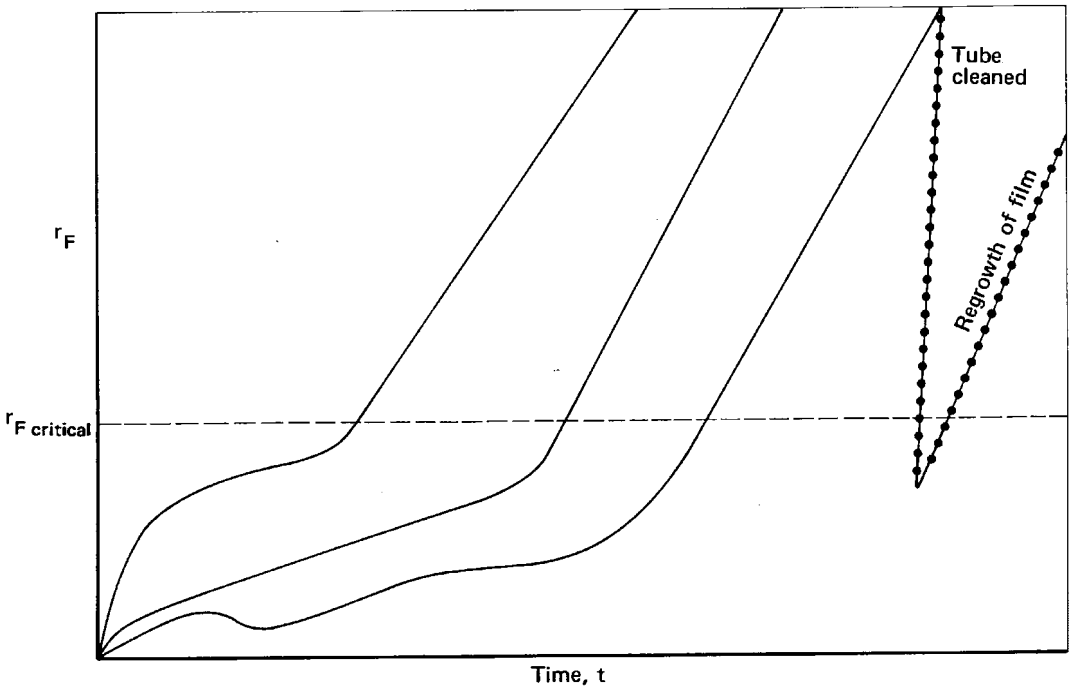

Fig. 16 — "Idealized" r_F development

where t is exposure time and T_2 is the generation time for the bacteria at the top of the film.

Data are available after only short periods of exposure and limited attempts at cleaning. Early work does indicate (see Fig. 15) that mechanical cleaning with a M.A.N. brush* can decrease r_F values to OTEC levels, but biofilm regrowth after mechanical cleaning bypasses the slower conditioning and initiation phases. Thus, cleaning each heat exchanger tube about once a week appears to be a satisfactory preliminary schedule. Recent studies (Liebert et al., 1979) indicate that copper-nickel tubes exhibit slower rates of increase in r_F than do stainless steel, titanium, or aluminum. This is consistent with the known cell-killing effect of copper. For copper, the increase in r_F seems to be related to a corrosion film rather than to microfouling. It is encouraging to see that Fetkovich's and

*The M.A.N. brush is part of a commercially available tube-cleaning system which is used on power plant condensers.

Liebert's studies both confirm that intermittent brushing can reduce r_F to acceptable levels. However, the early data are too fragmentary to properly assess the long-term value of mechanical cleaning and the potential advantage of any particular heat exchanger material for all cleaning modes.

Chlorination

At present, chlorination is the best biocidal treatment for the OTEC power system (Fava, 1977). We outline here several important aspects of chlorine chemistry, nomenclature, dose rates, and production.

Chlorine chemistry in freshwater has been well characterized (White, 1972). The situation in seawater is different because of the presence of the bromine ion, Br-, in concentrations of 65 mg/liter (note that 1 mg/liter = 1 ppm). Since traditional chlorination nomenclature is based on freshwater experience, it is appropriate to review the highlights of chlorine chemistry.

Chlorine gas added to water hydrolyzes quickly to form hypochlorous acid, a weak acid which partly dissociates to form hypochloride and hydrogen ion: At pH values above 3, no measurable molecular chlorine remains. The amount of HOCl and hypochloride ion depend on pH and temperature. At ambient temperature, pH < 8 results in more HOCl than OCl^-, with nearly all HOCl occurring when pH < 6. Since the OCl^- ion is much less effective biocidally than HOCl, it is the quantity of HOCl which is significant in antifouling and germicidal applications. The fraction of HOCl is known as the free available chlorine residual, and its success as a biocide appears to be related to its ability to penetrate cell walls and interfere with cellular enzyme processes. When ammonia is present, a series of chloramines is formed having long-lasting biocidal effects.

In seawater, brominated compounds analogous to chlorinated freshwater compounds are formed. However, analytical methods cannot distinguish between chlorinated and brominated compounds in seawater. Thus the nomenclature of freshwater practice has been carried over to seawater operation. In freshwater systems, free, combined, and total residual chlorine are determined by measuring both free and

total residual chlorine, and the combined residual is obtained by differencing. Free residual chlorine indicates the amount of hypochlorous acid and hypochloride ion, while total residual chlorine measures the amount of oxidizing chlorine present. The same terms are used in seawater, but their chemical significance is moot. Nevertheless, since they refer to residual oxidants in seawater which have analogous biocidal effects to their freshwater counterparts, the nomenclature presents no difficulty. Another important concept is that of chlorine demand. This is the difference between the amount injected and the total residual chlorine at the end of a period of contact. Thus, the chlorine demand of the seawater must be satisfied before residual chlorine appears. The chlorine demand depends on pH, temperature, contact time, chlorine levels, and seawater composition. It has been measured only a few times in the open ocean and coastal waters.

Chlorine demand seems to vary between 0.1 and 5 mg/liter, depending on location, laboratory, and time of contact. Since the demand increases with increasing contact time, and the flow time in heat exchanger tubes is measured in tens of seconds, the chlorine demand may be even less than the quantities cited above. Chlorine demand data at potential OTEC sites are necessary for accurate estimates of chlorination requirements, since seawater samples taken from different sites have demands which vary by an order of magnitude.

When temperatures are below 40°F, power plant chlorination is occasionally not used. Above this temperature, the required residual levels to maintain effective levels of antifouling activity are not known, but residual levels in the range 0.2 to 1 ppm would be expected for the evaporator and even lower levels on the cold-water side.

At the present time, it is only possible to speculate about chlorination doses and schedules to maintain clean heat transfer surfaces, but low dose continuous chlorination supplemented by higher dose shock chlorination appears to be favored on the basis of past experience with macrofouling. Power plant engineers employ continuous chlorination for hardshelled macrofoulers, and intermittent or shock chlorination for softer forms of marine life. As suggested earlier, there is little basis for extrapolation of current practice to the OTEC power systems.

For reasons of safety and cost, on-site production of chlorine by electrolysis of seawater is the most suitable method for large OTEC plants. Several commercial systems are available, with power requirements $\sim$ 2 kWh/kg of Cl_2 generated.

The quantities of chlorine that must be generated, circulated through the heat exchangers, and then discharged into the ocean can be estimated as a function of applied dose. If 0.1 ppm for the condenser and 0.2 ppm for the evaporator are required on a continuous basis, then a 100 MW plant entails the production and discharge of 1000 lb/hr of chlorine. If required effective doses were found to be higher, say 1 ppm for both seawater circuits, then over 5000 lb/hr of chlorine would be generated and then discharged into the ocean. Parasitic power losses for chlorine production are about 2 percent in the low dose example and about 10 percent in the higher dose example.

Environmental Effects of Chlorination

If low levels of chlorine are an effective biofouling countermeasure, then it may be expected that low levels are also toxic to marine organisms. A series of recent studies at Woods Hole (Capuzzo et al., 1976, 1977; Goldman et al., 1978) has demonstrated this toxicity. Larval species that spawn intermittently are seriously damaged. Among zooplankton, it was found that the smallest organisms were most affected, reflecting the inverse relation between size and metabolic rate. The most startling result is that significant decreases in larval respiration rates occur at virtually undetectable chlorine residuals. The adverse effects of chlorine addition are manifest long after the exposure period. These observations were made on marine species indigenous to the New England coastal area; measurements are currently being made on species sampled from OTEC sites, but data are not yet available.

These results and others suggest that the environmental impact of OTEC chlorination may be serious, particularly when the scale of chlorine discharge is considered (24,000 to 100,000 lb/day). Another factor is that chlorine may be even more toxic to marine organisms in a "pristine" ocean environment than in polluted coastal waters where organisms have learned to survive under environmental stress.

The Environmental Protection Agency (EPA) has established a limit of 0.2 ppm free residual chlorine, up to 2 hours a day, in power plant cooling water discharge. No guidelines have been developed for the open or "pristine" ocean, but it is likely that even more stringent limits may be set for OTEC operation. Nevertheless, chlorine demand characteristics at short exposure times may be small enough to permit the use of chlorine at effective dose levels with virtually undetectable residual quantities in the discharge plume.

The Woods Hole toxicity measurements can be used to support either of two environmental restrictions:

a. Chlorination not permitted at all unless followed by dechlorination (which may not be feasible for OTEC) or proof of negligible adverse effect on marine life.

b. Maximum limits imposed on chlorine dosage or residual levels.

A restriction of type b. could permit effective chlorination. However, measurements of Cl_2 demand and minimum doses required for biofouling control would be required first, as well as discussions with EPA and other environmental agencies about the special needs of the OTEC biofouling system. Along these lines, a DOE-EPA working group has been established to develop OTEC-specific chlorination standards.*

Mechanical Cleaning

On the basis of available data, it is realistic to expect that mechanical cleaning will play an important role in maintaining acceptable r_F levels. Ultrasonic methods are intriguing because of their proven laboratory value, but power requirements, cost, and feasibility have yet to be demonstrated for large-scale cleaning of tube-and-shell or plate heat exchangers. Preliminary studies by Pandolfini et al. (1979) are promising, but only when the heat transfer surface receives a sufficient intensity of ultrasonic radiation. Abrasive slurry methods, in which small quantities of mildly abrasive material such as sand or powdered walnut shells are introduced into the flowing seawater, have been suggested for plate-and-shell or enhanced heat exchangers,

*Personal communication from Lloyd Lewis, DOE.

where brushes or balls cannot be used (Mann, 1979). Very little data are available on abrasive slurry effectiveness and erosion as a function of velocity, material, heat exchanger type, etc., but anecdotal experience with heat exchangers in which the cooling water has a high naturally occurring concentration of solids is encouraging. Nevertheless, the use of abrasive slurries cannot yet be seriously proposed because of possibilities for erosion, loss of protective film, and the inevitable accumulation of slurry material within the heat exchanger due to trapping and imperfect flushing.

Thus, designers are led to several familiar and costly alternatives that must be specificially tailored to OTEC:

1. Short-term testing with mechanical M.A.N. brushes suggests that brushes may be capable of maintaining low values of r_F on smooth tube heat exchangers under simulated OTEC conditions. The complete M.A.N. tube cleaning system is a widely used commercial system in which brushes are propelled by water flow and are captured in a cage between cleaning cycles. Unfortunately, flow reversal is required to return the brushes to their original position. This required flow reversal, for an entire 100 MW OTEC heat exchanger system, requires extensive valving and piping and would be difficult to achieve. Reversible pump motors are available and, according to Lockheed, the time required to complete a cleaning cycle has a negligible effect on performance. A system in which flow reversal is required for only a limited number of tubes simultaneously is also under consideration, but requires considerable further development. An accurately indexed tube cleaning machine system has been proposed by TRW. This concept, which involves the mounting of brushes on long rods which are slightly longer than the heat exchanger tubes, an overhead crane, and careful positional indexing, is intended for vertical heat exchangers, but could be compatible with fluted-type enhancement on the seawater side. This concept requires demonstration.

2. The Amertap cleaning system is another widely used commercial tube cleaning system in which slightly oversized rubber balls are circulated continuously through heat exchanger tubes from upstream to downstream side under the pressure of the flowing water. The balls

are then recovered by screens and recycled back to their original distribution point. This system appears to be effective in modern power plant practice but requires considerable modification for OTEC consideration. In addition to serious questions about feasibility, the system is a costly one. This system cannot accommodate water-side enhancement, and the sponge balls, like the mechanical brush system, may carry calcium carbonate from a localized ammonia leak and thus provide nucleii for calcium carbonate scale condensation on the seawater side.

3. A batch approach, or cleaning in place system (CIP), has been proposed for compact plate heat exchangers. This is required because plate heat exchangers are usually dismantled for mechanical cleaning, while tube-and-shell exchangers are usually cleaned intact. It may be expected that chlorination or its equivalent would be required on all OTEC heat exchangers (both plate type and tube-and-shell type), but the manual mechanical cleaning cycle for plate heat exchangers could be extended by an effective CIP system. The proposed CIP system involves a tank for the mixing of cleaning solution, and appropriate pumps, piping, and valving for circulation through the plate heat exchanger. The cleaning solution may consist of detergents or strong alkalies combined with surfactants and settling agents. The cleaning solution would be used to clean a number of plate modules, and then diluted and neutralized prior to storage or discharge. The CIP solution can be retained on-board and reused with additions. The effectiveness of this system remains to be demonstrated.

MATERIALS AND CORROSION

Here we outline a set of materials options which appear to be suitable for OTEC applications. Both titanium and AL-6X stainless steel alloy are well qualified for OTEC heat exchanger use. Their corrosion and erosion resistance are excellent in seawater, and they undergo no serious corrosion or reaction in the presence of ammonia. Copper-nickel heat exchangers are widely used in power plants: the copper has good antifouling characteristics but may react with ammonia

and exhibit stress corrosion cracking unless clad or duplexed with another metal (Mann et al., 1979). Thus copper is not yet a serious contender for OTEC heat exchangers in spite of its appealing biocidal qualities. Aluminum is attractive because of its low cost and high thermal conductivity. Unfortunately, its susceptibility to corrosion in seawater, possible erosion of protective layers by mechanical cleaning, and galvanic and pitting effects, etc., all suggest that a 10 to 15 year service life can be expected from Alclad alloy. Titanium and AL-6X stainless are materials which are qualified for OTEC heat exchangers at the present time (LaQue, 1979a, b; Kinelski, 1979b). Other components and materials must be compatible with ammonia and must show suitable strength and corrosion resistance. The 400 series stainless steels appear to be suitable candidates. Piping for ammonia may also be constructed of stainless steel or stress-relieved steel. Seawater piping can be steel, clad with copper for its antifouling effect. Stainless steel is qualified for use in seawater pumps and valves. The hull and cold-water pipe could be constructed of steel and reinforced concrete, but fatigue loading on the cold-water pipe may be problematic. Other more technologically advanced materials such as fiber-reinforced plastics may also be suitable for the cold-water pipe (McGuinness et al., 1979). Antifouling coatings are under consideration.

THERMODYNAMIC ANALYSIS

The thermodynamic analysis is basic to estimating the size and cost of major components of the system. The OTEC power system under consideration is based on a Rankine cycle. It is convenient to discuss the cycle state points in terms of the relationship of temperatures and flows in the major components of an OTEC system. In addition to the warm- and cold-water inlet temperatures, there are four intermediary temperatures (warm- and cold-water discharge temperatures and working fluid turbine inlet and discharge temperatures) and two velocities (evaporator and condenser water velocities) that need to be specified to permit calculation of the heat transfer area required per unit net output, and other performance parameters for a given concept and set of component loss assumptions. A number of

other variables such as water velocity in cold-water pipe and vapor velocity in connecting pipes and headers enter into the performance calculation of the total system. Detailed studies by contractors, however, indicate that the four intermediary temperatures and two velocities effectively control the cost of the major components and therefore contribute to the principal design parameters that require overall optimization. The qualitative effects of these six cycle parameters on the overall performance can be summarized as follows:

- Increasing turbine inlet temperature (decreasing turbine discharge temperature) increases the gross work per unit turbine flow, but decreases the temperature difference in the evaporator (condenser) and therefore increases the heat exchanger size. Varying these parameters within thermodynamically admissible limits results in the heat exchanger area per unit net power increasing without limit at either end of the admissible range.
- Increasing the warm-water discharge temperature (decreasing the cold-water discharge temperature) results in a larger warm-water (cold-water) flow per unit working fluid flow, and hence in larger water pumping and ducting provisions, but it increases the log mean temperature difference in the evaporator (condenser) and hence decreases the heat exchanger size. Selection of water discharge temperatures therefore represents a compromise between water pumping provisions and heat transfer equipment. Similarly, the water velocities in the heat exchangers are chosen as a compromise between the heat exchanger size and the pumping power.

These six parameters thus affect the heat exchanger size and net cycle performance in an interrelated manner and should be treated simultaneously in the system optimization.* By contrast, other

*Optimization of total system cost is discussed in Sec. III, Cost Analysis. The optimization technique used in this study is presented in Appendix E.

variables such as water velocity in the cold-water pipe can be optimized separately without significantly perturbing the overall system optimality.

Approximate Optima

Results of earlier OTEC studies show that simplified approximate rules for selecting some (but not all) of these parameters can be quite satisfactory. In a closed-cycle OTEC plant operating over an overall temperature difference (ΔT overall), having a fraction, $\bar{x}$, of the ΔT overall across the turbine, the (gross) power output (for a certain heat load) will be proportional to $x \cdot \Delta T$, and the heat transfer surface area for a certain heat load will be inversely proportional to $(1 - x)\Delta T$ as a first approximation. Using the heat transfer area per unit gross power as an approximate surrogate for the cost per unit net power, it can be readily shown that the minimum is achieved when the turbine temperature drop is made equal to one-half the overall temperature drop.

In a similar way, the distribution of temperature drop between condenser and evaporator with substantially equal overall heat transfer coefficients is optimized when the ΔT across each heat exchanger is approximately the same. It does not appear that equally simplified relations exist for establishing desirable warm- and cold-water discharge temperatures or water velocities in evaporator and condenser.

Calculation Methods

The objective of this analysis is to evaluate the effect of component parameters and losses and hence to show the sensitivity of OTEC performance and cost to specific technical uncertainties. The analysis is not intended to produce detailed design information. In general, we emphasize parameters in novel components (e.g., heat exchangers, water pumping and ducting systems, and ocean engineering aspects) rather than those of reasonably straightforward turbomachinery and pumps. It was also an objective that the analysis be able to accept inputs from experimental programs on heat exchangers and other components. This affected the form of inputs used.

The thermodynamic analysis* is carried out on the basis of a unit flow of working fluid. Pumping requirements for the working fluid and warm- and cold-water loops are explicitly calculated, but hotel and miscellaneous parasitic electrical losses (due to the ammonia purification system, for instance) are input as a value per unit working fluid flow.

Heat exchanger tube† size is taken as an input because it is constrained to a small range by factors not readily expressed analytically. The heat exchanger is assumed to be made up of identical tubes having the same performance. No separate calculation is made for a subcooled section of the evaporator, but rather the same heat transfer correlation is used for the entire evaporator (like Abelson's calculation). The tube length and ammonia flow per unit tube are calculated using Abelson's "Case 3 algorithm." (Plate heat exchangers are treated in a substantially different way because the plate size is likely to be constrained by press size. See below.)

The evaporator and condenser heat transfer characteristics are input (separately) in terms of a "Wilson plot" (Michel, 1977) slope and intercept in order to simplify as much as possible the form of heat transfer inputs and to make it possible to use test data with a minimum of interpretation. Variations in heat exchanger concept, material tube size, and type and extent of heat transfer enhancement are manifested as changes in the Wilson plot slope and intercept. The Wilson parameters refer to clean tube conditions. Fouling of tube surfaces (due either to biofouling or to inorganic deposits on either side) is accounted for by introducing an additional fouling factor as a thermal resistance to heat flow.

The water-side pressure drops (including the effects of roughness in circular tubes) are treated as by Abelson. Water system pressure drops in the ducting and transfer arrangements are accounted for by a summation of the number of dynamic heads lost in bends, contractions,

---

*An exhaustive treatment of the thermodynamic analysis of closed-cycle OTEC can be found in Abelson, 1978.

†Treatment of plate-type heat exchangers is discussed later.

expansions, etc. Separate values are entered for cold- and warm-water ducting. We have assumed a mean ducting velocity of 6 ft/sec, in rough accordance with earlier contractor studies.

Vapor-side pressure losses are input as condenser and evaporator pressure drops in psi. It is assumed that the effect of these pressure drops on the effective condensing (evaporating) temperature is adequately approximated by taking the effective vapor saturation temperature corresponding to the arithmetic mean pressure in each heat exchanger.

Chlorination, if specified, is assumed done by on-board-generated sodium hypochlorite formed by electrolysis of seawater. The chlorination fraction can be separately specified for warm- and cold-water streams. The chlorination electrical power requirement is taken as 2.2 kW/lb/hr of equivalent chlorine produced.

Plate Heat Exchangers

The treatment of plate heat exchangers differs from that of the tube-and-shell heat exchangers in two basic aspects: First, rather than being subject to free design optimization in order to set the dimensions of the heat exchanger, it is assumed that the plate dimensions are constrained by the available manufacturing equipment. The assumed maximum active plate area is 10 × 4.5 ft. Preliminary exploration showed that substantially longer ($\sim$ 40 percent) plates would permit an increase of about 12 percent in overall heat transfer coefficient, but this possibility was not exploited. Second, available correlations from Lockheed (LMSC, 1979) and Alfa-Laval show the overall heat transfer coefficient to depend on the working fluid mass velocity, a dependence that is ignored in most correlations for tube-and-shell heat exchangers. The inclusion of this parameter is appropriate for plate heat exchangers because of the much smaller spacing and because of the importance of the mass velocity in getting liquid distribution in an evaporator. Appendix C contains correlations for overall heat transfer coefficient, adapted from the Lockheed PSD-II material (LMSC, 1979a).

OFF-DESIGN PERFORMANCE

The design point analysis of OTEC calculates the gross and net power, the water flows per unit ammonia flow, the heat exchanger tube lengths, the net power per unit tube, the turbine flow area per unit tube for given assumed turbine temperatures, and warm- and cold-water inlet and discharge temperatures and water velocities in tubes, given a set of component efficiencies and heat exchanger characteristics. The off-design problem treated here is to find, for a given "design point," how the net power varies with different warm-water temperatures during a year's operation at a site in the Gulf of Mexico.

First, it should be noted that there are in principle many different modes of off-design operation, only a few of which will be considered here. For instance, a constraint could be imposed that the water pumps operate at constant speed and flow. But such an operational constraint unreasonably penalizes the performance of OTEC in extreme conditions, making it inoperable in winter weather. It is clearly desirable, when searching for the best off-design operating conditions, to allow the water flow to vary, and that has been done in these calculations.

Component Characteristics

It is necessary to consider the variation in performance of certain components as they are operated away from their design points. The turbine is most important in this respect. We assume here that the turbine is constrained to operate at constant speed, producing alternator power of constant frequency. It therefore operates at a constant "wheel speed" although the "spouting velocity" (i.e., the turbine nozzle exit velocity) will change significantly as the overall ΔT across the plant changes. In a representative case, the spouting velocity varies from 917.7 to 778.0 ft/sec as the overall ΔT varies from 40° to 28°F. If the turbine were optimized at the higher temperature, the loss in efficiency at the lower temperature would be over 3 percent, and the loss in net power over 6 percent. In this analysis the turbine is designed for an intermediate temperature so that the loss in efficiency to swirl can be kept below 1 percent over

the entire temperature range. The turbine flow area can be changed, as has been demonstrated on experimental gas turbine turbomachinery, with minimal losses in efficiency. The turbine flow area is sized for optimal "design point" power plants at low ΔT. Designs involving both fixed flow area and variable flow area turbines have been synthesized and investigated in this study.

The heat exchangers are the dominant components of the power system and usually limit the amount of power that can be produced. There is no evident way that the surface area can be changed for off-design operation, but clearly the water velocity in the tubes can assume different values as overall temperature changes. Heat exchanger off-design performance is accounted for by expressing the overall heat transfer coefficient in terms of water velocity in the tubes.

Water pump off-design efficiency variations were not considered, because the pump speed was made proportional to flow so that the pump efficiency for a fixed water circuit would be independent of flow. The components required to achieve variable pump speed were included in the power system.

Method of Off-Design Performance Calculation

Performance calculations (including the effects of turbine efficiency variation, as noted above) are made using the "design point" algorithms for a range of heat exchanger exit temperatures and tube velocities. A detailed explanation is given in Appendix G. Briefly, a graphical method is used to plot turbine flow area per heat exchanger tube against tube length, for a water exit temperature and tube velocity. The heat exchanger area per unit net power is then plotted against tube length. A set of plots of this type is made for each overall ΔT of interest. A "design point" of a given conceptual OTEC plant at a given overall ΔT with fixed geometry heat exchangers and turbines is then entered into similar charts for other overall ΔT's to find the plant's off-design performance.

The same charts can be used to estimate the performance of plants using a variable flow area turbine, and the variation in turbine nozzle area called for can be estimated, as well as the overall performance advantage achievable by such means.

Site-Dependent Average Power Calculation

The best "design point" overall ΔT for a plant to operate year-round depends, among other things, on the seasonal variation in temperature difference available. It can be argued that power generated at different times of the year has different values. That approach would require different weighting of the monthly output, and would represent a simple modification to the present calculation. Here we assume that OTEC would supply part of the base-load requirements--in the Southern United States largely supplied by coal--and that the value of OTEC is in reducing the coal consumption. We also assume that the variation in the cost of coal-produced base-load power is negligible through the year. Therefore we have not in these calculations weighted the value of power differently through the year, and the optimal design is taken as that one which maximizes the simple time-averaged power over one year.

Tables 1 and 2 show, for two sites in the Gulf of Mexico--one off Tampa and the other off New Orleans--the average power produced over the year for an OTEC with variable area turbine and for the best fixed area turbine, as a fraction of that which would be produced by a 40°F overall ΔT design operating continuously at 40°F. This "standard" reference value of ΔT overall is essentially arbitrary. It is adopted because a large fraction of the OTEC design studies have been made for that value. In Table 1, it is assumed that as the overall temperature difference increases over 40°F, the additional power generation capability of the OTEC plant--some 25 percent--can be accommodated by the electrical components: generator, switch gear, transformers, rectifiers, and transmission cable. In other words, those components have a higher rating than the nominal plant rating at 40°F. In general, the somewhat higher cost of these components is justified by the handsomely better performance on a seasonal average basis. Table 2 shows the effect on the average power (again relative to a 40°F design operated continuously at 40°F) if the rating of the electrical components is arbitrarily limited to the plant rating at 40°F. Comparison with Table 1 shows that a penalty in averaged power of about 8 percent results if the electrical components are not uprated.

Table 1

AVERAGE POWER OVER YEAR
(Relative to 40°F Design Plant Operated at 40°F Overall ΔT)
(Electric Components Not Constraining)

Tampa Site	
Variable area turbine design	0.90
Best fixed area turbine design	0.88
New Orleans Site	
Variable area turbine design	0.78
Best fixed area turbine design	0.75

Table 2

AVERAGE POWER OVER YEAR
(Relative to 40°F Design Plant Operated at 40°F)
(Power Limited to Power at 40°F)

Tampa Site	
Variable area turbine design	0.84
Best fixed area turbine design	0.81
New Orleans Site	
Variable area turbine design	0.72
Best fixed area turbine design	0.70

OCEAN SYSTEM*

For commercial OTEC, several platform configuration studies (Westinghouse, 1978) tended to eliminate all except the ship-form or spar. At the present time, it seems warranted to consider both concrete and steel fabricated hulls for ship-forms. The greater familiarity and ease of fabrication in existing shipyards makes steel ships a contender. The spar form has many advantages and some offsetting disadvantages, particularly with fabrication facilities and deployment. The design layout of the platform should permit economies to be realized by the appropriate choice of power system modular size. However, this is not fully established as fact at the present time.

*This subsection is based on contributions by J. Roney, a consultant to The Rand Corporation.

The cold-water pipe (CWP) is in development and evolution. Several basic materials appear usable for an OTEC CWP, and there are a number of conceptual configurations.

Earlier platform studies considered either fixed or flexible connections for the CWP at the hull, where the flexible connections would be achieved by some form of gimbal or hinged joint or spherical ball joint. A rigid CWP structure using steel, concrete, or plastic (such as fiberglass-reinforced plastic) in a fixed joint configuration has stress levels high enough to require a thicker CWP wall.

A multi-point mooring system has been established in the platform studies and other ocean engineering analyses. A single-point moor for commercial plants will require the electric power riser cable to endure conditions beyond the capabilities of current technologies under the best OTEC conditions.

Platform Technology

Two principal structural materials have been considered: steel and reinforced concrete. Steel hull designs use well-established procedures by naval architects. In spite of existing guides for specific designs and experience with cost estimation and verification, there has been a recent history of cost overruns with naval ships constructed at private shipyards.

Concrete hulls do not enjoy the depth of experience that steel hulls do. Most of the reinforced concrete technology is in other fields, and the application to marine structures is somewhat limited. Much concrete technology in the marine environment is related to the offshore petroleum industry where the very large structures such as Ekofisk and Condeep are milestones, but are bottom-seated, gravity-moored structures and not floating platforms. On the other hand, the Arco barge is a prototype of an OTEC-like concrete platform.

The lack of experience with concrete hulls results in a higher level of uncertainty in cost estimates and possibly in more conservative designs and thus higher costs than a more mature technology. The use of concrete hulls for plants may require special qualification steps to establish their acceptability.

Platform Size Requirements

The size and dimensions of a platform are related directly to the volume and layout area needed for the power modules. The following table shows the platform dimensions and volumes allowed by Gibbs and Cox in their designs for the four options indicated (John J. McMullen, 1979):

	Horizontal Units		Vertical Units	
Heat Exchanger Rating (MWe)	Dimensions (H × W × D, ft)	Volume (10^6 ft^3)	Dimensions (H × W × D, ft)	Volume (10^6 ft^3)
25	155 × 125 × 110	2.13	105 × 105 × 164	1.81
50	180 × 155 × 135	3.77	135 × 120 × 192	3.11

The compactness of the vertical heat exchanger is reflected in the figures. The horizontal heat exchanger power system modules are 120 percent of the volume of the vertical heat exchanger modules. The 50 MWe modules are 175 percent of the volume of the 25 MW modules, reflecting an equivalent volume savings of 12 to 15 percent.

Cold-Water Pipe

The requirement to suspend a conduit approximately 100 feet in diameter and 3000 feet long from a platform that is subject to movement in all three axial directions and rotation about any of the axes is indeed demanding. Some progress has been made in conceptual designs and analysis of the CWP. The state of technological development can be summarized as follows: (1) There are a number of feasible and promising configurations and materials which are candidates for CWP fabrication, (2) the analytic tools for CWP engineering require more development, and (3) although it appears feasible to manufacture a CWP that can survive the loads imposed, including extreme storm conditions, the long lifetime requirements still pose considerable problems that can influence total life-cycle costs due to maintenance or replacement.

Early design concepts called for a relatively rigid, rugged structure such as a concrete cylinder some 80 feet in diameter, following

the methods of reinforced concrete construction as applied in marine industries. Relatively little attention was given to the deployment of such a massive structure. The full nature of the dynamic loadings were not appreciated until recently. The high stresses due to platform motions are now recognized, and a need for a degree of flexibility at the CWP-platform connection has been identified. The character of wave-induced drag and inertial hydraulic loads and current-induced drag loads are under study. Analytical tools such as the Paulling (1970) model are being developed. Attention is being focused on broadening the concepts and uses of materials such as fiber-reinforced plastics, steel, and compliant materials, e.g., nylon-reinforced rubber.

A greater appreciation of the complexity of the deployment problem has emerged. Noteworthy is the detailed attention given to deployment methods for the multi-sectioned concrete CWP.

Materials

The problems associated with materials for cold-water pipe fabrication are more severe than anticipated. The high cycle number and lack of knowledge of fatigue properties in the seawater environment present considerable difficulty to CWP designers. Even steel--about which much more is known--has appreciable uncertainties.

Although the high stress levels induced by platform motions can be greatly reduced by flexible connections, thus reducing direct bending loads, the translatory movements and the direct hydrodynamic loads on the pipe produce high stress levels and require correspondingly thick walls. There is a paucity of good fatigue performance data. The net effect is a degree of uncertainty that is likely to persist for many years.

Systems Analysis

Although two systems studies by National Oceanic Atmospheric Administration (NOAA) contractors are under way, some potentially imaginative approaches remain to be explored, e.g., a combined CWP mooring system/riser cable design. In composites, it may be productive to

consider different materials over the length of the pipe. From information presented at the Cold-Water Pipe Symposium in January 1979 (NOAA/DOE, 1979), the interaction of the cold-water pipe, mooring system, and riser cable problems was recognized and a systems-oriented approach is being instituted. A systematic approach is also evident in designs for spar-type platforms. A tension-leg moor, using the cold-water pipe as a mooring system member, provides many advantages, and systems of this type have been proposed (Gibbs and Cox, 1979a).

POWER TRANSMISSION

Transmission Requirements

The output of each OTEC power system module will be AC electric. The power delivered to the user will also be AC, and any transmission from shore on an existing grid will necessarily be AC. Thus, the transmission system will be receiving and delivering AC power, which is a compelling case for AC transmission. Unfortunately, the insulation requirements for undersea cable dictate cross-section designs that have much higher capacitance per unit length than for overland cable. As a result, the reactive power losses in the transmission of AC are unacceptably large when distances are 60 miles or more.*

Consequently, DC transmission is indicated for distances of 50 n mi or more. For in-between distances, there will be a trade-off between the reactive losses for AC transmission and the losses due to current rectification aboard the platform and current inversion at shore, plus the capital, maintenance, and replacement costs of rectifiers and inverters if DC were used.

Environmental Conditions

The OTEC plants will be at sites where the seabed is 4000 ft deep or more. The distance from shore will vary by site from several miles to 150 miles or more. The cable will be submerged.

---

*AC power via overland lines over long distances is transmitted by supplying reactive power at intermediate stations.

The submerged cable must be buried when the seabed is shallower than 300 ft to protect it from seagoing vessels. Burial lengths will vary by site from several miles to 100 miles or more. An alternative to this method of protecting the cable from damage is to establish an appropriate "stay-away" zone along the shallow segment of the cable crossing.

The unburied portion of the submerged cable will rest on the seabed, except for the riser segment near the OTEC platform.

The ease of burial will depend on the seabed, which will vary among sites. Burial will be especially difficult where the seabed is rocky. Table 3 lists some characteristics of the two sites considered in this study.

Table 3

REPRESENTATIVE SITE CHARACTERISTICS[a]

New Orleans	
Distance of plant from shore	81 n mi
Depth at plant	4800 ft
Bottom condition	Sandy
Number of platforms	6 or 12
Net power output per platform	500 MW (6 platforms) or 250 MW (12 platforms)
Cable burial length	58 n mi
Florida West Coast	
Distance of plant from shore	148 n mi
Depth at plant	4200 ft
Bottom condition	Sandy
Number of platforms	6 or 12
Net power output per platform	500 MW (6 platforms) or 250 MW (12 platforms)
Cable burial length	81 n mi

[a]The platform sizes were chosen arbitrarily in Morello et al. (1978) for an OTEC plant with a total generating capability of 3000 MWe.

Other environmental effects on cable installation include subsurface current forces directly on the cable and surface and atmospheric forces on the vessel from which the cable is deployed.

Once the cable is installed, the environmental effects of primary concern are those producing static and dynamic loads on the riser segment. We will discuss these in a separate subsection.

Preliminary Cable Configuration

The cable configuration shown in Fig. 17 has been proposed by the contractors:

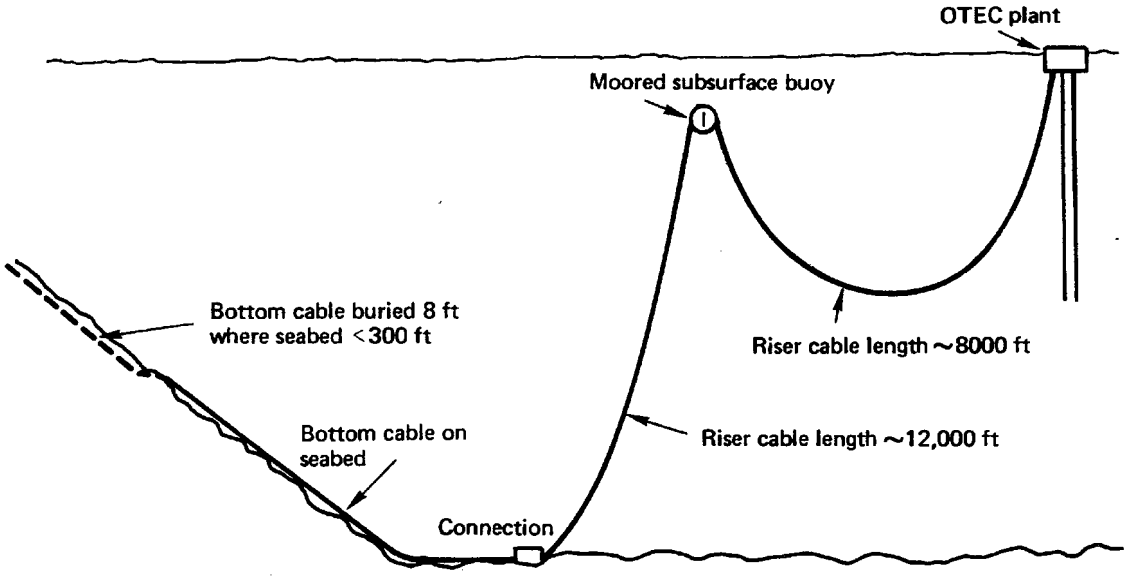

Fig. 17 — Proposed cable configuration

Instead of a direct riser connection, a moored subsurface assembly with a two-segment riser cable has been proposed to relieve the cable of stresses it would otherwise encounter. With the configuration shown above, tension due to in-plane and out-of-plane static drag forces is reduced considerably. Also, the "node" at the subsurface buoy raises the fundamental frequency of "vibrating string" motion. Finally, the three-point mooring substantially reduces the chafing action of the lower segment against the seabed.

Number of Cables

Theoretically, the absolute minimum number of individually insulated conductors required for delivery of OTEC output is one. In such a case, the power transmitted by the cable would be monopolar DC or single-phase AC--the seawater would form the return segment of the loop.

Practically speaking, however, a single conductor system would present a number of safety, shielding, and electrolysis problems. Furthermore, whereas practical OTEC generator design calls for three-phase AC, single-phase AC transmission to reduce cable costs would hardly be cost effective. Thus, practical minimal requirements are two conductors for bipolar DC transmission or three conductors for three-phase AC. Additional conductors may be dictated by the electrical load to be transmitted.

An additional conductor over and above the number required for electrical transmission would provide redundancy in case a single conductor fails. However, this design philosophy is suspect if the most likely failures are common mode failures, i.e., those involving more than one conductor at a time. Thus, if redundancy is important, the individual conductors should be as structurally independent as possible. Even so, the effects of current and platform dynamics on the riser segment will not be very different among conductors.

Implantment, Imbedment, and Repair

General restrictions on the handling of power cables include adherence to the allowable limits on tension, torsion, and bending, care against local abrasion, etc. The cables themselves must be compatible with the manner of handling, or vice versa. For example, any armoring must be double layered in opposite directions or otherwise configured so that the cable does not twist under tension, which has implications on limits of coiling prior to implantment.

Another general problem is joining of cable lengths. Joints are potential weak points--the longest cable lengths attainable should be the goal, both for manufacture and assembly.

A third general problem is environmental conditions. The operation should be planned to commence when environmental conditions are

favorable, and not be aborted altogether should these conditions become more adverse.

A fourth problem, peculiar to oil-filled cables, is maintenance of an intense pressure in excess of the ambient pressure at the depth the cable is at any time, yet not excessive relative to the ambient pressure at shallow depth. Temperature transients, which will affect the volume of oil inside the cable, also have to be accounted for.

A dedicated cable-laying ship would be most suitable for the laying task from the standpoint of stability, maneuverability, and navigational accuracy. However, it is clearly the most expensive alternative. Furthermore, it is not suitable for shallow waters or very narrow confines, which some of the representative routes traverse.

Bulk carriers outfitted with laying equipment would be suitable for very short distance laying operations. However, they would probably require tugs for towing and improved navigation during implantment. Barges present similar problems as bulk carriers, except that the requirement for tugs is more intensified. Barges appear to be an especially attractive choice when a large portion of the cable route is in very shallow waters.

Laying machines suitable for large power cables in seabeds as deep as 4000 to 6000 ft must be developed to avoid cable damage during payout. For example, for a bottom cable of 5 in. diameter and weighing 35 lb/ft in air, the braking equipment must be designed for 140,000 lb. The current state of the art for undersea cable installation is 1800 ft depth, with 60,000 lb of braking force.

In shallow water, the prominent consideration is the cost of burial. The cable length to be imbedded is as great as 1000 n mi for the 12 cables envisaged for the Florida West Coast. The embedment cost is very high, and the time involved is on the order of years.

In very shallow waters, repair of oil-filled cable can be performed by divers. Repair of other cable is performed on the surface. The conventional method is grappling for the cable in the vicinity of the fault, laying the grappled segment across the repair barge, and replacing a suitable length after installation of two flexible joints.

Conventional Cable Systems for Underwater Applications

1. Solid Paper-Impregnated Cable (PI). PI cable has a central core conductor, surrounded by a partially conducting shield. Several layers of special paper tapes are then tightly wound around the shield. The assembly is vacuum-impregnated with a special insulating oil. This sheath also provides a moisture barrier and protects the interior against abrasion and other damage mechanisms.

Thus far, PI has been the most widely used cable for underwater applications. Specific usage includes:

- o Corsica-Italy crossing: 105 km length, 500 m maximum depth, 200 kV DC, copper conductor, 850 kCM* cross section.
- o Sweden-Laeso Island: 65 km length, shallow water, 250 kV DC, copper conductor, 1250 kCM cross section.
- o British Columbia-Vancouver Island: 27 km length, 200 m maximum depth, 300 kV DC, copper conductor, 800 kCM cross section.
- o Skaggerak (Denmark-Sweden) connection: 125 km length, 500 m maximum depth, 250 kV DC, copper conductor, 1600 kCM cross section.

A prominent problem with PI cable is its vulnerability to failure caused by oil migration (i.e., draining) when positioned on a slope of but modest inclination. Furthermore, migration may be hastened by oil viscosity reduction at typical 75° to 80°C conductor temperature under full load.

In view of its limited AC load-carrying ability and the oil migration problem, it is clear that, in the absence of extensive development efforts to remedy these limitations, PI cable is not a suitable candidate for any part of an AC line or for the riser segment of a DC line; it is a potential candidate for the bottom segment of a DC line where the seabed is more or less horizontal.

PI cable is also sensitive to handling during implantment. However, the other candidate cable types appear to exhibit comparable or

---

*kCM = thousand circular mils. One circular mil = $\frac{\pi}{4} \times (10^{-3})^2$ sq in.

greater sensitivities. The handling problems will be discussed in a separate subsection.

2. Paper-Impregnated, Gas Pressure-Assisted Cable (PG). This is a variation of PI cable where nitrogen gas is applied internally through the conductor interstices. It eliminates the problem of gaseous voids that are formed in PI cable from thermal expansion and contraction under load cycling. As such, the maximum allowable AC capability is increased significantly--the current state of the art is 138 kV. Potential capabilities of 220 kV AC or 350 to 400 kV AC have been envisaged by Pirelli Cable Systems.

The current usage of PG cable is primarily underground. Two significant underwater applications are:

- o British Columbia-Vancouver Island: 25 km long, 180 m deep, 138 kV AC, copper conductor, 1000 kCM cross section.
- o Cook Strait connection: 39 km long, 250 m deep, 250 kV DC, copper conductor, 1000 kCM cross section.

The oil migration problem that makes PI cable unsuitable for non-horizontal geometry also applies to PG cable. However, because it can accommodate the higher voltages, PG is a potential candidate for the bottom segment of an AC cable.

One prominent difficulty in the implantment of PG that may be insurmountable is the maintenance of pressure equilibrium with the environment. Because it is not pressurized until after implantment, it will be subject to additional external pressures when laid in deep water. Then, upon pressurization, any shallow water segment will be subject to excess internal pressure.

3. Self-Contained Oil-Filled Cables (OF). This is another variation of PI cable in which the central core is a passageway through which high pressure oil (about 50 psi) is applied from an external source. An external metallic sheath, generally of lead reinforced with strong tapes, contains the internal pressure. With the high pressure oil to counteract expansions and contractions due to thermal fluctuations, loads up to 750 kV AC can be accommodated.

Primary existing applications of this cable include:

- o Long Island Sound: 18 km length, shallow water, 400 kV AC, copper conductor, 2000 kCM cross section.
- o British Columbia-Vancouver Island (2nd crossing): 27 km length, 250 m depth, 300 kV DC, copper conductor, 800 kCM cross section.
- o Mallorca-Menorca: 44 km length, shallow water, 132 kV AC, copper conductor, 2000 kCM cross section.
- o Denmark-Sweden: 7 km length, shallow water, 400 kV AC, copper conductor, 2000 kCM cross section.
- o Tsuguru Strait: 44 km length, 290 m depth, 250 kV DC, copper conductor, 1200 kCM cross section.

This type of cable offers the largest range of possibilities for both bottom and riser applications. The voltages under consideration for OTEC are readily attainable; there is no oil migration problem, and there is no pressure equalization problem during implantment or in situ.

The primary identifiable problem, which will have to be examined more thoroughly, is that of hydraulic transients, which will have a prominent effect for the connection lengths under consideration.

4. High-Pressure Oil-Filled Pipe Cable (HPOF). Rather than the external sheath found on OF, this variant of PI places the paper-insulated conductor directly through a steel pipe which is subsequently flooded with oil and pressurized. HPOF is especially applicable to three-phase AC, because the incremental cost of two additional conductors within a pipe is relatively small. HPOF cable delivers up to 550 kV AC; it is the most reliable system for transmitting high voltage power underground. Current submarine usage is limited to short connections, on the order of a nautical mile, in shallow waters.

This type of cable appears to be a potential candidate for the bottom segment of the OTEC transmission system, where it can be continuously supported. Because each segment is rigid, deployment by conventional means (e.g., winch, reel, coil) is inapplicable.

Technology for joining, recovery, and repair will also have to be established.

5. Compressed-Gas Insulated Cables (CGI). CGI cable was designed to transmit bulk power at extra high voltages over short distances on land. It is available as a single-conductor or three-conductor line. The basic single-conductor construction consists of two concentric aluminum cylinders, 40 to 60 ft long, supported internally by insulating spacers. Sections are welded to achieve the desired length, after which the annulus between cylinders is filled with SF_6 gas at 50 psi. At capacities as great as 800 kV AC, the power carrying capability of this cable far exceeds that of any other.

CGI cable does not appear to be a serious candidate for OTEC. A 15 in. diameter pipe would be required to handle 345 kV. Such a pipe would have a buoyancy of 50 lb/ft in seawater and would collapse at a depth of 800 ft. Moreover, it would require a special coating for protection against corrosion. This type pipe is especially sensitive to handling because the position of the central conductor must be intact.

6. Extruded Dielectric Cables (E). Typical extruded insulation cables consist of a central conductor, a surrounding shield, insulation, an outer conducting shield, and an extruded insulating jacket. Typical insulation is cross-linked polyethylene.

Extruded dielectric cable is simplest in construction, lowest in cost, and least sensitive to handling. State-of-the-art usage is 150 kV AC, with a potential capability of 350 kV AC or DC. Its primary existing usage is underground. A notable underwater application is the Anchorage, Alaska cable: 138 kV AC, 22,000 ft length, shallow water, 500 kCM conductor cross section.

Unfortunately, the current reliability record of extruded dielectric cables is not impressive, and the reasons are not clear. The belief is that the polyethylene insulation deteriorates in the presence of moisture. Furthermore, there is a strong belief that extruded cables will never be acceptable for deep water, i.e., in the presence of significant hydrostatic pressure, because microscopic voids in the insulation cannot be eliminated.

Nevertheless, because of the potential advantage of extruded insulation cable cited earlier, plus its relative merits for riser applications, it is definitely a candidate for OTEC applications.

Leading Candidate Bottom Cables

New Orleans. The transmission requirement for this site is 3000 MW over an 81 n mi distance. For this distance, only DC transmission can be considered. The primary candidate between the point and shore appears to be two pairs of OF cables, each pair carrying ± 500 kV. If a tie point is not used, then the power to be transmitted for each plant is either 250 MW or 500 MW, in which case conventional PI cable at ± 200 kV or ± 300 kV, respectively, appears to be the leading candidate.

Florida West Coast. The requirement for this site is 3000 MW over a 148 n mi distance. Hydraulic pressure losses preclude the use of OF cable for these distances unless an additional intermediate feeding point is installed, in which case two cable pairs, each at ± 500 kV, would be used.

Otherwise, PG cable appears to be the only reasonable candidate for the tie point to shore link. Because ± 400 kV appears to be the upper voltage limit for this type of cable, three cable pairs would be necessary. A considerable cable development effort will probably be required to accommodate the depth variations of hydrostatic pressure that will be encountered.

With the latter solution, conventional PI cables would connect the individual plants with the tie point. However, because ± 300 kV is the existing upper limit for this type cable, additional R&D to bring the capacity up to ± 400 kV would be required to avoid the expense of voltage conversion at the tie point.

If the points were not used, then the leading candidate is conventional PI all the way, as with the New Orleans case.

Riser Cable Segment

Riser cable characteristics are markedly different from those of the bottom cable. Whereas the bottom cable extends from shore to the

OTEC plant site, a distance varying from a few miles to a few hundred miles, depending on the site, the primary consideration is cost of cable, cost of implantment, cost of imbedment where the water is shallow, and ability of cable to withstand the implantment loads. The only significant structural load on the bottom cable, once implanted, is hydrostatic pressure, whose value is easily determined.

The riser cable, on the other hand, must bridge a vertical distance of only a mile or so. For this reason, the costs of material and implantment are insignificant compared with those of the bottom cable. However, whereas the latter is fixed at both ends and continuously supported along its length, the riser cable experiences forced motions at its upper end and forces along its unsupported length. The upper end forcing function is the OTEC platform dynamic response to wind and surface wave forces. Current-induced, quasi-static drag forces and oscillatory forces due to vortex shedding act on the cable along its entire unsupported length. Consequently, the major analysis and design consideration regarding the riser cable is its ability to maintain its electrical and structural integrity under the in situ loads.

Loads on Riser Cable. The current and voltage loads on the riser cable segment will be governed by those for which the bottom cable is designed to carry (dictated by the OTEC plant output and distance to shore). The loads are:

1. *Dead Weight.* The riser cable is expected to be denser than seawater. A flexible cable suspended under its own weight assumes the well-known catenary configuration. The tension in such a cable is a function of span and degree of sag. Excess tautness results in high initial tensions that get even higher when "live" loads are superimposed. It also raises the strumming frequency. The latter two problems are discussed below.

Excess sag, on the other hand, means more cable, hence more cable weight. It also renders the cable vulnerable to looping, which if followed by a sharp increase in tension, can produce a kink or hockle, either of which can lead to electrical failure. It also results in larger swaying amplitudes.

2. *Quasi-Static Drag Forces.* The drag force due to current generally will have components parallel and perpendicular to the vertical plane of the cable. Its magnitude will depend on current velocity, cable cross section, and length normal to the direction of flow.

3. *Strumming.* The phenomenon of strumming refers to cable oscillations in the plane normal to the direction of current flow. The oscillations are induced by out-of-phase pressure variations arising from vortex shedding on either side of the cable. The strumming frequency varies directly with current velocity and inversely with cable diameter. A resonance condition is set up when the strumming frequency is approximately equal to a natural frequency of cable vibration or a harmonic thereof. With insufficient damping, strumming at a natural frequency would cause an amplitude buildup, with time, leading to a peak-load structural failure. This is not the case here because the inertia and viscosity of the surrounding seawater medium provide external damping. Also, because the unsupported cable length is so great, any significant strumming forces occur at high multiples of the cable's fundamental frequency, where internal damping is very prominent.

The real importance of strumming is two-fold: (1) it can lead to structural failure due to fatigue and (2) it dramatically increases the static drag force on the cable by providing, in essence, a larger effective cross section normal to the flow. The latter phenomenon can be accounted for in peak-load design, once the multiplicative effect on drag is known. However, fatigue resistance can only be confidently deduced from experimental data on prototype cable. Because a cable is a complex configuration of structural and other elements, no degree of confidence can be attached to analytic deductions of cable fatigue properties from corresponding values for component materials.

4. *OTEC Platform Motion.* Some form of station keeping will be provided for the OTEC platform. The obvious possibilities are single-point mooring, three-point mooring, or dynamic positioning using thrusters. Regardless, its motion will have six degrees of freedom.

Presumably the riser cable will be slack to the extent that it offers negligible resistance to OTEC platform motion. In this case,

the platform dynamics can be decoupled from the riser cable, and once the platform dynamics have been deduced, the boundary condition at the upper end of the riser cable becomes a displacement vector whose coordinates are time-varying functions.

This displacement vector can more conveniently be described by an in-plane and out-of-plane component, each being a bounded function of time, i.e., having a frequency spectrum.

Platform motion is thus an additional source of cable fatigue.

5. *Implantment and Repair Loads.* The riser cable will be subjected to special loads during implantment and during recovery and repair operations. These are peak-loading situations that must be accounted for.

6. *Additional Loads.* Another possible load source is chafing of the riser cable against an adjacent surface, possibly the ocean floor or some surface in the vicinity of the upper termination point.

The corrosive effects of seawater are well-known. The cable exterior surface must be corrosion resistant and, equally important, must be watertight because the cable material will probably be very vulnerable to corrosion.

An additional load to be reckoned with is marine growth. Generally, the growth will increase slowly, but steadily, with time. It will affect the statics and dynamics of the cable in a number of ways:

a. The cable weight will increase.
b. Its cross section, and hence the static drag force, will increase.
c. Its natural frequencies of vibration will be shifted downward.

The effects of these time-varying phenomena must be accounted for in a complete analysis.

There are two prominent sources of thermal loads on the cable. One is the temperature profile of the ocean and its diurnal variation. Another is changes in electrical current passing through the cable conductor due to changes in OTEC power output. However, for each source the temperature differences are quite small insofar as thermal strains are concerned.

Another potential load source is marine animal life, e.g., shark bite or barnacle infestation. The cable will have to be armored or otherwise rendered suitably tough to accommodate these uncontrollable effects. There is also the potential of human interference, such as fishing nets or trawl lines, as well as the possibility of the keel of a large ship contacting the riser cable. Seagoing vessels will probably have to be kept away from the vicinity of the riser cable.

Riser Cable Design Integrity

Cable integrity refers to maintenance of its electrical load-carrying capability; partial or complete failure refers to a loss of this capability. Although it is difficult to envisage structural failure without electrical failure, the converse is not necessarily true. For example, any condition causing leakage of seawater through the insulation will produce immediate electrical failure, although the cable may remain structurally intact.

The previous subsection identified various sources of loading on the riser cable. Three categories of effects of this loading can be discerned. *Peak loads* refer to "worst" cases, for example, tensions due to maximum undersea currents, snap loads due to the most severe surges by the OTEC platform, maximum bending during implantment, severe fish bite, etc. *Time-increasing effects* result from corrosion, marine growth or buildup, creep, or other monotonic phenomena. *Fatigue* results from cyclic loads, wherein each cycle is within tolerable limits but their accumulation causes failure.

A typical cable is not amenable to the preferred type of analysis procedure in which data on the individual elements comprising the structure are synthesized to determine its properties. First, the mechanical properties of a cable's components may not be adequately known. Second, their configuration makes synthesis of component data difficult. Even when a prototype cable becomes available, properties such as fatigue resistance under cyclic loading will require a long time for experimental determination. The successful development of riser cable will require an iterative procedure of detailed analysis, design, modeling, manufacture, and testing.

III. COST ANALYSIS

The objective of this section is to provide a general perspective on OTEC costs. We used a general system approach to generate OTEC cost estimates and accomplish the following tasks: (1) determine the distribution of OTEC capital costs by subsystem, (2) perform sensitivity analyses on several areas of engineering and cost uncertainty to identify those areas having the greatest potential impact on total system cost, and (3) compare cost estimates of alternative OTEC configurations to determine the impact on capital cost and the cost of electricity (COE) of major design changes.

The Rand methodology, which is oriented to the total system level (but supported by component level analysis), emphasizes sensitivity to cost and engineering uncertainties and can be easily updated and expanded. It focuses on closed-cycle commercial-size plants of 240-400 MWe located in the Gulf of Mexico (specifically Tampa and New Orleans). All generated power is cabled to shore.

The principal output of this analysis is recurring capital cost. Nonrecurring costs such as RDT&E and industrial facility modification are not included. Nor are financial/incentive plans such as shipbuilding subsidies, lease-leverage financing, and tax preferences considered. An additional output is the bus-bar cost of electricity, determined in accordance with the methodology outlined in the Electric Power Research Institute's *Technical Assessment Guide*.*

Cost is defined as cost to the procuring organization and therefore includes overhead, general and administrative expense, and fee. All cost values in the Rand methodology are in constant 1978 dollars. The total constant dollar start-of-operation capital cost, which is the primary cost output and the basis for calculating the capital component

*It should be noted that DOE has published a standardized guideline for the computation of unit production costs such as the cost of electricity (see memorandum for distribution from Stuart W. Ray, Director, Office of Planning and Regulatory Program Evaluation, subject: Financial Costing Guidance for the Policy and Fiscal Guidance, March 28, 1979). However, it did not become available to Rand until the analysis portion of the study was completed.

of the cost of electricity, includes the costs of the power, ocean engineering, and transmission subsystems, as well as contingency, architect-engineer services, interim replacement (the cost of replacing components whose expected life is less than that of the facility as a whole), and interest during construction. No credit is taken for residual or scrap value.

The labor improvement curve is applied at the component level rather than at the total platform or major subsystem level. Furthermore, it is intended to capture the impact of repetition only, not cost reductions obtained as a result of new design concepts or manufacturing technologies. The methodology does not address potential resource limitations of either raw materials or construction facilities.

To make the problem more manageable, it was necessary to limit the number of subsystem alternatives considered, as indicated below:

Subsystem	Alternatives Incorporated into Rand Methodology	Alternatives Not Incorporated into Rand Methodology
Heat exchanger	Tube-&-shell, plate	Serpentine coil
Platform	Ship, spar	Tuned sphere, submersible
Cold-water pipe	Single, integral pipe	Detached pipe, multiple pipes
Mooring	Three-point static	Dynamic
Riser cable attachment	Subsurface buoy	Mooring line, CWP

The cost estimates are subject to a degree of both cost-estimating and requirements uncertainty.* The cost-estimating uncertainty stems from questions such as the proper cost-capacity relationship to be used for a given component or simply from the doubt inherent in any cost estimate irrespective of the certainty with which design and performance characteristics are known (e.g., uncertainty concerning raw material

*All default cost and sizing factors are based on data obtained from contractor reports.

prices). There are also uncertainties in design and performance characteristics. For example, the minimum cold-water pipe wall thickness as well as the optimum power module layout and platform configuration are yet to be firmly established.

The cost element subject to the greatest degree of uncertainty is operations and maintenance (O&M). First, no operational experience is available to develop a comprehensive component reliability and maintainability analysis. Second, there is no connection in the cost model between component design and O&M costs. Thus the methodology is not suitable for detailed component design tradeoffs. However, even with pessimistic assumptions concerning reliability and maintainability, O&M costs are never a very significant portion of the OTEC cost of electricity.

Although cost is the most important consideration in justifying the development of a new technology for eventual commercialization, it is not the only criterion used by utilities and DOE to evaluate a new system. However, because most evaluation criteria other than cost tend to be nonquantifiable and subjective, no attempt is made here to provide system ratings for them.

OVERVIEW OF COST METHODOLOGY

The Rand OTEC cost methodology is a set of estimating relationships keyed to the cost breakdown structure shown in Table 4. It is oriented to the total system level, emphasizes sensitivity to cost and engineering uncertainties, and requires a minimum of input. It is based on the engineering analyses in Sec. II. Outputs of the thermodynamic analysis which are passed to the cost module and which influence system sizing (and thereby cost) are:

Condenser/evaporator chlorine dosage (ppm)

Total electrical losses per unit ammonia flow rate (kW/lb/sec)

Ratio of cold/warm-water flow to ammonia flow

Cold/warm-water pump power per unit ammonia flow rate (kW/lb/sec)

Net electrical power per unit ammonia flow rate (kW/lb/sec)

Reflux ratio	
Number of condenser/evaporator plates per pound of ammonia per second (plates/lb/sec)	Plate heat exchanger
Condenser/evaporator active tube length (ft)	Tube-and-shell heat exchanger
Condenser/evaporator ammonia mass flow rate per tube (lb/sec/tube)	Tube-and-shell heat exchanger

Table 4

COST BREAKDOWN STRUCTURE

- Power System
  - Heat exchangers
  - Working fluid subsystem
  - Seawater pumps
  - Biofouling control
  - Turbines
  - Generators
  - Electrical auxiliaries
  - Instrumentation and control
  - Start-up/stand-by power
  - Component installation
- Ocean Engineering
  - Platform
  - Cold-water pipe
  - Mooring
- Transmission
  - Rectifier
  - Riser cable
  - Bottom cable
  - Shore terminal station
  - Deployment/installation
- Architect and engineer (A&E) services
- Contingency
- Interim replacement
- Interest during construction

Among the more important options available to the user of the cost module are platform capacity (MWe); number of modules per platform; platform type (barge or spar); platform material (concrete or steel); cold-water pipe material (concrete, steel, fiber-reinforced plastic, or elastomer); heat exchanger type (tube-and-shell or plate); heat exchanger material (titanium or aluminum); and the number of seawater pumps per module. In addition to the thermodynamic and user

option inputs, there are also a number of default cost and sizing factors stored as part of the model but subject to user override.

The cost methodology employs six different types of estimating relationships to project OTEC component costs. These six forms are distinguished as follows:

Labor and Material	C = burdened labor rate × labor requirement + material unit price × material requirement
Constant	C = a (reference cost is known and is not expected to vary within size or design constraints of this study)
Factor	C = aQ (cost is based on simple cost factor or rule-of-thumb [e.g., $ per pound or % of other cost])
Linear	C = a + bQ (cost is based on assumption that relationship is linear; coefficients determined by fitting line to two or more data points)
Exponential Scaling	$C = C_{REF} (Q/Q_{REF})^a$ (applied primarily to components of similar design but varying size where cost and size of reference design are known; exponent frequently estimated)
Other	Multi-variable exponential (contractor-derived estimating relationships)

The total system cost synthesized from the component and subsystem cost estimates is then optimized with respect to the design parameters. The optimization is based on a nonlinear programming technique known as Sequential Unconstrained Minimization Technique (SUMT), described in Appendix E.

RESULTS

This subsection presents a reference case, the distribution of capital costs by subsystem, a sensitivity analysis with respect to several areas of engineering and cost uncertainty, and cost estimates of alternative OTEC configurations to show the impact of major design changes.

Reference Case

A detailed description of the reference case, including input definitions and output printouts, is provided in Appendix F. It is briefly defined as follows. HX is heat exchanger.

Site: Tampa	Mechanical cleaning: none
Rated ΔT: 40°F	Platform type: ship
Platform capacity: 400 MWe	Platform material: concrete
HX type: tube and shell	CWP material: steel
HX tube material: titanium	Platform number: 8
HX location: internal	Year of dollars: 1978

As indicated on Printouts 4 and 6 in Appendix F, the reference OTEC configuration has a constant-dollar start-of-operation capital cost of $3430/kWe and a bus-bar cost of electricity of 96 mills/kWh. Of the 96 mills/kWh value, the capital component accounts for 92 percent of the total.

The distribution of the reference case constant-dollar start-of-operation capital cost is shown in Fig. 18. The heat exchangers are the single most important cost category (25 percent), followed closely by interest during construction (IDC) (20 percent). The platform, balance of power system, transmission system, and contingency categories each account for about 10 percent. The mooring, cold-water pipe, and A&E service categories each average about five percent of the total.

Viewed another way, the three hardware-oriented cost groups (power system, ocean engineering, and transmission) account for about two-thirds of the capital cost whereas the service-finance oriented

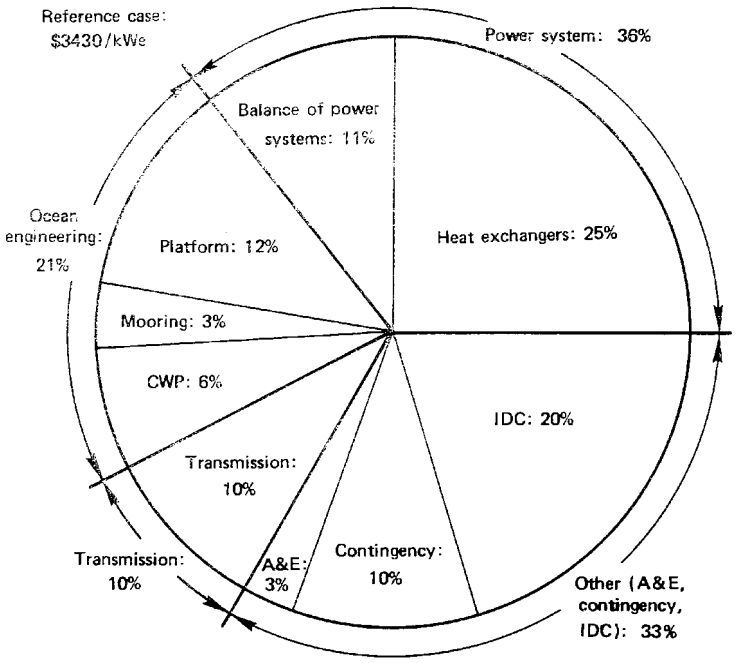

Fig. 18—Distribution of constant-dollar start-of-operation capital cost

category (A&E services, contingency, and IDC) accounts for approximately one-third.

Sensitivity Analysis

A sensitivity analysis was conducted to identify those areas having the greatest potential impact on total system cost. Each of the factors of interest was increased by one percent. The results are shown in Figs. 19 and 20. None of the variables affect total system cost (capital or COE) by as much as one-fourth of one percent. This is to be expected since with the exception of the heat exchanger, there is no dominant component. The engineering variables having the greatest potential impact on total system cost are the condenser and evaporator water-side heat transfer effectiveness and the water pump efficiency. The cost-related variables having the greatest potential impact on total system cost are the tube material cost factor, the platform material unit cost, and the contingency factor.

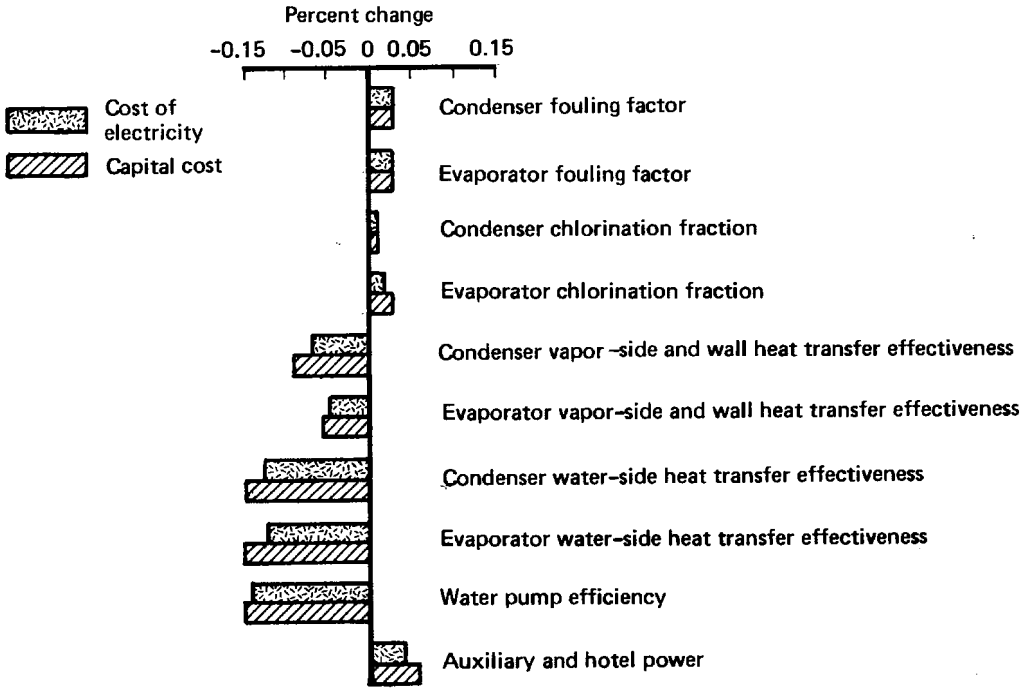

Fig. 19 — Percent change in cost due to 1 percent increase in single engineering variable

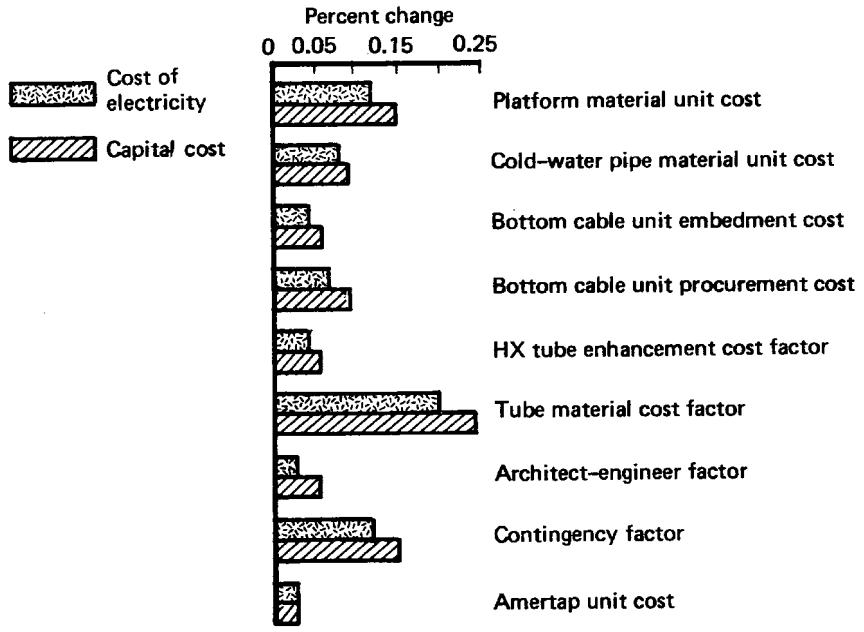

Fig. 20 — Percent change in cost due to 1 percent increase in single cost variable

Alternative Design Assumptions

The cost variations due to major changes in OTEC design assumptions are shown in Table 5. Although most of the cases are fairly self-explanatory, several deserve further elaboration.

Platform Capacity. Cases 1 and 2 suggest that OTEC costs increase substantially in units below 200 MWe in size. As indicated in Fig. 21, ocean engineering, transmission, and other (A&E services, contingency, and IDC) costs increase sharply as platform capacity decreases. Power system costs, however, remain relatively constant.

Platform Type. On the basis of capital cost, the ship and spar configurations (Case 3) are approximately equal, but on the basis of COE, the spar is approximately 11 percent more costly. This is due to the *estimated* O&M penalty the spar must pay for detachable power modules.

Heat Exchanger Location. By placing the heat exchangers external to the platform (Case 4), a capital savings of 7 percent is achieved, primarily in platform costs. However, on the basis of COE there is no cost advantage to doing this since the capital savings are offset by the *estimated* O&M penalty for externally mounted heat exchangers.

Alternative Site. The cost of electricity for a 400 MWe plant at New Orleans (Case 6) is estimated to be 12 percent greater than the cost of a similar plant at Tampa, even though the New Orleans capital cost is 4 percent less. The capital cost savings are primarily the result of lower transmission costs since the New Orleans site is closer to shore. However, in computing the COE, these capital cost savings are more than offset by New Orleans' lower production level caused by the smaller New Orleans temperature differential (see Table 6).

Length of Construction Period. A two-year increase in the length of the construction period (Case 16) increases capital cost by 8 percent and COE by 7 percent. By the same token, it is estimated that if the construction period were shortened to 3 years (Case 17), the capital cost would be reduced to approximately $3160/kW and COE to 89 mills/kWh.

In the cost methodology, the effect of the construction period length is strictly on interest during construction. In reality, however, a lengthening of the construction period is generally a result

Table 5

COSTS OF ALTERNATIVE OTEC DESIGN ASSUMPTIONS

Case ID Number	Title	Variable Changes			Capital Cost		COE	
		Variable	Old Value	New Value	$/kWe	% Change	Mills/kWh	% Change
--	Reference case	--	--	--	3430	--	96	--
1	Platform capacity	Platform capacity (MWe)	400	250	3830	+12	106	+11
2	Platform capacity	Platform capacity (MWe)	400	100	5350	+56	146	+52
3	Platform type	Platform type	Ship	Spar	3470	+1	106	+11
4	HX location	HX location	Internal	External	3190	-7	97	+1
5	Platform material	Platform material	Concrete	Steel	3860	+13	107	+12
6	Alternative site	Site	Tampa	New Orleans	3280	-4	107	+12
7	CWP material	CWP material	Steel	Concrete	3350	-2	94	-2
8	CWP material	CWP material	Steel	FRP	3260	-5	92	-4
9	CWP material	CWP material	Steel	Elastomer	3330	-3	94	-3
10	HX pairs per module	HX pairs per module	1	2	3510	+2	98	+2
11	HX design concept	HX design concept	Bundle	Unit	3620	+6	101	+5
12	Water box requirement	Water box requirement	No	Yes	3630	+6	101	+6
13	Mechanical cleaning	Mech. cleaning type	None	Amertap	3540	+3	99	+3
14	Mechanical cleaning	Mech. cleaning type	None	M.A.N. brush	3530	+3	99	+3
15	Facility life	Facility life (years)	30	20	3430	0	100	+4
16	Length of construction period	Const. period (years)	5	7	3700	+8	103	+7
17	Length of construction period	Const. period (years)	5	3	3160	-8	89	-7
18	Seawater pump cost expectations	Pump cost expected	Optimistic	Conservative	3540	+3	99	+3
19	Overload capacity	Overload capacity	Yes	No	3390	-1	103	+7
20	Modules per platform	Modules per platform	8	16	3620	+6	101	+5
21	Modules per platform	Modules per platform	8	40	4010	+17	111	+16
22	Fouling factor doubled	Fouling factor[a]	C=.0001 E=.00025	C=.0002 E=.00050	3610	+5	101	+5
23	Chlorination fraction increase to 1 ppm	Chlorination	C=.00000010 E=.00000025	C=.0000010 E=.0000010	3780	+10	105	+10
24	Maintenance availability	Maintenance availability factor	.9	.8	3430	0	108	+12
25	Maintenance availability	Maintenance availability factor	.9	.7	3430	0	123	+28
26	O&M costs doubled	Fixed O&M factor Variable O&M factor	16.0 1.5	32.0 3.0	3430	0	103	+8

Table 5--Continued

Case ID Number	Title	Variable Changes			Capital Cost		COE	
		Variable	Old Value	New Value	$/kWe	% Change	Mills/kWh	% Change
27	Tube material	Tube material Tube thickness	Titanium .028	Aluminum .083	3660	+7	102	+6
		Wilson plot intercept	C=.00073[a] E=.00041	C=.00059 E=.00027				
		Wilson plot slope	C=.00420 E=.00385	C=.00410 E=.00376				
28	Tube outside diameter	Tube outside diameter	1	2	3780	+10	105	+9
		Wilson plot intercept	C=.00073 E=.00041	C=.00073 E=.00041				
		Wilson plot slope	C=.00420 E=.00385	C=.00485 E=.00445				
29	Vertical HXs	HX orientation HX pairs per module	Horizontal 1	Vertical 5	3210	-6	90	-6
		Enhancement	C=none E=linde	C=flute E=flute				
		Mech. cleaning type Assorted thermal	none	TRW brushes				
30	HX type	HX type	Tube & shell	Plate	2960	-14	87	-9
		Plate material Plate design Assorted thermal	-- --	Titanium Gasketed				
31	Low cost	Case 30 changes CWP material Contingency factor Construction period Tax preference	-- Steel .15 5 --	-- FRP 0 4 3.24%	2330	-32	60	-37
32	Temp. variation	Warm water temp. in	80°F	81°F	3330	-3	93	-3
33	Temp. variation	Cold water temp. in	40°F	41°F	3610	+5	101	+5
34	Water-side heat transfer enhancement	Wilson plot slope	C=.00420 E=.00385	C=.00159 E=.00160	2940	-14	83	-14
35	Water-side heat transfer enhancement	Case 34 changes Tube enhancement fixed cost component	-- C=0 E=.07	-- C=0 E=.14	3140	-8	88	-8
		Tube enhancement variable cost component	C=0 E=.61	C=.41 E=1.22				

[a] C = condenser; E = evaporator.

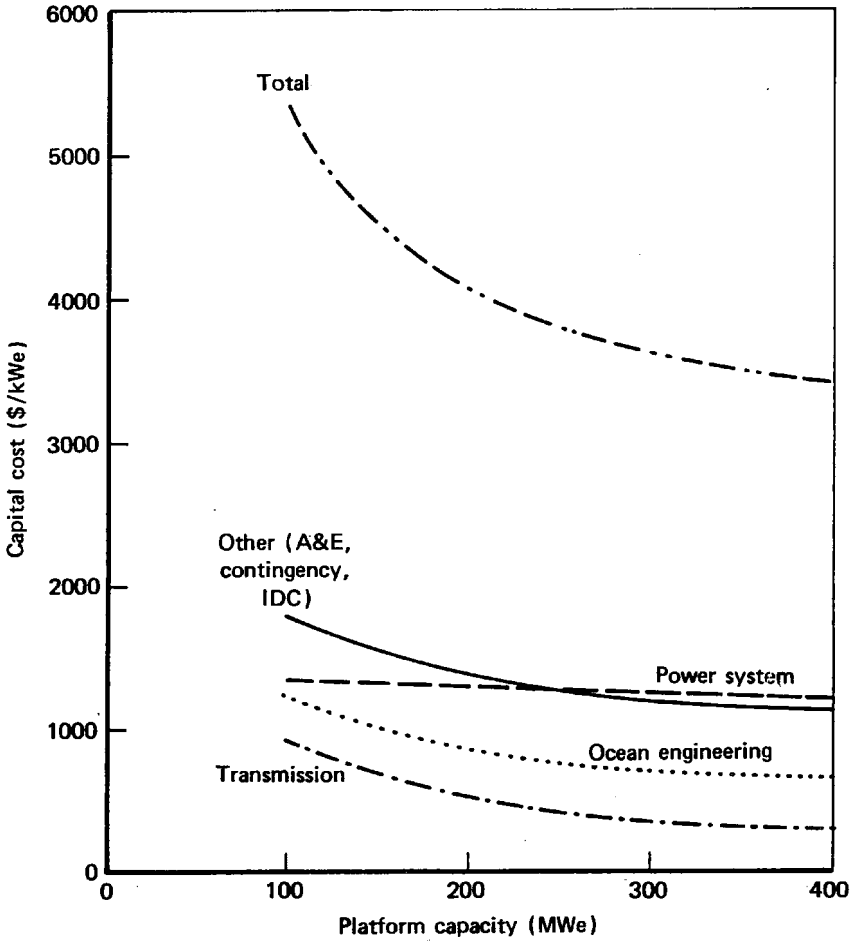

Fig. 21—Capital cost as a function of platform capacity

of other difficulties which cause cost increases in their own right. Thus, the 8 percent increase in capital cost associated with a longer construction period would more than likely be a minimum value.

Overload Capacity. The results of Case 19 suggest a 7 percent increase in COE if the generators, rectifiers, transmission cable, and inverters are not designed to accommodate an overload electrical capacity (during periods of peak temperature difference). This is because the small capital savings achieved by not overdesigning are more than offset by the lost production capability:

	Annual Production (kWh)
With overload capability	2.78×10^9
Without overload capability	2.60×10^9

Table 6

COST COMPARISON FOR ALTERNATIVE SITES

Capital Cost ($/kWe)	*Tampa*	*New Orleans*
Power system	1230	1270
Ocean engineering	740	700
Transmission	330	230
Other (A&E, IDC, and contingency)	1130	1080
Total	3430	3280
Cost of Electricity (mills/kWh)		
Capital	89	99
O&M	7	8
Total	96	107
Production (kWh/year)	2.78×10^9	2.40×10^9

Modules per Platform. Cases 20 and 21 suggest that modules should be built to their maximum feasible capacity as dictated by appropriate engineering design considerations. A greater number of smaller modules result in diseconomies of scale (with respect to capital cost) for the ammonia loop components, seawater pumps, turbines, and generators. Additionally, packing (platform volume requirements) of a greater number of smaller modules is generally estimated to be less efficient than the packing of a fewer number of larger modules.

Biofouling. Cases 22 and 23 indicate that the system cost is not very sensitive to fairly substantial variations in biofouling parameters. A doubling of the evaporator and condenser fouling factors causes a 5 percent increase in system cost. For chlorination requirements, a tenfold increase in the condenser plus a fourfold increase in the evaporator result in a 10 percent increase in the total system cost.

Maintenance Availability. As mentioned previously, this study has not been concerned with O&M factors such as maintenance availability. However, the results of Cases 24 and 25, which are shown in Fig. 22, clearly indicate the criticality of this factor to the OTEC cost of electricity.

Tube Material. As indicated in Case 27, the substitution of aluminum for titanium as the tube material results in an increase in

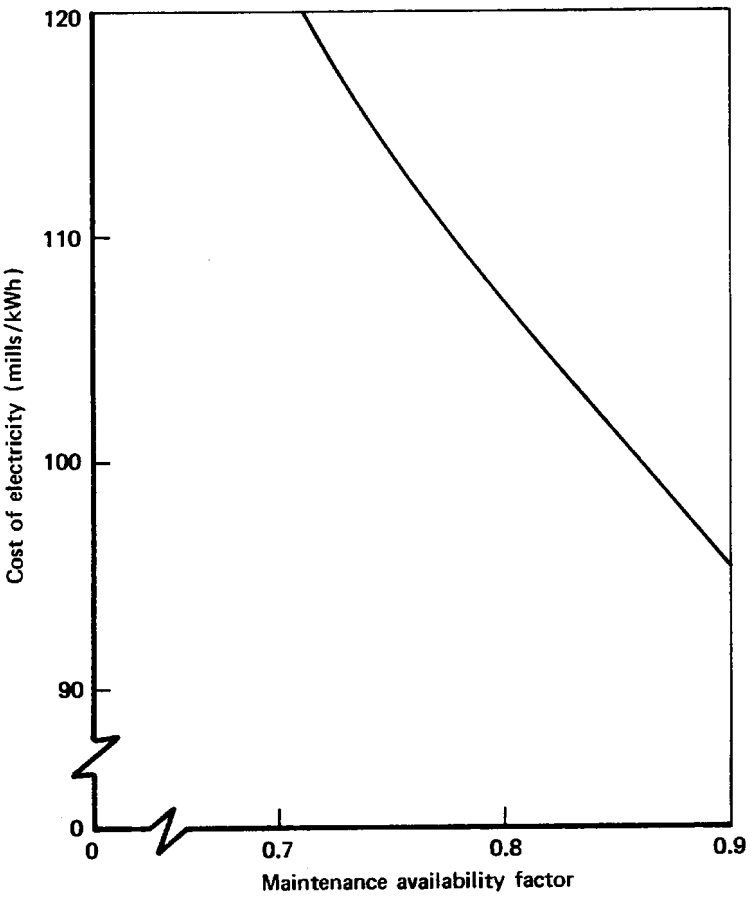

Fig. 22—COE as a function of maintenance availability factor

capital cost of 7 percent and a COE of 6 percent. Although the aluminum heat exchangers are cheaper than the titanium heat exchangers on a one-for-one basis, it is estimated that they will have to be replaced twice over the facility life of 30 years. It is the cost of this interim replacement that makes the aluminum option more expensive.

Vertical Heat Exchangers. The use of vertically oriented tube-and-shell heat exchangers (Case 29) reduces both capital cost and COE by 6 percent. The vertical heat exchangers are generally estimated to be smaller than their horizontal counterparts, resulting directly in reduced heat exchanger costs and indirectly in reduced platform costs.

Heat Exchanger Types. The switch from a titanium tube-and-shell heat exchanger to a titanium plate heat exchanger (Case 30) results in

a capital cost reduction of 14 percent and a COE reduction of 9 percent. The plate heat exchanger, which is considerably more compact than the tube-and-shell heat exchanger, results directly in reduced heat exchanger costs and indirectly in reduced platform, CWP, and mooring costs (ocean engineering components), as illustrated in Table 7.

Table 7

COST COMPARISON FOR DIFFERENT HEAT EXCHANGER CONFIGURATIONS

($/kWe)

	Tube and Shell	*Plate*
Heat exchangers	840	610
Balance of power system	390	420
Ocean engineering	740	630
Transmission	330	330
Other (A&E, IDC, and contingency)	1130	970
Total	3430	2960

However, part of this capital savings is offset by the *estimated* higher O&M costs caused by the more extensive cleaning requirements (closed-loop detergent once every 28 days; disassembly at some longer interval).

(Mills/kWh)

	Tube and Shell	*Plate*
Capital	89	79
O&M	7	8
Total cost of electricity	96	87

Low Cost. The low-cost case (31) is defined as follows:

- Use of projected low-cost components:
  - Plate heat exchanger
  - FRP cold-water pipe
- No unknowns during construction (elimination of contingency)

- o Construction period of 4 years
- o Tax preference of 3.24 percent (fixed charge rate reduced from 18 percent to 15 percent).

The result of these assumptions is to reduce capital cost by 32 percent (to $2330/kWe) and the cost of electricity by 37 percent (to 60 mills/kWh).

Water-Side Heat Transfer Enhancement. The performance and cost estimation program developed for OTEC has been applied to estimate the potential effect of water-side heat transfer enhancement on the system performance and cost (Cases 34 and 35). Using the general approach outlined in Appendix B, the effects of water-side enhancement on cost are found to be favorable, resulting in a reduction of system capital cost on the order of 8 to 14 percent of the base case, depending on the cost of incorporating the required tube roughness. Note that these two cases utilize fouling factors and chlorination requirements identical to the reference case. Any complex cleaning requirements which may be entailed by this type of enhancement have not been accounted for.

IV. CONCLUDING REMARKS

The evaluation of a complex advanced technology like OTEC requires *a total system approach*. This is necessary to uncover R&D disparities, if any, among major critical systems and to provide for the necessary interaction among the subsystems so as not to result in suboptimizations that may jeopardize an otherwise viable program. This study has examined two important system issues: the engineering uncertainties surrounding major component subsystems and the sensitivities of cost estimates to such uncertainties. It has focused on closed-cycle OTEC for delivery of electric power in the United States. System-level analyses of performance and cost of complete commercial OTEC systems have been made using inputs from component analyses and thermal-resource data for sites in the Gulf of Mexico, feeding the west coast of Florida and New Orleans areas.

A reference design was selected to provide a datum for comparison and sensitivity analysis. It is a plant with a platform capacity of 400 MWe approximately 150 n mi west of Tampa, Florida. The power system is based on a tube-and-shell heat exchanger using titanium for tube material. The total system capital cost has been estimated at $3400 per kWe in 1978 dollars at start of operation. Of this, the power system accounts for 36 percent, the ocean system 21 percent, and the transmission system 10 percent. The remainder ($\sim$ 33 percent) includes interest during construction (20 percent), contingency (10 percent), and architect and engineer services (3 percent).

Within the power system, the heat exchangers represent 25 percent of the cost. Thus, it represents an important cost element, but is by no means the sole driving force of the system cost. The research and development of advanced heat exchangers constitute a large portion of DOE's current OTEC program effort.

In state-of-the-art heat exchangers, warm water flows through a series of tubes and ammonia flows along the outside of the tubes. A large envelope known as a shell contains the pressurized ammonia. The heat transfer efficiency of such an exchanger can be enhanced using

tubes with special surfaces. Current DOE OTEC research programs on heat exchanger enhancement are concentrated on the ammonia vapor side of the tube-and-shell heat exchanger. Enhancement on the water side is a technical opportunity that awaits exploitation. Preliminary analysis shows that the effect can be impressive, leading to a possible reduction of capital cost by 8 to 15 percent depending on the cost of incorporating the required tube roughness. Serious efforts to verify calculated performance, cleanability, and producibility of the enhanced surfaces are warranted.

If ammonia is permitted to flow on the inside of the tubes and water on the outside, the shell can be eliminated. This is referred to as the plate-type heat exchanger. Plate-type heat exchangers cost less than the shell-and-tube variety but have a lower heat transfer efficiency. The plate-type heat exchanger constitutes an important R&D element in the present OTEC program. Our analysis indicates their use may reduce capital cost by perhaps 15 percent.

All OTEC heat exchangers will be susceptible to biofouling, the buildup of marine organisms on tube surfaces. Biofouling reduces heat transfer efficiency. Studies indicate that biofouling can be controlled by mechanical methods employing brushes, sponge rubber balls, slurries, or water jets. Consideration is also given to the potential use of chemicals such as chlorine to inhibit biofouling.

Compared to standard practices in marine power plants that circulate seawater, OTEC's requirements for controlling biofouling are much more stringent because OTEC operates with a much lower thermal gradient.

Reasonable control of biofouling is vital to the satisfactory performance of heat exchangers in a closed-cycle OTEC. Early ocean tests have been encouraging. Biofouling rates in the open ocean appear to be less than those in coastal regions. The effect of the biofouling factor on cost is moderate; we find that a 100 percent increase in fouling factor from the baseline for the evaporator and condenser causes a 5 percent increase in system cost. This estimate of sensitivity, however, must be qualified since it does not account for possible design

problems resulting from cleaning requirements, perturbations in flow patterns, and other considerations.

A wide range of cleaning concepts has been suggested to deal with biofouling. Mechanical cleaning methods are likely to be effective, although experimental evidence is needed to confirm this encouraging trend. Heat transfer enhancement using special surfaces aggravates the biofouling problem. Feasibility and effectiveness of mechanical cleaning methods will be severely taxed in both enhanced tube designs and plate-type heat exchangers.

Chemical controls are effective for macro-fouling. Many designs rely on chlorination, but owing to the large quantity of chlorine involved (a discharge of 5000 lb/hr, for a 400 MW plant), this method of controlling biofouling will be subject to regulatory policies. On the other hand, as in the case of the biofouling factor, total system cost is not very sensitive to chlorination requirements. A tenfold increase in condenser chlorination requirements plus a fourfold increase in evaporator chlorination requirements resulted in a 10 percent increase in the system cost.

The cost, life, and corrosion resistance of heat exchanger materials are important. Aluminum, titanium, and other metals are candidates. Aluminum is inexpensive, but it will be susceptible to corrosion and thus may not last long enough to amortize its initial cost. Titanium has a higher initial cost than aluminum but resists corrosion better and thus will last longer. The use of aluminum requires interim replacement, which makes this option more expensive--an increase in capital cost of 7 percent and COE of 6 percent.

The OTEC submarine transmission cable and cold-water intake pipe also pose significant engineering challenges. The massive cold-water pipe for a plant in the 250 to 400 MWe range will have dimensions never before attempted. It is expected that developments in off-shore technology, particularly the designs and accomplishments of the petroleum industry, will play an important role in the development of structures for the OTEC ocean system.

The cold-water pipe, its fabrication, deployment, and coupling to the platform will require a concerted engineering effort to produce advances beyond the state of the art. For small plants (10 to 40 MW) the problems are not likely to be critical. Where commercial-scale plants are concerned, however, considerably more effort will be necessary. Material is an important consideration not only because of the structural loadings that must be withstood but also because of the cost resulting from the sheer size and volume in question. Four types of material have been considered in this analysis: steel, concrete, elastomer, and fiberglass-reinforced plastic (FRP). Steel is the most expensive and FRP the least, resulting in a reduction of 5 percent in the capital cost and 4 percent in COE. Design concepts vary widely and probably cannot be established until more experimental data become available from R&D programs yielding scalable results. As a result, cost estimates for the cold-water pipe are highly uncertain.

The underwater cable that transmits OTEC power to shore will have to be designed for unusual conditions. The bottom cable will be located at great depth and may have to extend as far as 200 miles. The riser portion of the cable will have to rise several thousand feet from the ocean floor to the OTEC platform, where it will be attached in a way that permits platform motions that could be significant. As in the case of the cold-water pipe, cost estimates for the submarine cables are tentative in this analysis; there are significant engineering uncertainties, particularly in the riser cable. Although a submerged or pendant buoy approach for the riser cable has been selected by DOE's principal contractor, its optimal configuration has yet to be established. Advances in cable technology are crucial to the success of the mainland power mission. Acceleration of cable development should reduce cost uncertainty, which is probably greater for this component than for any other in the program.

The technological risk will be much reduced once a demonstration article of appropriate scale has been operated at sea for some time. At present, both the proliferation of concepts for the cold-water pipe and the dearth of concepts for riser cable configuration indicate the engineering uncertainties and the limits of our analytical capability to fully study the problems.

The OTEC plant is a complex system with a very large number of components. No single component dominates the cost of the total system; neither should it be expected that perturbations of any single engineering or cost variable will cause dramatic changes in the total system cost. In fact, the cost sensitivity of the total system to any one variable is small. For instance, an increment of one percent in any of the engineering and cost variables considered resulted in a variation of the system cost of less than one-fourth of one percent. Nevertheless, it is of interest to note that among the thermodynamic variables, the water-side heat transfer effectiveness and the water pump efficiency have the greatest impact on total system cost.

Like most advanced technologies, OTEC has been the subject of conflicting statements and wide and differing ranges of cost estimates. Most of the major OTEC issues, particularly those dealing with financing schemes and market penetration, cannot be resolved at this early stage of R&D. Cost variations resulting from major changes in the design concepts, however, have been estimated in this study. Figure 23 and Table 8 illustrate some of the results.

Questions of economic feasibility are related first to component costs (dollars per kW) and ultimately to energy costs (mills per kW-hours). Plant costs estimated by various contractors have ranged over a factor of 4. Our estimate of the total system capital cost for the reference case with tube-and-shell heat exchangers is $3430 per kWe (in 1978 dollars). A lower estimate of $2500 per kWe is achieved with the use of projected low-cost components such as plate-type heat exchangers and a FRP cold-water pipe, the elimination of contingency costs, and a shorter (four-year) construction period. Honest differences exist among independent cost estimates. In most cases, these differences can be readily isolated and explained. In a concept like OTEC in which there is no actual cost experience, the estimates tend to be sizeable extrapolations from (sometimes remotely) related work. The completeness as well as the rationality of such extrapolations are additional sources of uncertainty.

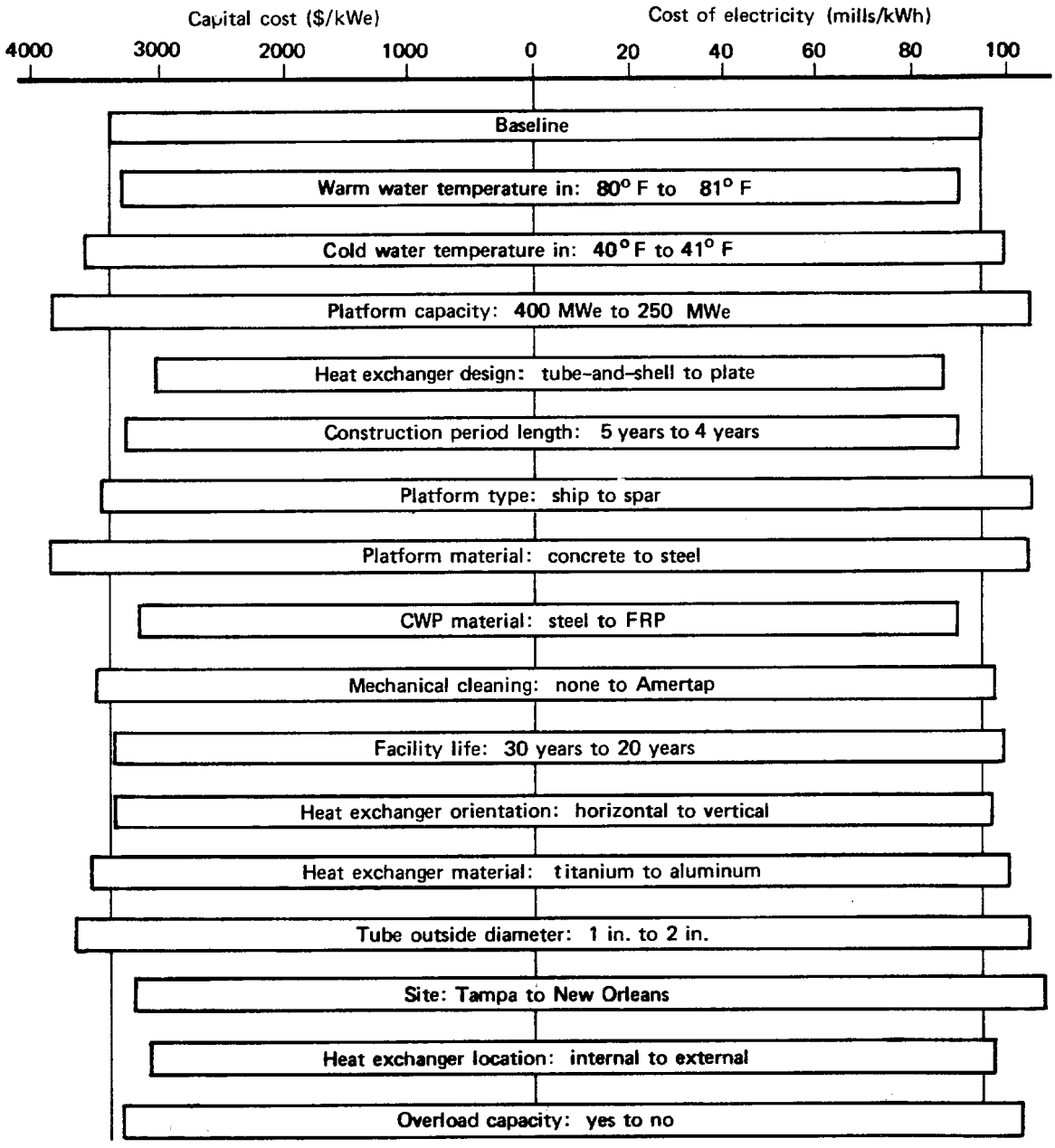

Fig. 23 — Cost variations due to major changes

Table 8

COST VARIATIONS DUE TO MAJOR CHANGES

Variation	Percent Change	
	Capital Cost ($/kW)	COE (Mills/kWh)
Site: New Orleans vs. Tampa	-4	+12
Heat exchanger location: external vs. internal	-7	+1
Overload capacity: no vs. yes	-1	+7

Estimates of OTEC cost of electricity are highly uncertain. Quoted energy costs below 60 mills per kWh are probably optimistic. The economic viability of the OTEC system is a very sensitive function of the plant's availability. High availability may be aided by modularity and on-line cleaning, though conditions peculiar to ocean operation introduce more uncertainties. Note, however, that it is the capacity factor, the product of availability, and a second factor related to the seasonal variation of the surface-to-bottom temperature difference (10 percent reduction in this quantity leads to about a 50 percent loss in output) that determines power cost. Capacity factors of 60 to 80 percent are estimated for the Gulf region.

Summarizing, the power system and the platform appear to be within the state of the art, although opportunities for water-side heat transfer enhancement in the heat exchangers still await exploitation. Mooring and station-keeping technologies require further development and adaptation. The submarine cable system and cold-water pipe (CWP) present major technical risks. The cable design parameters remain uncertain; the optimal configuration for the riser cable needs to be established and validated. A major development program including large-scale tests may be necessary to validate cold-water pipe designs. Materials such as fiberglass-reinforced plastic appear promising, but a more extensive data base than is currently available needs to be developed, particularly on fatigue properties. Both the CWP and the

riser cable are amenable to numerical analysis. The amount of engineering information that can be generated with appropriate computer modeling could be extremely useful, as well as cost effective, in complementing the necessary experimental work. A systematic effort in this direction is required.

Independent estimates of the total system cost differ but remain comparable. No single component dominates or determines the cost of the system. Such estimates are highly sensitive to costing methodologies and financing schemes and incentives. Among the three major subsystems, estimates for the cold-water pipe and underwater cable are much more uncertain compared with that for the power system.

Appendix A

HEAT EXCHANGER DESIGN FACTORS: A GRAPHICAL METHOD

For the types of heat exchangers applicable to the OTEC concept, the heat transferred may be expressed as

$$q = UA\,\Delta T_{LM} = \dot{m}c_p(T_1 - T_2) = \dot{m}c_p\,\Delta T_{in}\,(1 - \exp\,[-\,UA/\dot{m}c_p]) \qquad (A.1)$$

where U = overall heat transfer coefficient

A = heat transfer area

ΔT_{LM} = log-mean temperature difference

$\dot{m}$ = mass flow rate of water

C_p = specific heat

$(T_1 - T_2)$ = water temperature change

ΔT_{in} = temperature difference between inlet water and ammonia streams

e = base of natural logarithms

The overall heat transfer coefficient, U, is a function of the individual heat transfer coefficients of the several resistances

$$\frac{1}{U} = \frac{1}{h_{NH_3}} + \frac{1}{h_{wall}} + \frac{1}{h_F} + \frac{1}{h_{H_2O}} \qquad (A.2)$$

where the h's denote the heat transfer coefficients of the ammonia evaporation or condensation, the tube wall, the water-side fouling, and the water convective cooling or heating, respectively.

For a given heat quantity and water flow rate, the required heat transfer area is inversely proportional to the overall heat transfer coefficient. Thus any increase in overall heat transfer coefficient results in a decreased requirement for heat transfer area. Typical values of the individual heat transfer coefficients are listed in Table A.1 for OTEC shell-and-tube heat exchangers, along with the

Table A.1

TYPICAL VALUES OF HEAT TRANSFER COEFFICIENTS[a]
AND ENHANCEMENT POSSIBILITIES

(OTEC shell-and-tube heat exchangers)

Coefficient	Typical Values (Approximate)		Enhancement Possibilities (Approximate)	
	Minimum	Maximum	Minimum	Maximum
h_{NH_3}	1500		3×	5×
h_{wall}	5,000	10,000		
h_F	2,000	5,000		
h_{H_2O}	600	1,000	2×	3×
U	330	508		
U[b]			386	698
U[c]			570	1,304

[a]The units of the heat transfer coefficients are those of the English engineering system, Btu/(hr)(sq ft)(°F), which seem to be those used in OTEC calculations. For conversion to the metric S.I. system, W/(m^2)(°C), multiply by 5.6784.

[b]With ammonia-side enhancement.

[c]With both ammonia- and water-side enhancements.

enhancement possibilities. Overall heat transfer coefficients with only ammonia-side enhancement result in increases of 17 to 37 percent over the unenhanced values. If water-side enhancement is also used, *additional* increases of 48 to 87 percent result. Thus enhancement on both sides can result in an approximate doubling of the overall heat transfer coefficient and a consequent halving of the required heat transfer area.

Actually the direct trade-off of overall coefficient and area is too restrictive and does not take account of the effects of varying water flow rate. One should include the possibility of varying the water flow rate in the OTEC heat exchangers, both because of the effect on the required area and because of the appreciable power required for

water pumping. The various complex trade-offs possible for the OTEC heat exchangers are perhaps best seen by examining the last form of Eq. (A.1):

$$\frac{q}{\Delta T_{in}} = \dot{m}c_p \left(1 - \exp\left[- UA/\dot{m}c_p\right]\right) \qquad (A.3)$$

As written in this form, the specified quantities are on the left and the design variables are on the right. The relation of these variables is illustrated in Fig. A.1, where UA is plotted versus $\dot{m}c_p$ with lines of constant $q/\Delta T_{in}$ and of constant $UA/\dot{m}c_p$. For a given specified design value of $q/\Delta T_{in}$ (required heat to be transferred and available temperature difference), there is a minimum value of UA below which the design requirement cannot be satisfied regardless of the water flow rate. Similarly there is a minimum water flow rate below which the design requirement cannot be satisfied no matter how high UA may be. The design values of these two quantities must then lie above these minimum values. Typical designs have values of 1.5 to 2 times these minima.

The type of diagram in Fig. A.1 is particularly useful for visualizing the design trade-offs possible in the OTEC heat exchangers. For a given specified heat quantity and a given available temperature difference, a design is confined to the central line on Fig. A.1. Sliding up and down this line involves trade-offs between degree of enhancement (U), the heat exchanger area (A), and the water flow rate ($\dot{m}$). Cost considerations of these three factors will dictate where on this line an optimum design lies. This diagram is also useful for depicting the effects of the annual transients in available temperature difference and the effects of the buildup of biofouling; both of these can be countered (e.g., to keep the heat quantity constant) to some extent by adjustment of the water flow rate.

Going further into the details of the heat exchanger design and the effect of various design parameters on performance, the vaporizing and condensing side heat transfer coefficients are usually determined empirically by, e.g., the Wilson-plot procedure (Coombs and Murphy,

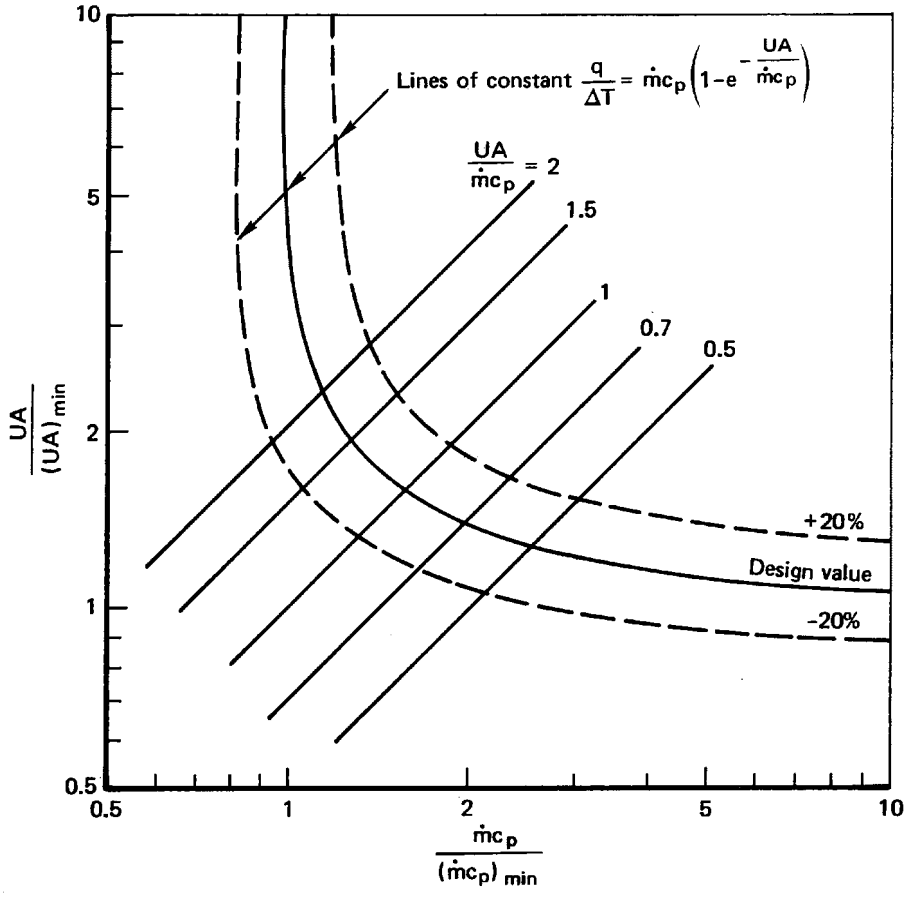

Fig. A.1 — Relationship between U, A, and m in heat exchanger design

-1978). Various techniques of enhancing these coefficients have been developed. In the case of the evaporator, these appear to be either the use of proprietary porous surfaces to provide additional nucleation sites for boiling or provide a flow mechanism for direct evaporation from the surface of a thin film. As indicated in Table A.1, these techniques provide enhancement by a factor of three to five.

Except for the effects of biofouling, the water-side heat transfer coefficients in unenhanced tubes and passages are more predictable. Although the classic Dittus-Boelter equation (see e.g., Chapman, 1974)

$$c_H = 0.023\ Pr^{-0.6} Re^{-0.2}$$

is frequently used, it is more accurate* to use a modified† form of the Petukov equation (Petukov, 1964)

$$\frac{(c_F/2c_H) - 1}{\sqrt{c_F/2}} = 13.13\ (Pr^{2/3} - 1) \qquad (A.5)$$

where c_H = dimensionless heat transfer coefficient = $h/c_p \rho V$
h = heat transfer coefficient
ρ = fluid density
V = fluid velocity
Pr = Prandtl number = $c_p(\mu/k)$
μ = viscosity
k = thermal conductivity
Re = Reynolds number = $D\rho V/\mu$
D = tube diameter, or passage equivalent diameter
$c_F = \tau_w/\frac{1}{2}\rho V^2$
τ_w = shear stress at wall

The dimensionless friction coefficient for smooth passages is expressed by the classic Prandtl-Nikuradse expression (Nikuradse, 1932)

$$\frac{1}{\sqrt{c_F}} = 4.0 \log_{10}(Re \sqrt{c_F}) - 0.40 \qquad (A.6)$$

*For example, the Petukov equation represents the recent Argonne data for the Union Carbide evaporator (Lewis and Sather, 1978) better than does the Dittus-Boelter equation; this appears to account for the apparent discrepancy between "theory" and experiment.

†The original coefficients have been modified slightly to yield the Reynolds analogy $c_H = c_F/2$ at $Pr = 1$.

The pressure drop through the tube or passage is

$$\Delta p = 4c_F \frac{L}{D} \frac{\rho V^2}{2} \tag{A.7}$$

and the water pumping power (not including entrance and exit losses) for an exchanger, having N tubes of length L, is

$$P = \Delta p \; N \frac{\pi}{4} D^2 V = c_F A \frac{\rho V^3}{2} \tag{A.8}$$

Note that the heat transfer area

$$A = N\pi DL, \tag{A.9}$$

the water mass flow rate

$$\dot{m} = N \frac{\pi}{4} D^2 \rho V, \tag{A.10}$$

and the number, diameter, and length of the tubes are all interrelated.

In the case of heat transfer enhancement on the water side of an OTEC heat exchanger, the relations presented above (Eqs. (A.4), (A.5), and (A.6)) for smooth tubes and passages may be modified. In the case of enhancement by an increase of surface area over that of a cylindrical tube (e.g., a fluted tube), these relations are approximately valid. For an enhancement involving a change in the convective heat transfer mechanism, these equations need to be modified.

Appendix B

HEAT EXCHANGE DESIGN OPTION AND WATER-SIDE ENHANCEMENT

To illustrate both some of the design options and the possible advantages of water-side enhancement discussed in Sec. II, we will consider a specific example in which an unenhanced shell-and-tube heat exchanger is modified by water-side enhancement. Denoting the unenhanced smooth-surface basic design by the subscript s and specifying an unchanged heat quantity, q, and available temperature difference, ΔT, Eq. (A.1) yields

$$\frac{q}{q_s} = 1.0 = \frac{\dot{m}}{\dot{m}_s} \cdot \frac{1 - e^{-\frac{\dot{m}_s}{\dot{m}} \frac{UA}{U_s A_s} \left(\frac{U_s A_s}{\dot{m}_s c_p} \right)}}{1 - e^{-\frac{U_s A_s}{\dot{m}_s c_p}}} \tag{B.1}$$

For this example, we choose

$$\frac{U_s A_s}{\dot{m}_s c_p} = 0.5$$

$$\frac{V}{V_s} = 0.8,\ 1.0$$

$$\frac{U_s}{h_s} = 0.8$$

$$D = \text{constant}$$

and assume a water-side enhancement which increases both the heat transfer and friction by a factor of two

$$\frac{c_H}{c_{H_s}} = \frac{c_F}{c_{F_s}} = 2.0$$

As will be seen later in this appendix, this appears to be possible (and even conservative) using certain types of surface roughness.

The results of this example are shown in Fig. B.1, where various design parameters, in ratio to the unenhanced values, are shown as functions of the parameter $UA/\dot{m}c_p$. If the velocity and $UA/\dot{m}c_p$ remain the same, the number of tubes and the mass flow rate are unchanged; however, the area and tube length are reduced by about 40 percent and the pumping power increased by about 20 percent.

A more interesting possibility is that represented by the dashed lines in the figure corresponding to a water velocity of 0.8, the unenhanced value, and an increase in $UA/\dot{m}c_p$ to about unity. In this case the mass flow is reduced by 40 percent and the area by 25 percent. The tube length is increased by about 10 percent.

As noted previously, the design selection will depend on the relative costs of heat transfer area and of pumping power, as well as on biofouling of the surface. Ultimately an optimization would have to take into account the performance of the enhanced heat transfer surface as a function of Reynolds number; the tube diameter and water velocity would be adjusted accordingly. This will be discussed below.

Although the example presented above was for a shell-and-tube heat exchanger, the same general trends would appear in the analysis of a plate heat exchanger for the effects of various design parameters.

The plate heat exchangers being considered in the current program have about the same overall heat transfer coefficient as the shell-and-tube exchangers and consequently about the same required heat transfer area; they are, however, much more compact. The design characteristics of plate heat exchangers are relatively unexplored and less generally understood, with some performance details either proprietary or undetermined. There also appear to be more uncertainties of the efficacy of cleaning the plate heat exchangers. In the case of the Lockheed/Alfa-Laval plate heat exchanger design (LMSC, 1979b), the ammonia-side and water-side heat transfer coefficients are comparable in value (i.e., the ammonia-side coefficient is smaller and the water-side coefficient is larger than the shell-and-tube values). The ammonia-side coefficient is also dependent on the ammonia mass flow rate and temperature. Heat

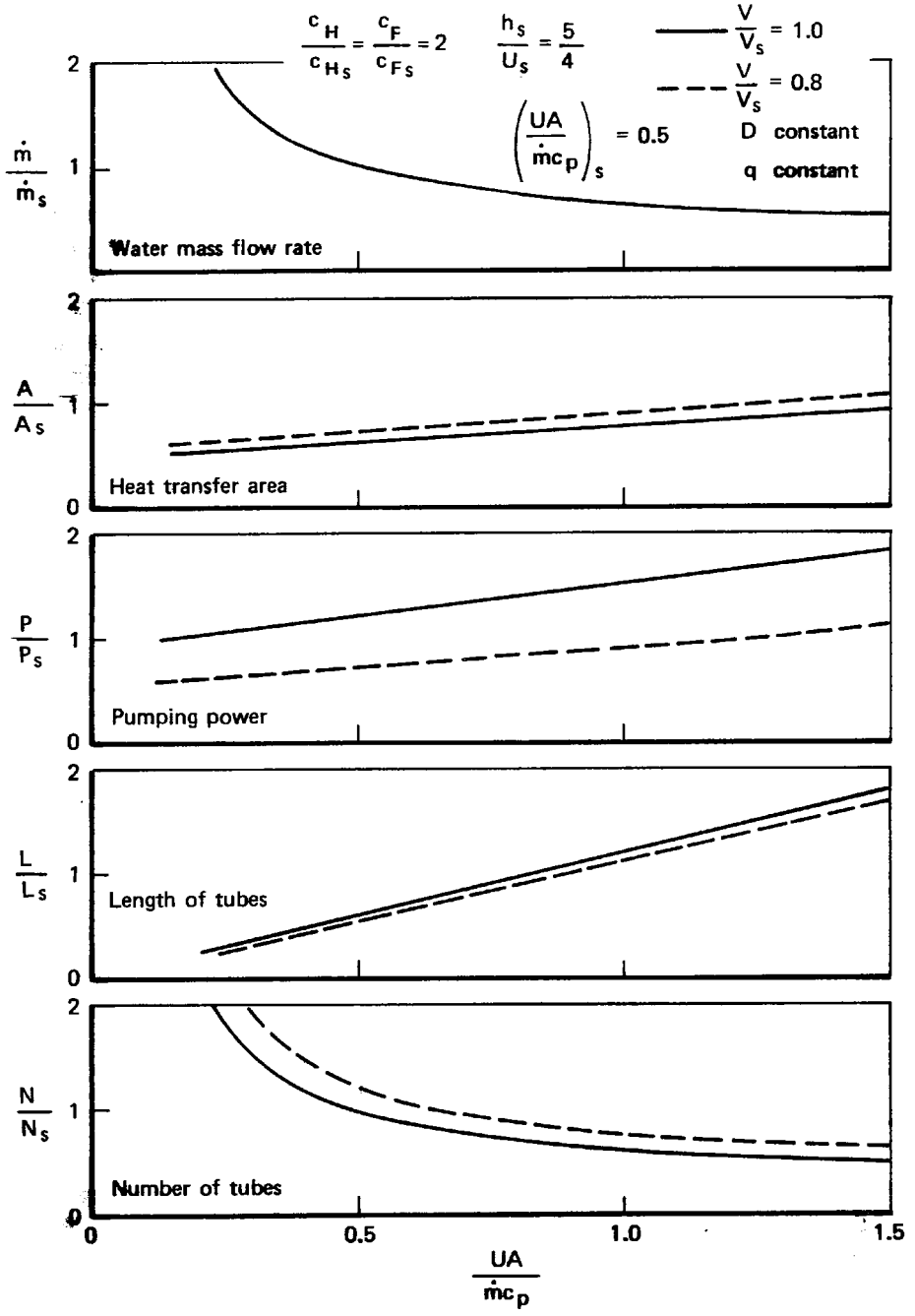

Fig. B.1 — Effects of water-side heat transfer enhancement on the design parameters of a shell-and-tube heat exchanger. Possible variation of these parameters is shown in ratio to their unenhanced number.

transfer enhancement in this exchanger consists of the corrugations in the plate surfaces which produce both an area increase and presumably increased heat transfer by film thinning on the ammonia side and increased turbulence on the water side.

Appendix C

CORRELATIONS FOR OVERALL HEAT TRANSFER COEFFICIENTS IN PLATE HEAT EXCHANGERS

For the condenser,

$$\frac{1}{\bar{U}} = .1084\left(\frac{A_{H_2O}/A_{NH_3}}{\dot{W}_{H_2O}/\dot{W}_{NH_3}}\,\rho_{H_2O}v_c 3600\right)^{-.5595} + 3.256\left(\rho_{H_2O}v_c\ 3600\right)^{-.667}$$

$$+ .002 + \text{fouling factor (hr ft}^2\ ^\circ\text{F/Btu}$$

The plate area per lb per sec of NH_3 flow (AHTC) is

$$AHTC = \frac{Q_{cond} \times \frac{1}{U} \times 3600}{\Delta T_{LM}}\ ft^2/lb/sec$$

The water flow pressure drop (DPPLTC) in the plate is (lb/in^2)

$$DPPLTC = 35.02 \times 10^{-12} \times \ell \times \left(\rho_{H_2O}v_c\ 3600\right)^{1.9}$$

The water flow entrance and exit losses (DPEXE) are (lb/in^2)

$$DPEXE = \frac{15\left(\rho_{H_2O}\right)v_c^{\ 2}}{2 \times 32.2 \times 144}$$

Similar expressions apply for the evaporator, again based on the Lockheed/Alfa-Laval correlations.

The water velocity in the heat exchangers (v_c above, or v_e for the evaporator) must be chosen so that the plate length ℓ (in the water

flow direction) is equal to the specified 4.5 ft. It is also given as a fraction of temperatures, water velocity, and plate spacing by

$$\ell = \frac{3600\ \rho_{H_2O} v_c \frac{S}{2} c\rho_{H_2O} \left(T_{w_i} - T_{w_o}\right)}{\bar{U}\ \Delta T_{LM}}$$

where S is the plate spacing in feet.

Appendix D
FOULING RESISTANCE

We consider an OTEC heat exchanger, where heat is exchanged between flowing water and condensing or evaporating ammonia (NH_3).

From Eq. (A.2),

$$\frac{1}{U} = \frac{1}{h_{NH_3}} + \frac{1}{h_{wall}} + r_F + \frac{1}{h_{H_2O}}$$

For both tube-and-shell and plate-and-shell heat exchangers, total heat transfer is $Q = UA\Delta T_{LM}$, where A is the heat transfer area, U is the overall heat transfer coefficient, and ΔT_{LM} is the log mean temperature difference, viz:

$$\left(T_{H_2O}\right)_{in} - \left(T_{H_2O}\right)_{out} \Big/ \ell n \left[\left(T_{H_2O}\right)_{in} - T_{NH_3} \Big/ \left(T_{H_2O}\right)_{out} - T_{NH_3}\right]$$

To illustrate the degradation in performance as a result of fouling, we calculate the dependence of total heat transfer on r_F when the inlet water temperature, flow rate, surface area, and ammonia-side temperature are fixed. We write $1/U = (1/U_o) + r_F$, where U_o refers to a clean surface value. Since

$$Q = \left[\left(T_{H_2O}\right)_{in} - \left(T_{H_2O}\right)\right]_{out} \cdot \dot{m}C_p$$

where $\dot{m}$ is the water flow rate, simple manipulation leads to

$$Q = \dot{m}C_p\left[\left(T_{H_2O}\right)_{in} - \left(T_{NH_3}\right)\right]\left[1 - e^{-\frac{UA}{\dot{m}C_p}}\right]$$

and

$$\frac{Q}{Q_o} = \frac{1 - e^{-\frac{UA}{\dot{m}C_p}}}{1 - e^{-\frac{UA}{\dot{m}C_p}}}$$

From the relation $U = U_o/(1 + r_F U_o)$, we can write $U/U_o \sim r_F U_o$. Thus heat exchanger performance is more sensitive to r_F at large values of U_o, and enhanced OTEC heat exchangers may suffer greater reductions than do conventional unenhanced systems.

Appendix E
OPTIMIZATION

To perform a quantitative evaluation, the total OTEC system is modeled so that the algorithms are flexible enough to accommodate a variety of system designs. At the same time, they are detailed enough to provide a reasonably accurate portrayal of the system's performance.

The power system is modeled by building on the thermodynamic and cycle analysis discussed in Sec. II. This includes the working fluid and heat exchanger performances, power requirements for warm-water and cold-water pumps, and generator net power output. The design parameters for the ocean system are interfaced with power system requirements in the sizing algorithms. A separate set of algorithms provides the calculations for the transmission system.

The outputs from the engineering models of the three major subsystems form the bases for the cost estimating algorithm (see Sec. III). These are then linked together to form the total system cost equation which is used as the objective function to be minimized in the optimization process.

The sequential unconstrained minimization technique (SUMT) (Fiacco and McCormick, 1968; Mylander et al., 1971) used in this analysis is probably the best known of the interior penalty methods for solving nonlinear programming problems. The version used here requires a set of user subroutines derived from the engineering and cost models. They provide the computation of the specific problem function, the gradient of the functions, input routines and specifications of parameters, options, and tolerances.

The optimization problem is formulated in the following form:

$$\begin{aligned} &\text{Minimize} && f(X) \\ &\text{Subject to} && g_i(X) \geq 0,\ i = 1, 2, \ldots, m \\ & && h_i(X) = 0,\ i = mH, \ldots, m + n \end{aligned}$$

where the elements of X are the decision variables entering into the designs and performance calculations in the engineering and cost models. In the present formulation for the OTEC system, the necessary regularity and convexity conditions have been met. The theoretical requirements for SUMT to be guaranteed to find a local minimum include the existence of point(s) which satisfy the inequality constraints and that there not be a local minimum at points where the X vector goes to infinity. Furthermore, if certain convex conditions are satisfied, then the local minimum found is a global minimum.

SUMT uses a penalty function to transform the constrained optimization problem into a sequence of unconstrained problems of the form:

$$P(X,r) = f(X) - r \sum_{i=1}^{m} \ln g_i(X) + \frac{1}{r} \sum_{i=m+1}^{m+n} [h_i(X)]^2$$

where P(X,r) becomes the function to be minimized. The inequality constraints cause a large penalty to occur as a boundary is approached. The equality constraints add a large penalty whenever h(X) departs from 0 in either direction. The size of the penalties is controlled by an arbitrary parameter, r. The algorithm solves the problem by solving a series of subproblems for $r_1 > r_2 > r_x \ldots > 0$. SUMT minimizes $P(X,r_n)$ in each subproblem to find the minimum of f(X) as r tends to 0. When a minimum of a subproblem is found, r is reduced by a factor assigned by the user, and the new subproblem is solved. The process continues until the convergence criteria chosen by the user is satisfied. Figure E.1 shows the computational sequence. Figure E.2 illustrates schematically the results of the sequence of subproblems and the notional shape of the penalty function.

As implemented in this study, the computations for both the objective function, i.e. total system capital cost or bus-bar cost of electricity, and the constraints, are indirect. That is to say, the independent variables over which the cost is minimized do not appear explicitly in the objective function or the constraints but rather enter into a series of intermediary calculations that link the engineering analyses and synthesis of the total system to a battery of cost estimating

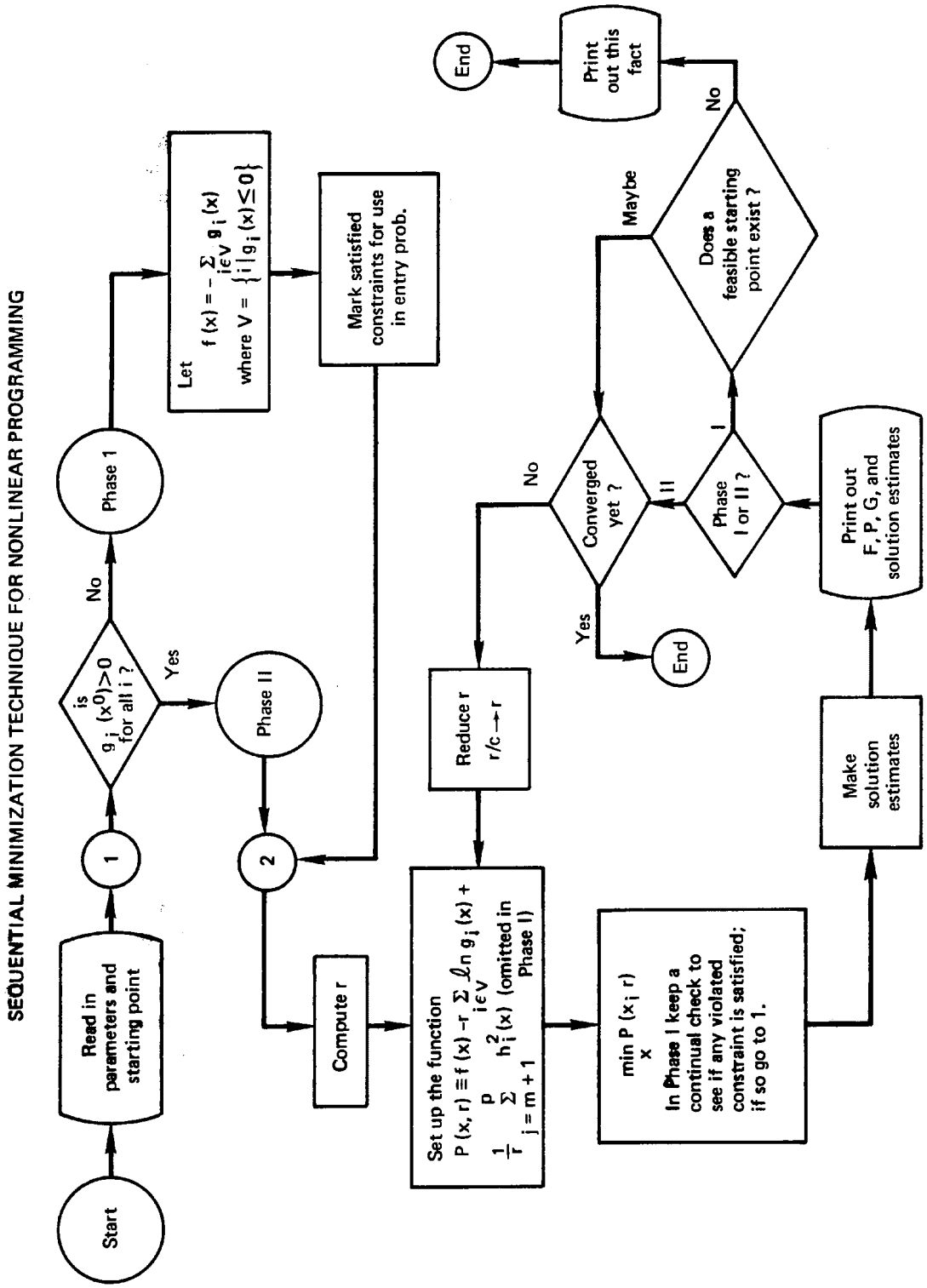

Fig. E.1—SUMT flow chart

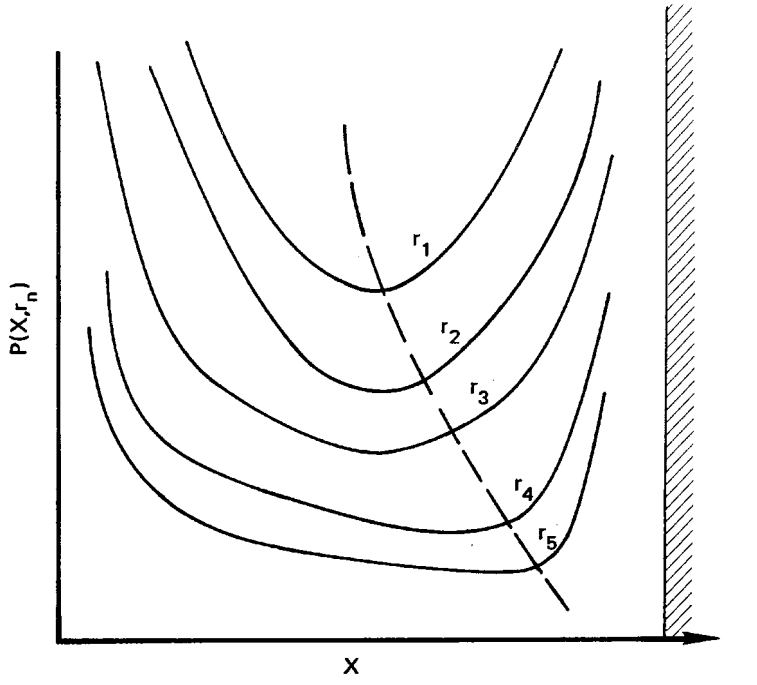

Fig. E.2 — SUMT sequence

relationships (CER). These in turn are combined to form the final objective function. In this manner, the resulting model retains maximum flexibility over the choice of design parameters and CER.

SUMT can efficiently converge to an optimum over as many as 100 independent variables. In its most aggregate form, the OTEC thermodynamic system design can be satisfactorily characterized by six engineering parameters: The outlet seawater temperatures of the evaporator and the condenser (TWWO, TCWO), the inlet and exit temperatures of the working fluid (T6, T7), and the water velocities in the condenser and the evaporator (VELC, VELE). Optimization of the total system cost over the variables subject to appropriate constraints governing the valid temperature ranges, the nonnegativity of net power produced, etc., has been found to be satisfactory when compared to a much more detailed formulation including a larger number of independent variables such as tube diameters. It was subsequently decided that variations of other engineering and cost parameters can be adequately handled by reoptimization. The results of such variations are given in Sec. III.

It was also found that the nonlinear problem formulated for OTEC is well behaved. Figures E.3, E.4, and E.5 show selected two-dimensional iso-cost contours. It can be readily seen that the problem is convex and the regularity conditions are satisfied within the range of interest of the variables.

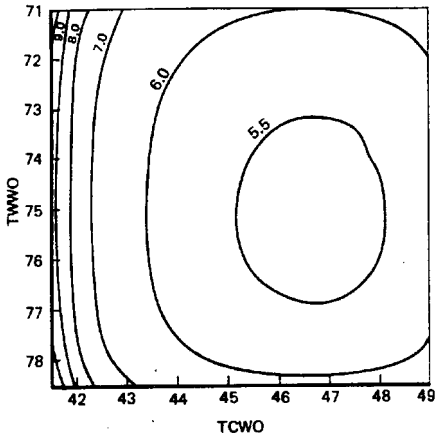

Fig. E.3—Iso-cost contours for constant T6, T7, VELC, and VELE

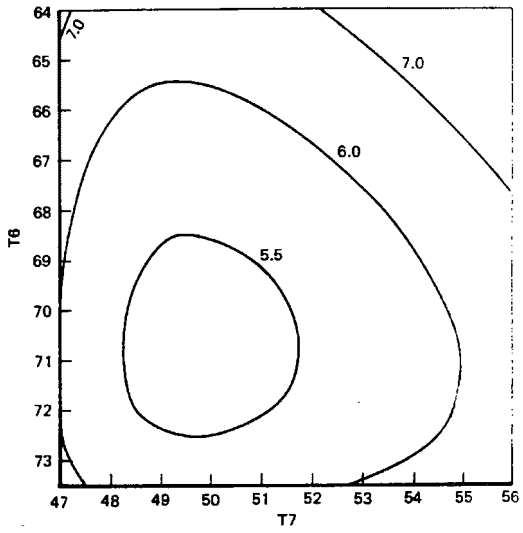

Fig. E.4— Iso-cost contours for constant TWWO, TCWO, VELC, and TELE

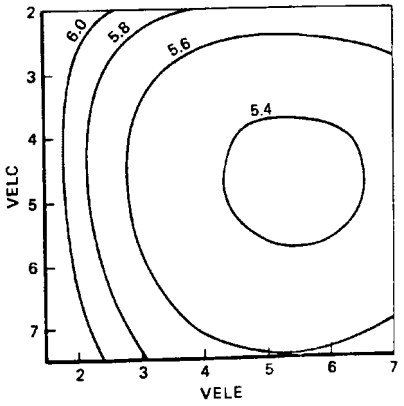

Fig. E.5—Iso-cost contours for constant TWWO, TCWO, T6, and T7

Appendix F

REFERENCE CASE: INPUT DEFINITION AND OUTPUT PRINTOUT

This appendix contains a reproduction of the reference case described in Sec. III. Thermodynamic module variables that define the reference case are listed in Table F.1. Cost module demand inputs which further define the reference case are listed in Table F.2. No changes were made to default factors.

The reference case output is shown as Printouts 1 through 6. Printouts 1 through 3 provide a recapitulation of assumed economic factors and site geographic/climatic conditions as well as sizing data regarding the ocean engineering, power, and transmission systems. Printout 4 is a summary of OTEC capital costs. Printout 5 details the heat exchanger and transmission system capital costs. Printout 6 shows the bus-bar cost of electricity.

As indicated on Printouts 4 and 6, the reference OTEC configuration has a constant-dollar start-of-operation capital cost of $3428/kWe and a bus-bar cost of electricity of 96 mills/kWh.

Table F.1

REFERENCE CASE THERMODYNAMIC VARIABLES

		Condenser	Evaporator
Input Constants			
Turbine efficiency	0.834		
Condensate pump efficiency	0.750		
Vapor Δ pressure (lb/sq in.)		0.500	0.800
Height change (ft)	50.0		
Reflux ratio	0.500		
Wilson plot intercept		0.00073	0.00041
Wilson plot slope		0.00420	0.00385
Fouling factor		0.00010	0.00025
Friction factor coefficient	0.316		
Friction factor exponent	-0.250		
Tube roughness	0.0002		
Minor losses, coefficient		4.100	2.580
CWP Δ pressure (lb/sq ft)	342.0		
Water pump efficiency	0.700		
Auxiliary hotel power (kW/lb NH_3/sec)	0.820		
Chlorination fraction		0.00000010	0.00000025
Tube inside diameter	0.944		
Warm-water inlet temperature (°F)	80.00		
Cold-water inlet temperature (°F)	40.00		
Optimized Variables			
Warm-water exit temperature (°F)	75.50		
Turbine inlet temperature (°F)	70.50		
Turbine exit temperature (°F)	50.00		
Cold-water exit temperature (°F)	46.50		
Tube velocity (ft/sec)		4.50	5.50
Calculated Output Variables			
Heat load (Btu/lb NH_3)		514.67	531.60
Generator power (kW/lb NH_3/sec)	17.599		
Log mean temperature difference (°F)		6.029	6.831
Water flow/ammonia flow		84.413	125.942
Overall heat transfer coefficient (Btu/(sq ft)(hr)(°F))		478.72	608.87
Unit tube ammonia flow (lb/sec)		0.01658	0.01358
Tube length (ft)		43.077	25.293
Condensate pump power (kW/lb NH_3/sec)	0.371		
Drain and reflux pump power (kW/lb NH_3/sec)	0.045		
Water pump power (kW/lb NH_3/sec)		1.836	1.157
Total pump power (kW/lb NH_3/sec)	3.4088		
Chlorination power (kW/lb NH_3/sec)		0.07293	0.22670
Total electrical losses (kW/lb NH_3/sec)	4.5284		
Net electrical power (kW/lb NH_3/sec)	13.07		
Condenser and evaporator heat transfer area/net power	84.319		

Table F.2

REFERENCE CASE COST MODULE DEMAND INPUTS

Site:	Tampa
Platform capacity:	400 MWe
Overload capacity:	yes
Modules per platform:	8
Platform type:	ship
Platform material:	concrete
CWP material:	steel
Platform number:	8[a]
Cold/warm-water pumps per module:	2/2
Ammonia feed pumps per module:	4
Capacity per ammonia feed pump:	.33
Ammonia recirculation pumps per module:	4
Capacity per ammonia recirculation pump:	.33
Turbines per module:	1
Heat exchanger type:	tube-and-shell
Heat exchanger location:	internal
Heat exchanger orientation:	horizontal
Heat exchanger design concept:	bundle
Water box requirement:	no
Number of condenser/evaporator bundles per HX:	14
Tube material type:	titanium
Tube outside diameter:	1.00 inch
Tube thickness:	.028 inch
Condenser/evaporator tube enhancement:	none/Linde
Mechanical cleaning type:	none
Number of HX pairs per module:	1

[a]The platform number is required for learning curve adjustments. For purposes of making inter-system comparisons of capital cost and the cost of electricity, it has been assumed that unit 8 is representative of a mature industry condition.

SYSTEM DESCRIPTION

GENERAL
SITE: TAMPA
NET POWER OUTPUT RATING (MWe) 400.
MODULES PER PLATFORM: 8
OVERRIDE CAPACITY: YES
PLATFORM #: 8
LENGTH OF CONSTRUCTION PERIOD (yrs): 5.00
FACILITY LIFE (yrs): 30
OVERALL CAPACITY FACTOR (decimal): 0.7938
DUE TO SEASONAL TEMP VAR (decimal): 0.8820
DUE TO MAINTENANCE (decimal): 0.9000
ANNUAL O&M
FIXED ($/kWe): 16.0000
VARIABLE (mills/kwh): 1.5000
ANNUAL RATE OF INFLATION (decimal): 0.060
ANNUAL COST OF CAPITAL (decimal): 0.100
FIXED CHARGE RATE (decimal): 0.1800
SEA CONDITIONS (100 year storm)
SIGNIFICANT WAVE HEIGHT (ft): 45.8
CURRENT (knots): 5.0000
WIND VELOCITY (knots) 114.00
OCEAN DEPTH (ft): 4590.
DISTANCE FROM SHORE (nautical miles): 148.0

OCEAN ENGINEERING

PLATFORM
TYPE OF PLATFORM: SHIP
POWER MODULE LOCATION: INTERNAL
CONSTRUCTION MATERIAL: CONCRETE
STRUCTURAL WEIGHT (long tons): 331083.
OPERATING DISPLACEMENT (long tons): 673177.
DIMENSIONS (ft): - - - SHIP - - -
LENGTH: 887.3013
BEAM: 278.8660
DEPTH: 126.7574

COLD WATER PIPE
VOL FLOW (cuft/hr): 145073232.
MATERIAL: STEEL
INSIDE DIAMETER (ft): 92.4744
WALL THICKNESS (ft): 0.1068
LENGTH (ft): 3100.
DEPTH OF PIPE BOTTOM (ft): 3200.
SECTION LENGTH (ft): 100.0000
ASSEMBLY CONCEPT: ASSEMBLY-AT-SEA
HULL CONNECTION TYPE: GIMBAL BEARING
EXPECTED LIFE (yrs): 30

MOORING
CONCEPT: FIXED, MULTI-POINT
LINE TYPE: WIRE-CHAIN
ANCHOR TYPE: CONCRETE BLOCK
LEGS PER PLATFORM: 3
LINES PER LEG: 6
LINE LENGTH (feet per line): 9180.
ANCHOR WEIGHT (lbs / anchor): 41003120.
EXPECTED LIFE (yrs): 30

Printout 1

```
POWER SYSTEM
  HEAT EXCHANGERS
      HX PAIRS (EVAP + COND) PER MODULE:        1
      HX TYPE:  TUBE AND SHELL
      HX ORIENTATION:  HORIZONTAL
      HX DESIGN CONCEPT:  BUNDLE
                                          EVAPORATOR        CONDENSER
      NUMBER OF BUNDLES PER HX               14                14
      TUBES
          MATERIAL:                       TITANIUM          TITANIUM
          ENHANCEMENT TYPE:                  LINDE              NONE
          OUTSIDE DIAMETER (in):           1.0000            1.0000
          WALL THICKNESS (in):             0.0280            0.0280
          ACTIVE LENGTH(f t):             25.2928           43.0765
          ACTUAL LENGTH(f t):             25.6928           43.4765
          NO OF TUBES PER HX:           281591            230679
      TUBESHEETS
          SIZE (ft):                      14.2845           12.9288
          BASEPLATE MATERIAL:               STEEL             STEEL
          BASEPLATE THICKNESS (in)        2.1376            2.0178
          CLADDING MATERIAL:             TITANIUM          TITANIUM
          CLADDING THICKNESS (in):         0.25              0.25
      TUBE SUPPORT PLATES
          SIZE (ft):                      14.2845           12.9288
          THICKNESS (in):                  0.5264            0.5034
          NUMBER:                             8                14
          MATERIAL:                         STEEL             STEEL
      SHELL
          INSIDE DIAMETER (ft):           93.4308           84.5638
          THICKNESS (in):                  4.7865            4.3485
          OVERALL LENGTH (ft):            25.6928           43.4765
          MATERIAL:                         STEEL             STEEL
  SEAWATER PUMPS
      MODULE PUMP POWER (MWe):      11.45
                                      WARM WATER        COLD WATER
      NUMBER PER MODULE:                   2                 2
      VOLUMETRIC CAP/PUMP (cuft/hr):  13527864.          9067077.
  AMMONIA PUMPS
                                       FEED PUMPS     RECIRC PUMPS
      NUMBER PER MODULE:                   4                 4
      CAPACITY PER PUMP (decimal):        0.33              0.33
      VOLUMETRIC CAP/PUMP (cuft/hr):   114746.           57373.
  BIOFOULING
      CHEMICAL
          CHLORINATION
              CHLORINE REQMTS FOR MODULE EVAPORATOR(S) (lbs/hr):      434.
              CHLORINE REQMTS FOR MODULE CONDENSER(S) (lbs/hr):       116.
      MECHANICAL
          SYSTEM TYPE:  NONE
          CLEANING FREQUENCY (passes per day):      0.0
  TURBINES
      AXIAL, DOUBLE FLOW, SINGLE STAGE EACH END, 1800 RPM
      NUMBER PER MODULE:      1
      GROSS POWER PER TURBINE (MWe):    67.32
  GENERATORS
      SYNCHRONOUS, TOTALLY ENCLOSED, 1800 RPM HYDROGEN-COOLED,
       BRUSHLESS AC EXCITER
      NUMBER PER MODULE:      1
      GROSS POWER PER GENERATOR (MWe):  80.79
```

Printout 2

```
TRANSMISSION SYSTEM
        250 kV DC
        ONE CIRCUIT PER PLATFORM
        NUMBER OF CABLES PER PLATFORM (incl spares):    3
        RISER CABLE
            TYPE:  SOLID DIELECTRIC, ALUMINUM CONDUCTOR
            ATTACHMENT: SUB-SURFACE BUOY
            LENGTH (ft):                  21700.00
            EXPECTED LIFE (yrs):  30
        BOTTOM CABLE
            TYPE:  PAPER IMPREGNATED, COPPER CONDUCTOR
            SUSPENSION: DEPTHS ≤ 300 FT: EMBEDMENT
                        DEPTHS > 300 FT: FLOOR
            LENGTH (nautical miles):      148.00
            EMBEDMENT DISTANCE (nautical miles):    85.00
            EXPECTED LIFE (yrs):  30
```

Printout 3

CAPITAL COSTS FOR PLATFORM # 8	$/kWe
POWER SYSTEM	
HEAT EXCHANGERS	
EVAPORATORS	446.
CONDENSERS	395.
WORKING FLUID SUBSYSTEM	
PUMPS(FEED AND REFLUX)	18.
PIPING	8.
VALVES	41.
INVENTORY, STORAGE, CLEAN-UP, PURGE	12.
SEA WATER PUMPS	
COLD WATER PUMPS	37.
WARM WATER PUMPS	51.
POWER SUPPLY AND CONTROL	14.
BIOFOULING CONTROL	
CHEMICAL	30.
MECHANICAL	0.
TURBINES	26.
GENERATORS	42.
ELECTRICAL AUXILIARIES	26.
INSTRUMENTATION AND CONTROL	20.
START-UP/STAND-BY POWER	9.
MISC EQUIPMENT ITEMS	0.
COMPONENT INSTALLATION	60.
OCEAN ENGINEERING	
PLATFORM	
HULL STRUCTURE	280.
BALANCE OF SEAWATER CIRCUITS	39.
SUPPORT SYSTEMS, OUTFITTING	86.
DEPLOYMENT	3.
COLD WATER PIPE	
SECTIONS	149.
HULL CONNECTION AND SCREENS	49.
DEPLOYMENT	16.
MOORING	
LINES, ANCHORS	114.
DEPLOYMENT	1.
TRANSMISSION	
RECTIFIER (SHIP-BOARD)	27.
RISER CABLE	11.
BOTTOM CABLE	147.
SHORE TERMINAL STATION	38.
DEPLOYMENT/INSTALLATION	
RECTIFIERS/INVERTERS	7.
RISER/BOTTOM CABLES	98.
A&E SERVICES	90.
CONTINGENCY	359.
INTERIM REPLACEMENT	
EVAPORATOR TUBES	0.
CONDENSER TUBES	0.
COLD WATER PIPE	0.
MOORING LINES	0.
RISER CABLE	0.
BOTTOM CABLE	0.
START-OF-CONSTRUCTION CAPITAL COST	2749.
ESCALATION AND INTEREST DURING CONSTRUCTION	1280.
START-OF-OPERATION CAPITAL COST	4029.
CONSTANT-DOLLAR START-OF-OPERATION CAPITAL COST	3428.

Printout 4

HEAT EXCHANGER BREAKDOWN ($/kWe)

	- - FIRST UNIT - - MATERIAL	LABOR	TOTAL	AVG FOR PLATFORM # 8 MATERIAL	LABOR	TOTAL
EVAPORATOR						
TUBES	289.	56.	345.	289.	26.	314.
TUBESHEETS	29.	18.	47.	29.	8.	37.
TUBE SUPPORT PLATES	3.	20.	22.	3.	9.	12.
SHELL	8.	14.	22.	8.	6.	14.
OTHER	13.	34.	47.	13.	16.	28.
SUB-TOTAL			483.			405.
FEE			48.			41.
DESIGN ALLOWANCE			0.			0.
TOTAL			531.			446.
CONDENSER						
TUBES	264.	46.	310.	264.	21.	285.
TUBESHEETS	24.	14.	39.	24.	7.	31.
TUBE SUPPORT PLATES	3.	28.	32.	3.	13.	16.
SHELL	11.	19.	30.	11.	9.	19.
OTHER	4.	9.	13.	4.	4.	8.
SUB-TOTAL			423.			359.
FEE			42.			36.
DESIGN ALLOWANCE			0.			0.
TOTAL			466.			395.

TRANSMISSION SYSTEM BREAKDOWN
(AVERAGE FOR PLATFORM # 8)

	- - - -	$/kWe	- - - -
RECTIFIER (SHIP-BOARD)	31.		
HARDWARE		27.	
INSTALLATION		4.	
RISER CABLE	13.		
HARDWARE		11.	
CABLE			6.
ACCESSORIES			5.
DEPLOYMENT/INSTALLATION		1.	
BOTTOM CABLE	244.		
HARDWARE		147.	
CABLE			147.
ACCESSORIES			0.
DEPLOYMENT/INSTALLATION		97.	
TRANSPORTATION			5.
FLOOR LAYING			4.
EMBEDMENT			88.
SHORE TERMINAL STATION	42.		
INVERTER		40.	
HARDWARE			36.
INSTALLATION			4.
FACILITY		3.	
TOTAL TRANSMISSION SYSTEM	329.		

Printout 5

BUSBAR COST OF ELECTRICITY

	mills/kwh
CAPITAL	88.7250
O&M	7.1679
TOTAL	95.8929

Printout 6

Appendix G
OFF-DESIGN CALCULATIONS

The *design point* analysis calculates the gross and net power, the water flows per unit ammonia flow, the heat exchanger tube lengths, the net power per unit tube, and the turbine flow area per unit tube for a set of assumed turbine temperatures, warm- and cold-water inlet and discharge temperatures and water velocities in tubes, component efficiencies, and heat exchanger characteristics. The *off-design problem* treated here is to find, for a given "design point," how the net power varies with different warm-water temperatures during a year's operation at a given site. The task of off-design analysis is, for given heat exchanger and turbine flow area,* to find the cycle conditions (and hence the performance) that satisfy detailed heat and power balances for components, and flow continuity in the turbine.

The off-design performance analysis must take into account changes in component performance as the system moves away from its design point. The turbine efficiency is an important parameter that varies with off-design conditions. Figure G.1 shows the variation in turbine efficiency that has been used in the present study. Turbine efficiency is a parabolic function of the velocity ratio, i.e., the ratio of the pitch-line wheel speed to the theoretical spouting velocity. Stodola (1945) shows that for single stage, impulse turbines (as used in OTEC) this is a good approximation to observed data. The velocity ratio is taken as 0.5 at the "design" conditions; a constant RPM is used, and the velocity ratio (and hence the efficiency) can be found at other conditions from the thermodynamic calculation.

---

*The turbine flow area can be changed, as has been demonstrated on experimental gas turbine turbomachinery, with generally small losses in efficiency. The turbine flow area for optimal "design point" power plants at low ΔT is about 25 percent larger than at high ΔT. Both fixed flow area and variable flow area turbines were investigated. There is no evident way that the surface area of heat exchangers can be changed for off-design operation, but clearly the water velocity in the tubes can assume different values as overall temperature changes.

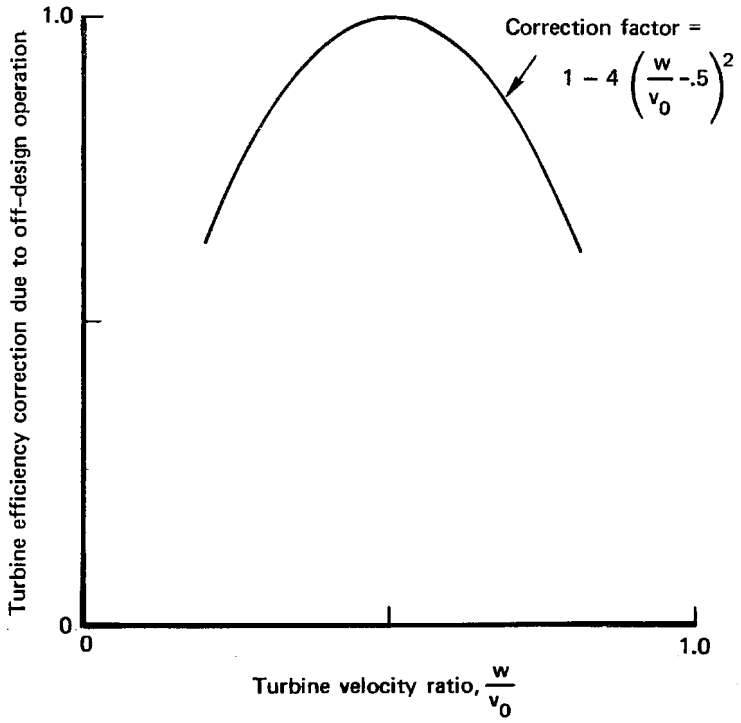

Fig. G.1 — Turbine efficiency correction at off-design

Off-design operation of the heat exchangers is accounted for by considering the heat transfer characteristics in terms of a Wilson plot that gives the overall heat transfer coefficient as a function of water velocity in the passages. In the examples shown here, we used Wilson-plot heat transfer data given by Michel (1977).

Off-design variations in water pump efficiency have been neglected because the preponderance of water pumping will occur at a constant pump velocity ratio (hence efficiency). The water passages are substantially fixed in geometry, and the variation in pumping-loss coefficients for a given design turn out to be negligibly small.

Performance calculations, including the effects of turbine efficiency variation, are made using the "design point" algorithms, for a range of heat exchanger exit temperatures and tube velocities and a given overall ΔT. Typically, the results of these algorithms may be graphically represented as in Fig. G.2 and Fig. G.3. Figure G.2 is a plot of turbine flow area per heat exchanger tube versus tube

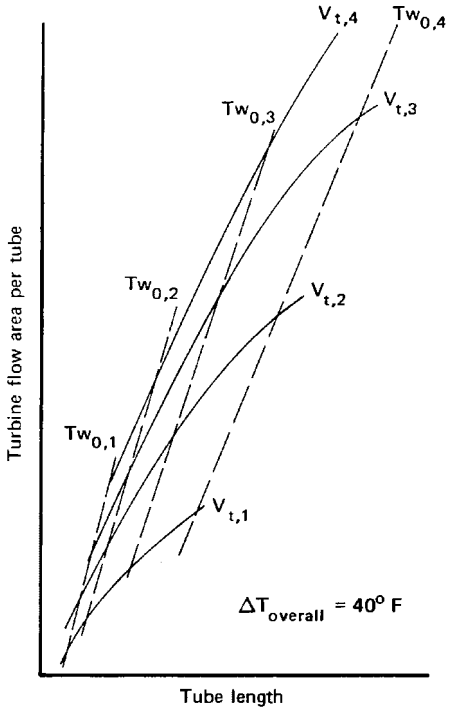

Fig. G.2 — Turbine flow area versus tube length

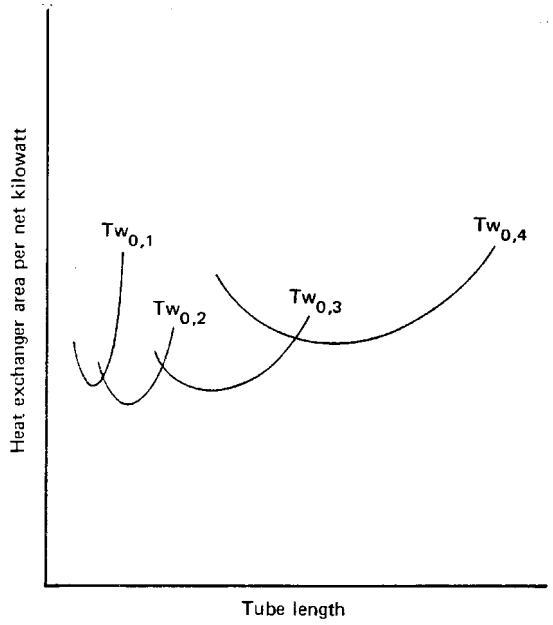

Fig. G.3 — Area per kW versus tube length

length, with lines of water exit temperature and tube velocity. Figure G.3 is a plot of A_{hex}/P versus tube length, with the same parameters. A set of plots of this type can be made for each overall ΔT of interest, and the off-design performance can be found for various "design point" power plants. The two principal "geometrical" constraints on operating conditions--tube length and turbine flow area per tube--are taken as the coordinates of Fig. G.2. A "design point" of a given conceptual OTEC plant at a given overall ΔT with fixed geometry heat exchangers and turbines will fix values for these parameters, and these values can be used to enter similar charts for other overall ΔT's to find the plant's off-design performance.

These same charts can be used to estimate the performance of plants using a variable flow area turbine, and the variation in turbine nozzle area called for can be estimated, as well as the overall performance advantage achievable by such means.

Typical results of such calculations can be represented in a form as shown in Fig. G.4. This is a plot of net plant power per square foot of heat exchanger area as a function of the overall ΔT available. The upper line is the locus of design points optimized to produce (under a certain set of component assumptions) the maximum net power per square foot of heat exchanger area at each overall ΔT. No plant of this class can be better than this line. The physical differences among the optimized plants are typically moderate, resulting in moderate to small component performance changes (for instance, in turbine efficiency and in water velocity in heat exchangers) as the power plant is operated off-design.

The dashed line on Fig. G.4 represents the performance versus overall ΔT for a plant with a variable flow area turbine. This performance will fall slightly below that of the locus of design points, because (1) the turbine off-design variation in efficiency has been taken into account, and (2) the tube length cannot be ideal over the entire range. But the performance over most of the range of interest is within 2 percent of the locus of design points, and at the extreme low temperature range is down about 5 percent.

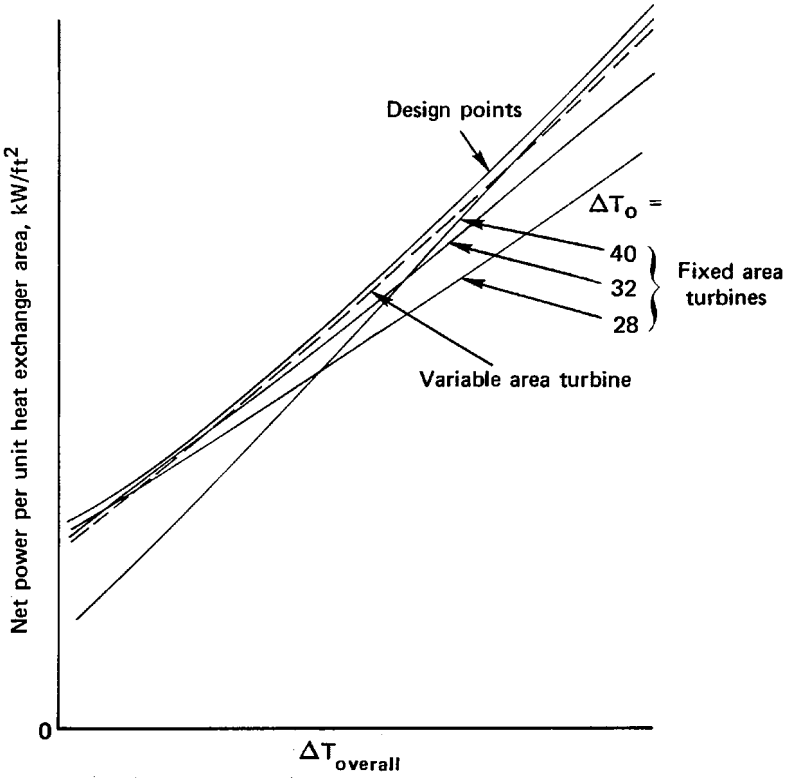

Fig. G.4 — Net power versus ΔT characteristics

The use of fixed geometry turbines results in larger deviations from the ideal. The lower solid lines in Fig. G.4 represent the off-design performance achievable with designs optimized at various temperatures, using fixed geometry turbines. The choice of a design at either extreme of the temperature range will result in relatively poor performance at the other end of the range. The percentage deviation from the locus of design points is most extreme at the low temperature end. A choice of an intermediate design point temperature can result in relatively small deviations from ideal performance over the entire range.

Figure G.5 has been used to calculate the average power available over the entire year. We assume that OTEC would supply part of the base-load requirements in the Southern United States largely supplied by coal. We also assume that the variation in the cost of base-load power is negligible through the year. Therefore, in these calculations the value of power is not weighted differently through the year,

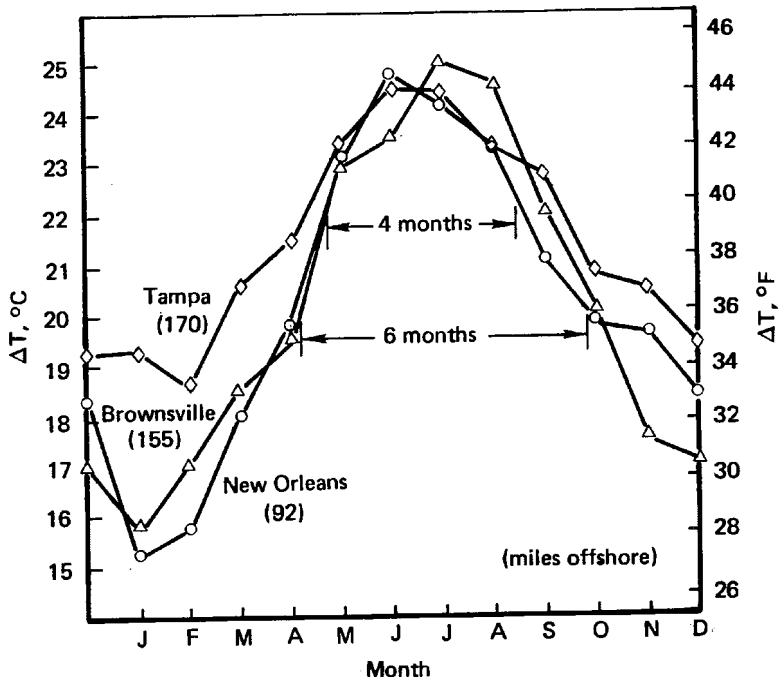

Fig. G.5—Seasonal variations in temperature difference
Surface to 3000 ft

and the optimal design is taken as that one which maximizes the simple time-averaged power over the year.

REFERENCES

Abelson, H., *OTEC Power System Performance Model*, The MITRE Corporation, MTR-7924, August 1978.

Berger, L. R., W. F. McCoy, and J. R. Berger, "Biofouling Assays for OTEC Pipes," *Proceedings of the Ocean Thermal Energy Conversion (OTEC) Biofouling, Corrosion, and Materials Workshop*, Argonne National Laboratory, ANL/OTEC-BCM-002, January 8-10, 1979, p. 38.

Bergles, A. E., and M. K. Jensen, *Enhanced Single-Phase Heat Transfer for Ocean Thermal Energy Conversion Systems*, Oakridge National Laboratory, ORNL/Sub77/14216/1, April 1977.

Bryers, J. D., W. G. Characklis, N. Zelven, and M. G. Nimmons, "Microbial Film Development and Associated Energy Losses," in G. L. Dugger (ed.), *Proceedings of the Sixth OTEC Conference*, preprint, Vol. 1, Conf. 790631/1, 1979.

Capuzzo, J. M., S. A. Lawrence, and J. A. Davidson, "Combined Toxicity of Free Chlorine, Chloramine, and Temperature to Stage 1 Larvae of the American Lobster (Homarus Americanus)," *Water Research*, Vol. 10, 1976, pp. 1093-1099.

Capuzzo, J. M., J. C. Goldman, J. A. Davidson, and S. A. Lawrence, "Chlorinated Cooling Waters in the Marine Environment: Development of Effluent Guidelines," *Marine Pollution Bulletin*, Vol. 8, No. 7, July 1977, pp. 161-163.

Capuzzo, J. M., J. A. Davidson, S. A. Lawrence, and M. Libni, "The Differential Effects of Free and Combined Chlorine on Juvenile Marine Fish," *Estuarine and Coastal Marine Science*, Vol. 5, 1977, pp. 733-741.

Chapman, A. J., *Heat Transfer*, 3d ed., Macmillan and Co., New York, 1974.

Characklis, W. G., "Attached Microbial Growths--Vol. II. Frictional Resistance Due to Microbial Slimes," *Water Research*, Vol. 7, 1973, pp. 1249-1258.

Chet, I., P. Asketh, and R. Mitchell, "Repulsion of Bacteria from Marine Surfaces," *Appl. Microbiol.*, Vol. 30, 1976, pp. 1043-1045.

Claude, G., "Power from the Oceans' Thermal Gradients," *Mechanical Engineering*, Vol. 52, 1930, pp. 1039-1044.

Coombs, S. K., and R. W. Murphy, "Experimental Studies of OTEC Heat Transfer Condensation of Ammonia on Vertical Fluted Tubes," *Proceedings of the Fifth Ocean Thermal Energy Conversion Conference*,

Miami Beach, Florida, February 20-22, 1978, Vol. III, September 1978, pp. VI-111, VI-112.

Corpe, W. A., "Marine Microfouling and OTEC Heat Exchangers," in R. H. Gray (ed.), *Proceedings of the Ocean Thermal Energy Conversion (OTEC) Biofouling and Corrosion Symposium*, USDOE-PNL, October 10-12, 1977.

Costerton, J. W., G. G. Geesey, and K. J. Cheng, "How Bacteria Stick," *Scientific American*, Vol. 238, No. 1, January 1978, pp. 86-95.

Dawson, D. A., and O. Trass, "Mass Transfer at Rough Surfaces," *Int. J. Heat Mass Trans.*, Vol. 15, 1972, pp. 1317-1336.

DePalma, V. A., D. W. Goupil, and C. K. Akers, "Field Demonstration of Rapid Microfouling in Model Heat Exchangers: Gulf of Mexico, November 1978," in G. L. Dugger (ed.), *Proceedings of the Sixth OTEC Conference*, preprint, Vol. 1, Conf. 790631/1, 1979.

Dipprey, D. F., and R. H. Sabersky, "Heat and Momentum Transfer in Smooth and Rough Tubes at Various Prandtl Numbers," *Int. J. Heat Mass Trans.*, Vol. 6, 1963, pp. 329-353.

Electric Power Research Institute, *Technical Assessment Guide*, PS-866-SR, Palo Alto, California, June 1978.

Fava, J. A., and D. L. Thomas, "Use of Chlorine for Antifouling on Ocean Thermal Energy Conversion (OTEC) Power Plants," in R. H. Gray (ed.), *Proceedings of the Ocean Thermal Energy Conversion (OTEC) Biofouling and Corrosion Symposium*, USDOE-PNL, October 10-12, 1977.

Fetkovich, F. G., "Interpretation and Implications of OTEC Biofouling Data," *Proceedings of the Ocean Thermal Energy Conversion (OTEC) Biofouling, Corrosion, and Materials Workshop*, Argonne National Laboratory, ANL/OTEC-BCM-002, January 8-10, 1979.

Fetkovich, F. G., G. N. Grannemann, L. M. Mahlingam, and D. L. Meier, "Measurements of Biofouling in OTEC Heat Exchangers," *Proceedings of the Fifth Ocean Thermal Energy Conversion Conference*, Miami Beach, Florida, 1978.

Fiacco, A. V., and G. P. McCormick, *Nonlinear Programming: Sequential Unconstrained Minimization Techniques*, John Wiley and Sons, Inc., New York, 1968.

Gazley, C., Jr., G. M. Harpole, L. S. Yao, W. H. Krase, I. Catton, J. Grzesik, and W. Matyskiela, *Prediction of Thermal Hydraulic Performance and Gas-Cooled Breeder Reactors*, The Rand Corporation, R-1978-EPRI, 1977.

Gibbs and Cox, Inc., *Ocean Thermal Energy Conversion (OTEC) Platform Configuration and Integration*, Report 18351-10 (W-10,030), New York, July 1978.

Gibbs and Cox, Inc., *OTEC-10 and -40 MWe Modular Applications Platform Star Conceptual Design*, Final Report, Report 18641-3, Washington, D. C., April 1979.

Goldman, J. C., J. M. Capuzzo, and G.T.F. Wong, "Biological and Chemical Effects of Chlorination at Coastal Power Plants," *Water Chlorination, Environmental Impact and Health Effects*, Vol. 2, Ann Arbor Science Publishers, Ann Arbor, Michigan, 1978.

Han, J. C., L. R. Glickman, and W. M. Rohsenow, "An Investigation of Heat Transfer and Friction for Rib-Roughened Surfaces," *Int. J. Heat Mass Trans.*, Vol. 21, 1978, pp. 1143-1156.

John J. McMullen Associates, Inc., *Reviews of Reports by Gibbs and Cox, Inc., Lockheed Missile and Space Corporation, and M. Rosenblatt and Sons on 400 MWe OTEC Plants*, New York, New York, June 1979.

Kinelski, E. H., "The Requirements for Biofouling, Corrosion, and Materials in the OTEC Program," *Proceedings of the Ocean Thermal Energy Conversion (OTEC) Biofouling, Corrosion, and Materials Workshop*, Argonne National Laboratory, ANL/OTEC-BCM-002, January 8-10, 1979a.

Kinelski, E. H., "Biofouling, Corrosion, and Materials Overview," in G. L. Dugger (ed.), *Proceedings of the Sixth OTEC Conference*, preprint, Vol. II, Conf. 790631/2, 1979b.

LaQue, F. L., "The Qualification of Metals and Alloys for OTEC Heat Exchangers," *Proceedings of the Ocean Thermal Energy Conversion (OTEC) Biofouling, Corrosion, and Materials Workshop*, Argonne National Laboratory, ANL/OTEC-BCM-002, January 8-10, 1979a.

LaQue, F. L., "Qualifying Aluminum and Stainless Steel for Tubes in OTEC Heat Exchangers," in G. L. Dugger (ed.), *Proceedings of the Sixth OTEC Conference*, preprint, Vol. II, Conf. 790631/1, 1979b.

Lewis, L. G., and N. F. Sather, *OTEC Performance Tests of the Union Carbide Fluid-Bundle Evaporator*, Argonne National Laboratory, ANL/OTEC-PS-1, December 1978.

Liebert, B. E., L. R. Berger, H. J. White, J. Moore, W. McCoy, J. A. Berger, and J. Larsen-Basse, "The Effects of Biofouling and Corrosion on Heat Transfer Measurements," in G. L. Dugger (ed.), *Proceedings of the Sixth OTEC Conference*, preprint, Vol. I, Conf. 790631/1, 1979.

Lockheed Missiles and Space Co., Inc., *Power System Development (PSD-II), Final Design Briefing*, supported by Alfa-Laval Thermal, Inc., 1979a.

Lockheed Missiles and Space Co., Inc., "Power System Development (PSD-II), Test Plan for the 0.2-MW_e Heat Exchanger Test Articles," Preliminary Draft, 1979b.

Lockheed Missiles and Space Co., Inc., *Ocean Thermal Energy Conversion (OTEC) Power System Development, Conceptual Design*, LMSC-D566744, January 30, 1978.

Mann, M. J., F. B. Bailey, and J. F. Mocker, "Qualification of a Duplex, Clad Material for OTEC," in G. L. Dugger (ed.), *Proceedings of the Sixth OTEC Conference*, preprint, Vol. I, Conf. 790631/1, 1979.

Mann, M. J., "An Abrasive Slurry Cleaning Technique for OTEC Plants," in G. L. Dugger (ed.), *Proceedings of the Sixth OTEC Conference*, preprint, Vol. I, Conf. 790631/1, 1979.

Massart, G. L., "The Tribulations of Trying to Harness Thermal Power," *Marine Technology Society Journal*, Vol. 8, No. 9, 1974, pp. 18-21.

McGuinness T., A. Griffin, and D. Hove, "Preliminary Designs of OTEC Cold Water Pipes," in G. L. Dugger (ed.), *Proceedings of the Sixth OTEC Conference*, preprint, Vol. I, Conf. 790631/1, 1979.

Melese-d'Hospital, G., "Merit Index for Gas-Cooled Reactor Heat Transfer," *Nucl. Sci. Engr.*, Vol. 50, 1973, p. 83.

Michel, J. W., "Analytical and Experimental Studies of OTEC Heat Transfer Problems at Oak Ridge National Laboratory," *Proceedings of the Fourth Annual Conference on Ocean Thermal Energy Conversion*, University of New Orleans, March 22-24, 1977.

Mitchell, R., "Mechanism of Biofilm Formation in Seawater," in R. H. Gray (ed.), *Proceedings of the Ocean Thermal Energy Conversion Biofouling and Corrosion Symposium*, USDOE-PNL, October 10-12, 1977.

Morello, A., and G. Gasparini, *Bottom Segment Design Underwater Cable Power Transmission System, Phase 1: Selection of Most Promising Cables for Various Plant Representative Sites*, Pirelli Cable Systems, Inc., New York, November 1978.

Mylander, C. W., R. L. Holmes, and G. P. McCormick, *A Guide to SUMT--Version 4*, Research Analysis Corporation, Report No. RAC-P-63, October 1971.

National Academy of Sciences, *Selected Issues of the Ocean Thermal Energy Conversion Program*, Marine Board, Assembly of Engineering, The National Research Council, Washington, D.C., 1977.

Nikuradse, J., "Gesetzmassigkeiten der turbulenter Stromung in glatten Rohren (Laws Governing Flow in Smooth Pipes)," VDI Forschungsheft 356, Beilage zu *Forschung auf dem Gebiete des Ingenieurwesens*, Ausgabe B, Band 3, September/October 1932.

Nikuradse, J., "Stromungsgesetze in rauhen Rohren (Laws of Flow in Rough Pipes)," VDI Forshungsheft 361, Beilage zu *Forschung auf dem Gebiete des Ingenieurwesens*, Ausgabe B, Band 4, July/August 1933 (NACA TM 1292, November 1950).

NOAA/DOE Cold Water Pipe Symposium, Applied Physics Laboratory, Johns Hopkins University, January 17-18, 1979.

Norris, R. H., "Some Simple Approximate Heat-Transfer Correlations for Turbulent Flow in Ducts with Rough Surfaces," in A. E. Bergles and R. L. Webb (eds.), *Augmentation of Convective Heat and Mass Transfer*, American Society of Mechanical Engineers, 1970, pp. 16-26.

Owen, P. R., and W. R. Thomson, "Heat Transfer Across Rough Surfaces," *J. Fluid Mech.*, Vol. 15, 1963, pp. 321-334.

Pandolfini, P. E., W. H. Avery, and F. K. Hill, *Experiments on Ultrasonic Cleaning of a Shell-Less Folded Aluminum Tube*, in G. L. Dugger (ed.), *Proceedings of the Sixth OTEC Conference*, preprint, Vol. 1, Conf. 790631/1, 1979.

Paulling, J. R., *Wave Induced Forces and Motions of Tubular Structures*, Eighth Symposium of Naval Hydrodynamics, sponsored by Office of Naval Research, Pasadena, California, 1970.

Petukov, B. S., "Heat Transfer and Friction in Turbulent Pipe Flow with Variable Physical Properties," *Advances in Heat Transfer*, Vol. 6, 1964, pp. 639-653.

Pilipenko, V. N., "Heat and Mass Transfer in Turbulent Flows Over a Rough Surface," *Heat Transfer--Soviet Research*, Vol. 9, 1977, pp. 78-82; originally published in *Proceedings of the 5th All-Union Conference on Heat and Mass Transfer*, Vol. 1, 1976, pp. 128-132.

Pirelli Cable Systems, Inc., *DOE-OTEC Project, Phase I, Selection of Bottom Cables*, New York, November 1978.

Schlichting, H., *Boundary Layer Theory*, 6th ed., McGraw-Hill Book Co., New York, 1968.

Slianciauskas, A. A., and M.-R. M. Drizius, "Calculation of Heat Transfer on Rough Surfaces," *Heat Transfer--Soviet Research*, Vol. 9, 1977, pp. 40-47; originally published in *Proceedings of the 5th All-Union Conference on Heat and Mass Transfer*, Vol. I, 1976, pp. 67-76.

Stodola, A., and L. C. Loewenstein, *Steam and Gas Turbines*, Vol. I, Peter Smith, New York, 1945, p. 222.

TRW, Inc. (Systems and Energy), *Ocean Thermal Energy Conversion (OTEC) Power System Development, Preliminary Design Report (Final)*, Report 1570, Redondo Beach, California, December 4, 1978.

U.S. Congress, Office of Technology Assessment, *Renewable Ocean Energy Sources, Part 1, Ocean Thermal Energy Conversion*, May 1978.

Webb, R. L., "Toward a Common Understanding of the Performance and Selection of Roughness for Forced Convection," *ASME Winter Annual Meeting*, ASME preprint 78-WA/HT-61, San Francisco, December 10-15, 1978.

Webb, R. L., and E.R.G. Eckert, "Application of Rough Surfaces to Heat Exchanger Design," *Int. J. Heat Mass Trans.*, Vol. 15, 1972, pp. 1647-1658.

Webb, R. L., E.R.G. Eckert, and R. J. Goldstein, "Heat Transfer and Friction in Tubes with Repeated Rib Roughness," *Int. J. Heat Trans.*, Vol. 14, 1971, pp. 601-617.

Webb, R. L., E.R.G. Eckert, and R. J. Goldstein, "Generalized Heat Transfer and Friction Correlations for Tubes with Repeated-Rib Roughness," *Int. J. Heat Mass Trans.*, Vol. 15, 1972, pp. 180-184.

Westinghouse Electric Corporation (Power Generation Division), *Ocean Thermal Energy Conversion Power System Development, Phase 1: Preliminary Design*, Lester, Pennsylvania, December 4, 1978.

White, G. C., *Handbook of Chlorination*, Van Nostrand, Reinhold, Company, New York, 1972.

Zener, C., "Solar Sea Power," *Preliminary Reports, Memoranda, and Technical Notes of the Materials Research Council Summer Conference Held at La Jolla, California, July 1973*, Vol. II, University of Michigan, Ann Arbor, 1973, pp. 201-206.